REPUBLIC OF IRAQ
MINISTRY OF HIGHER EDUCATION AND
SCIENTIFIC RESEARCH
AL-FURAT AL-AWSAT TECHNICAL UNIVERSITY
ENGINEERING TECHNICAL COLLEGE NAJAF

EXPERIMENTAL STUDY FOR ENHANCEMENT OF HEAT TRANSFER BY USING TINY AIR BUBBLES INJECTION INSIDE A SHELL AND COILED INTERNALLY- EXTERNALLY FINNED TUBE HEAT EXCHANGER

SAIF SALAH HASAN RAHEEMAH

M.TECH
IN MECHANICAL ENGINEERING TECHNIQUES OF POWER

2021

EXPERIMENTAL STUDY FOR ENHANCEMENT OF HEAT TRANSFER BY USING TINY AIR BUBBLES INJECTION INSIDE A SHELL AND COILED INTERNALLY - EXTERNALLY FINNED TUBE HEAT EXCHANGER

A THESIS

SUBMITTED TO THE DEPARTMENT OF MECHANICAL ENGINEERING TECHNIQUES OF POWER IN PARTIAL FULFILLMENT OF THE REQUIREMENTS FOR THE DEGREE OF MASTER OF THERMAL TECHNOLOGIES IN MECHANICAL ENGINEERING TECHNIQUES OF POWER (M.TECH)

BY

SAIF SALAH HASAN RAHEEMAH

Supervisor By

Prof. Dr. Ali Shakir Baqir

July / 2021

بسم الله الرحمن الرحيم

إِلَّا أَن يَشَاء اللَّهُ نَرفَع دَرَجَاتٍ مَن
نَشَاء وَفَوقَ كُل ذِي عِلمٍ عَلِيم

DISCLAIMER

I confirm that the work submitted in this thesis is my own work and has not been submitted to other organization or for any other degree.

Signature:

Name: Saif Salah Hasan

Date: /   / 2021

ACKNOWLEDGMENT

SUPERVISORS CERTIFICATION

We certify that the thesis entitled "**Experimental Study For Enhancement of Heat Transfer By Using Tiny Air Bubbles Injection Inside A Shell And Coiled Internally - Externally Finned Tube Heat Exchanger**" submitted by **Saif Salah Hasan** has been prepared under our supervision at the Department of Mechanical Engineering Techniques of Power, College of Technical Engineering-Najaf, AL-Furat Al-Awsat Technical University, as partial fulfilment of the requirements for the degree of Master of Techniques in Thermal Engineering.

Signature:

Name: Prof. Dr. Ali Shakir Baqir

(Supervisor)

Date: /   / 2021

In view of the available recommendation, we forward this thesis for debate by the examining committee.

Signature:

Name: Prof. Dr. Dhafer Menea Hachim

Head mechanical Eng Tech of power Dept.

Date: /   / 2021

COMMITTEE CERTIFICATION

We certify that we have read the thesis entitled "**Experimental Study for Enhancement of Heat Transfer by Using Tiny Air Bubbles Injection Inside a Shell and Coiled Internally -Externally Finned Tube Heat Exchanger**" submitted by **Saif Salah Hasan** and, as examining committee, examined the student's thesis in its contents. And that, in our opinion, it is adequate as a thesis for the degree of Master of Techniques in Thermal Engineering.

Signature:

Name: Prof. Dr. Ali Shakir Baqir

(Supervisor)

Date: /   / 2021

Signature: Signature:

Name: Lecturer. Dr. Salah M.Salih   Name: Asst. Prof. Dr.Zaid M.H. Al-Dulaimi

(Member)   (Member)

Date: /   / 2021   Date: /   / 2021

Signature:

Name: Prof. Dr. Majid H. Majeed

(Chairman)

Date: /   / 2021

Approval of the Engineering Technical College- Najaf

Signature:

Name: Asst. Prof. Dr. Hassanain Ghani Hameed

Dean of Engineering Technical College- Najaf

Date: /   / 2021

LINGUISTIC CERTIFICATION

This is to certify that this thesis entitled "**Experimental Study For Enhancement of Heat Transfer By Using Tiny Air Bubbles Injection Inside A Shell And Coiled Internally-Externally Finned Tube Heat Exchanger**" was reviewed linguistically. Its language was amended to meet the style of the English language.

Signature:

Name:

Date:

ABSTRACT

Transferring thermal energy efficiently require using a heat exchanger capable of producing the full thermal power of the energy supply at the lowest possible cost and time. Traditional surface style heat exchangers have significant disadvantages, such as the high heat transfer resistance of the surface, fouling issue, and increasing cost. So, any attempt to enhance the heat transfer characteristics of a surface-type heat exchanger enhances its thermal performance. The air bubble injection and finned helical coil tube are two of the most promising enhancement techniques recently suggested in a separate image.

So, in the present study, the effect of merged enhancement techniques, air injection and finned (internally-externally) helical coil tube on the thermal performance of a vertical counter-current coiled heat exchanger was investigated experimentally. The air was injected into the shell side of the heat exchanger as air bubbles with a variable diameter of (0.1,0.8, and1.5 mm) via sparger (spiral- shape plastic tube) with 1400 hole per meter, as a new injection method. Furthermore, the study was conducted to optimize the operational parameters of the void fraction 0.25 (air and water volumetric flow rates) of the shell side under laminar flow (316 $\leq$ Re $\leq$ 1223). The experiments were performed with volumetric cold water flow rate (Q_S) = 2,4,6,and 8 L/min,volumetric air flow rate (Q_a) = 0.5,1,1.5,and 2 L/min,air pressure=2,3,4,and 5 bar,volumetric hot water flow rate (Q_h) = 1,1.5,and 2 L/min,and working fluid (water) inlet temperature difference were 20 ºC. Studying the effect of varying the operating parameters on the overall heat transfer coefficient, effectiveness , temperature distribution along with shell side pressure drop, and effect of air pressure on the thermal performance of the heat exchanger was considered with and without air bubbles injection.Besides, that studied the effect of bubbles diameter, and distance of spiral fins (5,8, and 10mm) on the thermal performance of the heat exchanger.

The experimental results showed that the overall heat transfer coefficient and heat exchanger effectiveness were improved significantly due to air bubbles injection. Indeed, for a smooth tube, the maximum enhancement ratio of overall heat transfer coefficient with air to overall heat transfer coefficient without air was 152 %, and effectiveness with air to effectiveness without air was 111% at $Q_s = 6$ L/min,$Q_a = 2$ L/min,$Q_h = 2$ L/min.

On the other hand, for the finned tube, the maximum enhancement ratio of overall heat transfer coefficient with air to overall heat transfer coefficient without air was 92 % while, the effectiveness with air to effectiveness without air was 71% at $Q_s = 4$ L/min, $Q_a = 2$ L/min, and bubble diameter = 1.5mm.

Furthermore, the experimental results showed that the highest improvement ratio of (overall heat transfer coefficient of finned tube to overall heat transfer coefficient of smooth tube) for pitch fins (5,8, and 10mm) was (107%, 73%, 49%), respectively, and the ratio of (overall heat transfer coefficient of finned tube with air to overall heat transfer coefficient of smooth tube without air) for pitch fins (5,8, and 10mm) was (281%, 261%, 248%) respectively.

CONTENTS

LIST OF TABLES

CHAPTER TWO

CHAPTER THREE

CHAPTER FOUR

APPENDIX

LIST OF FIGURES

CHAPTER ONE

CHAPTER TWO

CHAPTER THREE

CHAPTER FOUR

APPENDIX

NOMENCLATURE

Symbol	Definition	Unit
As	The surface area of heat transfer	m²
C	Thermal capacity	J/s.k
c	Specific heat	J/kg.K
D_c	Curvature diameter	mm
d_i	Inner coiled tube diameter	mm
D_o	Outer diameter	mm
H	Height column	mm
h	Height coil	mm
k	Thermal conductivity	W/m.K
De	Dean number	-
L	Length	mm
m°	Mass flow rate	Kg/s
N	Number of turns	-
p	Coil pitch	mm
p_f	The pitch of the Spiral fin	mm
p_a	Air pressure	Bar
D_b	Diameter bubble	mm
R_c	curvature radius	mm
Re	Reynolds number	-
t	tubes thickness	mm
T	Temperature	K
q	Heat transfer rate	W
Q	Volumetric Flow rate	L/min
Q_a	Volumetric Air Flow rate	L/min
Q_h	Volumetric Hot water Flow rate	L/min
Q_s	Volumetric Cold water Flow rate	L/min
VF	Volume fraction	-
L/min	Litter per minute	-
W	uncertainty in the measurement	-
U	Overall heat transfer coefficient	W/m². k
U_s	Overall heat transfer coefficient (smooth tube)	W/m². k
U_f	Overall heat transfer coefficient (finned tube)	W/m². k
U_{sa}	Overall heat transfer coefficient (smooth tube with air)	W/m². k
U_{fa}	Overall heat transfer coefficient (finned tube with air)	W/m². k

U_{sa}/U_s	Enhancement ratio for Overall heat transfer coefficient (smooth tube with air) to Overall heat transfer coefficient (smooth tube without air)	-
U_{fa}/U_f	Enhancement ratio for Overall heat transfer coefficient (finned tube with air) to Overall heat transfer coefficient (finned tube without air)	-
U_{fa}/U_s	Enhancement ratio for Overall heat transfer coefficient (finned tube with air) to Overall heat transfer coefficient (smooth tube without air)	-
Δp	pressure drop	Psi
Δp_{ss}	pressure drop of shell with smooth coil	Psi
Δp_{sf}	pressure drop of shell with finned coil	Psi
Δp_{sc}	pressure drop inside smooth coil	Psi
Δp_{fc}	pressure drop inside finned coil	Psi
Subscripts		
a	Air	-
c	Cold fluid	-
h	Hot fluid	-
i	Inner	-
in	Inlet	-
o	Outer	-
out	Outlet	-
min	Minimum	-
LMTD	Logarithmic mean temperature difference	-
Greek Symbols		
ρ	Fluid Density	kg/m^3
μ	Dynamic viscosity	Pa.s
ε	Effectiveness	-
ε_s	Effectiveness of smooth tube	-
ε_f	Effectiveness of finned tube	-
ε_{sa}	Effectiveness (smooth tube with air)	-
ε_{fa}	Effectiveness (finned tube with air)	-
$\varepsilon_{sa}/\varepsilon_s$	Enhancement ratio for effectiveness (smooth tube with air) to effectiveness (smooth tube without air)	-
$\varepsilon_{fa}/\varepsilon_f$	Enhancement ratio for effectiveness (finned tube with air) to effectiveness (finned tube without air)	-

Chapter One

Introduction

CHAPTER ONE

INTRODUCTION

An effective energy conversion process requires a design that involves an appropriate equipment to achieve the highest possible thermal potential from the systems energy supply [1]. The heat exchanger is equipment that has almost been used in this operation. Therefore, the heat exchanger can clearly be described as a device that transfers thermal energy between two different energy content fluids. The heat exchanger can be practically divided into two major types: surface or indirect contact heat exchanger and direct contact heat exchanger [2]. Metallic walls separate hot and cold fluids in the former, and thermal energy is transferred through them. However, due to the high heat transfer resistance of the metal barriers, this form of heat exchanger's thermal potential is restricted in addition to the high cost resulting from the huge heat transfer area needed to overcome the low efficiency of the heat exchange. Although direct contact heat exchange does not have such issues, it refers to thermal energy transport between two or more fluid streams when they are brought into intimate contact with each other [2-7].

Researchers have proposed several heat transfer improvement strategies over the last few years to minimize costs, size, weight and increase the thermal efficiency of surface heat exchangers. These strategies can be classified into three groups: passive, active, and compound techniques, which will be outlined in the following:

1.1 Passive Heat Transfer Enhancement Technique:

This techniques generally used surface or geometrical modifications to the flow channel by incorporating inserts or additional devices. It promote higher heat transfer coefficients by disturbing or altering the existing flow behavior (except for extended surfaces), increasing the pressure drop. In the case of extended surfaces,

the effective heat transfer area on the extended surface is increased. Passive techniques hold the advantage over active techniques as they do not require any direct input of external power. However, this heat transfer enhancement methodology involves **[8-13].** Heat transfer augmentation by these techniques can be achieved by using:

- ❖ **Rough Surfaces:** These surface modifications mainly create disturbance in the viscous sub-layer region. These techniques are applicable primarily in single-phase turbulent flows.

- ❖ **Extended Surfaces:** Plain fins are one of the earliest types of extended surfaces used extensively in many heat exchangers. Finned surfaces have become very popular nowadays due to their ability to disturb the flow field apart from increasing heat transfer.

- ❖ **Swirl Flow Devices:** They produce swirl flow or secondary circulation on the axial flow in a channel. Helically twisted tape, twisted ducts & various forms of altered (tangential to the axial direction) are typical of swirl flow devices. They can be used for both single-phase and two-phase flows.

- ❖ **Surface Tension Devices:** These devices direct and improve liquid flow to boiling surfaces and from condensing surfaces. Examples include wicking or grooved surfaces.

- ❖ **Coiled Tubes:** In these devices, secondary flows or vortices are generated due to curvature of the coils, which promotes a higher heat transfer coefficient in single-phase flows and most regions of boiling. This leads to relatively more compact heat exchangers.

- ❖ **Displaced Enhancement Devices:** These inserts are used primarily in confined forced convection. They improve heat transfer indirectly at the heat exchange surface by displacing the fluid from the heated or cooled surface of the duct with bulk fluid from the core flow.

❖ **Use Of Additives:** This contains soluble polymers and gas bubbles in a single-phase liquid flow or liquid droplets in a gas flow. Besides, they require the addition of solid nanoparticles to strengthen the thermophysical properties.

1.2 Active Heat Transfer Enhancement Technique:

These techniques are more complex from the use and design point of view as the method requires some external power input to cause the desired flow modification and improvement in the rate of heat transfer. It finds limited application because of the need for external power in many practical applications. Compared to the passive techniques, these techniques have not shown much potential as it is difficult to provide external power input in many cases. Briefly, this strategy of improvement includes **[11, 12, 13]; v**arious active techniques are as follows:

❖ **Fluid Vibration:** Instead of applying vibrations to the surface, pulsations are created in the fluid itself. This kind of vibration enhancement technique is employed for single-phase flows.

❖ **Injection:** In this technique, the same or other fluid is injected into the primary bulk fluid through a porous heat transfer interface or upstream of the heat transfer section. This technique is used for the single-phase heat transfer process.

❖ **Jet Impingement:** This technique is applicable for both two-phase and single-phase heat transfer processes. In this method, fluid is heated or cooled perpendicularly or obliquely to the heat transfer surface.

❖ **Suction:** This technique is used for both two-phase heat transfer and single-phase heat transfer processes. Two-phase nucleate boiling involves vapor removal through a porous heated surface, whereas fluid is withdrawn through the porous heated surface in single-phase flows.

❖ **Surface Vibration:** They have been used primarily in single-phase flows. A low or high frequency is applied to facilitate the surface vibrations, resulting in higher convective heat transfer coefficients.

❖ **Electrostatic Fields:** Electrostatic fields like electric or magnetic fields or a combination of the two from DC or AC sources are applied in heat exchanger systems which induces more significant bulk mixing, force convection or electromagnetic pumping to enhance heat transfer. This technique is applicable in the heat transfer process involving dielectric fluids.

1.3 Compound Enhancement Techniques:

A compound augmentation technique is that where two or more than one of the techniques mentioned above is used in combination to improve further the thermal performance of a heat exchanger **[6]**.

1.3.1 Helically Coiled Tube Effect on Enhancement Heat Transfer:

According to the above-mentioned heat transfer enhancement techniques, curved tubes, particularly coiled tubes, have been adopted as essential passive methods due to their compact design. In addition, it has a high coefficient of heat transfer in comparison with the straight tubes **[14]**. Therefore, curved tubes are the most commonly used tubes in several heat transfer applications, such as air conditioning cooling systems, chemical reactors, food dairy processes **[14]**, and heat recovery **[15]**. The curved tube types are shown in Fig 1.1.
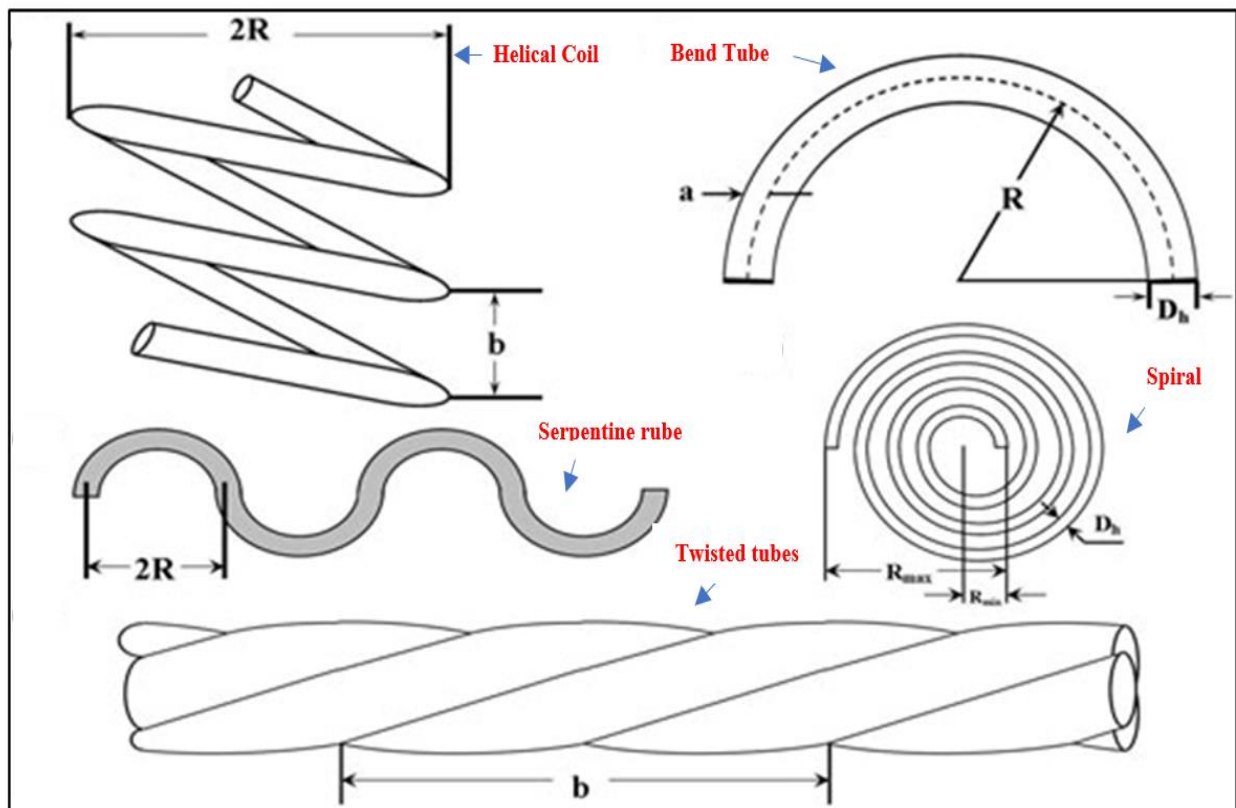
Figure 1.2: Types of curved tube geometries **[14]**.

Helically coiled tubes Fig.1.1 are the well-known type of curved tubes used in a large area of heat transfer applications. It provides a simple and effective means of heat transfer augmentation in a wide variety of industrial applications. The centrifugal forces caused by the curvature of the tube produce a secondary flow field with a circulatory motion pushing the fluid particles toward the core region of the tube. The intensity of the secondary flow field increases as the flow rate increases, and due to the stabilizing effects of this secondary flow, laminar flow persists to much higher Reynolds numbers in the helical coil than in straight tubes **[14]**. Consequently, the heat transfer performance differences between the coils and straight tubes are particularly distinct in the laminar flow region, which received most research attention **[16]**.

1.3.2 Secondary Flow in a Helical Coiled Tube:

The geometry of the shell and helically coiled tube heat exchanger is shown schematically in Fig.1.2. When a fluid flows in a helically coiled tube, and due to the interaction between centrifugal and viscous or frictional forces in the curved portion of the flow, a specific characteristic motion is known as secondary flow, as depicted in Fig.1.3. Secondary flow causes displaced fluid of curved pipes outer wall to the curved pipes inner wall. i.e., the fluid in the central region of the pipe moves away from the center of Curvature, and the fluid near the pipe wall flows towards the center of Curvature, but at the same time, this will increase pressure drop (Δp) **[17]**.

(d_t) is the tube diameter.
(d_c) is the coil diameter.
(d_{sh}) shell diameter.
(H_c) coil height.
(H_{sh}) shell height.
(d_v) shell inlet diameter.
(p) is the pitch coil.
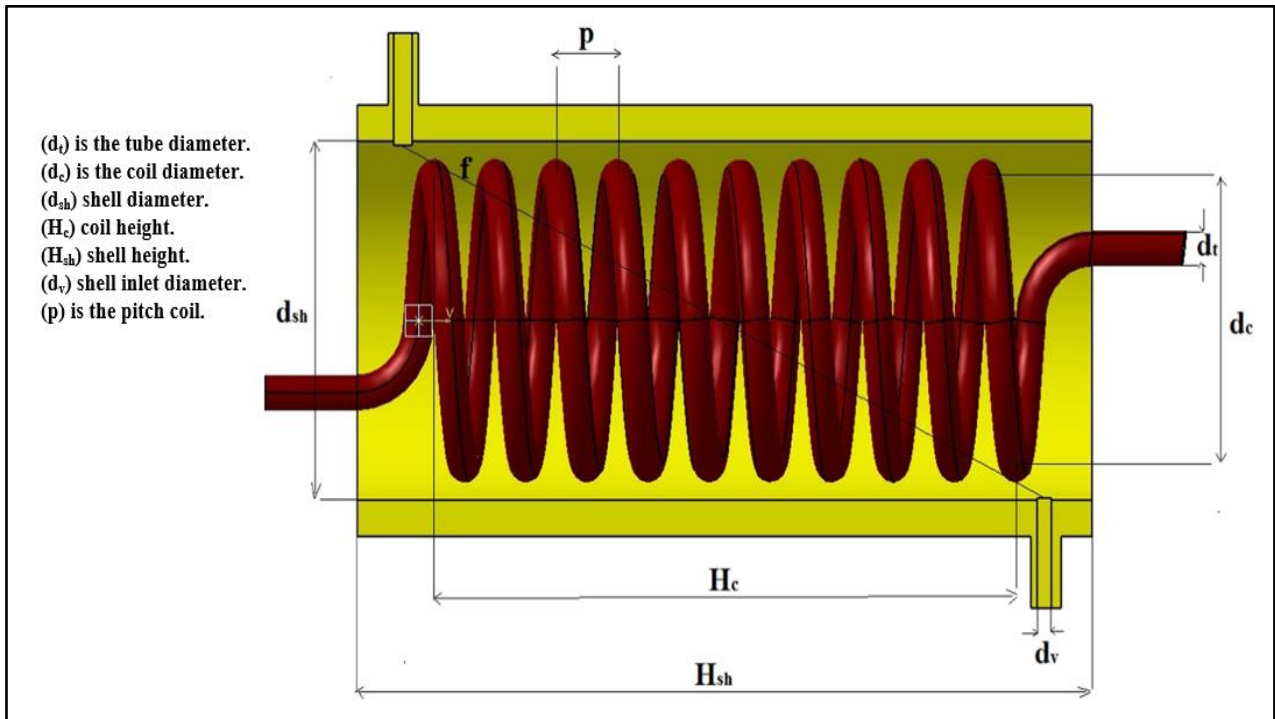
Figure 1.3: Schematic of shell and coiled tube heat exchanger **[17]**.

Dean was experimentally showed that the dynamical similarity of secondary flow depends on a non-dimensional parameter called Dean Number (De) **[18]**:

$$De = \left(\frac{d_t}{2R_c}\right)^{0.5} \left(\frac{d_t V_m}{\nu}\right) \tag{1.1}$$

Where De is the Dean Number,V_m are the mean velocity along the pipe, v kinematic viscosity, and d_t is the diameter of the pipe which is bent into a coil of radius R_c [18].
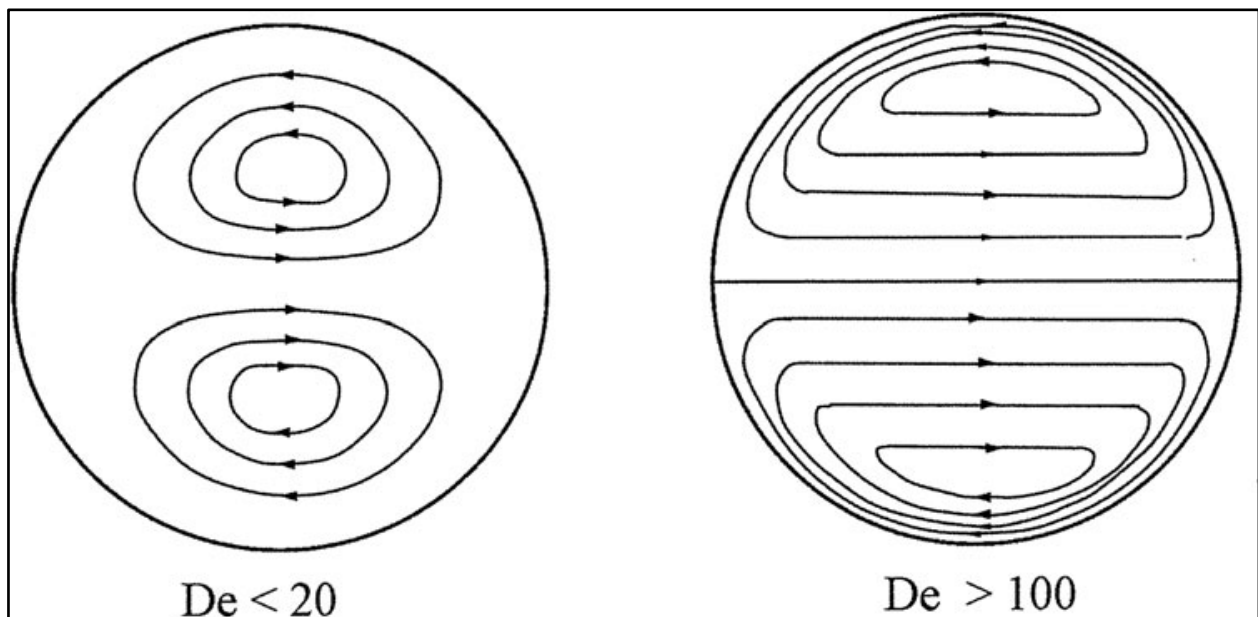
Figure 1.4: Secondary flow areas at low and high Dean Numbers [19].

So, to achieve the maximum thermal exchange in a minimum volume, the ratio of heat exchanger surface area (A_s) to its volume (V) that called area dencity (β) ,should be over($\beta > 700 \ m^2/m^3$) to form a compact heat exchanger [20]. Therefore, the choice usually fell out on coiled tube heat exchangers to achieve the maximum thermal exchange. since the coil tube is compact; therefore, it requires a smaller space. In addition, it is easy to produce, can operate at high pressure, and is suitable for use under conditions of laminar flow or low flow rates on the shell side. Thus, these heat exchangers can often be very cost-effective [21]. Consequently, the focus has begun to enhance further the thermal performance of the helical coiled tube heat exchangers using the different techniques mentioned above.

1.4 Heat Transfer Enhancement by Air Bubbles Injection into Shell Side of Heat Exchanger:

Any desire to improve the heat exchangers thermal performance leads to additional pressure drops, costs, electricity, material, and weight. For example, the turbulators mentioned above are significantly increased the pressure drop along with the heat exchangers. As a result, any attempt to minimize the pressure drop will reduce the increment of heat transfer. Therefore, experts are still looking for a technique that can improve the thermal performance of heat exchangers with a minimum possible pressure drop [20].

Some researchers have investigated sub-millimeter air bubble injection, such as **kitagawa et al. [22]**, as a heat transfer amplification technique for natural convection of static fluids. Several academic experiments have been conducted to explain bubbles fluid-dynamic behavior within liquids **Sadighi et al. [23]** recently suggested the direct application of tiny air bubbles to improve heat exchangers thermal characteristics. Air injection into any liquid contributes to the formation of air bubbles within the fluid. The quantity, shape, distribution, and scale of these air bubbles depend on the method used for air injection. As air bubbles are formed, they tend to float vertically through the liquid due to buoyancy. Air bubbles normal behavior will increase turbulence and break the boundary layer of fluid flow. Thus, tiny air bubbles vertical movement and stability can be used as an appropriate, efficient technique to increase heat exchangers thermal performance [24]. Fig 1.4 clearly describes the injection of air bubbles in a vertical shell and a coiled tube heat exchanger.
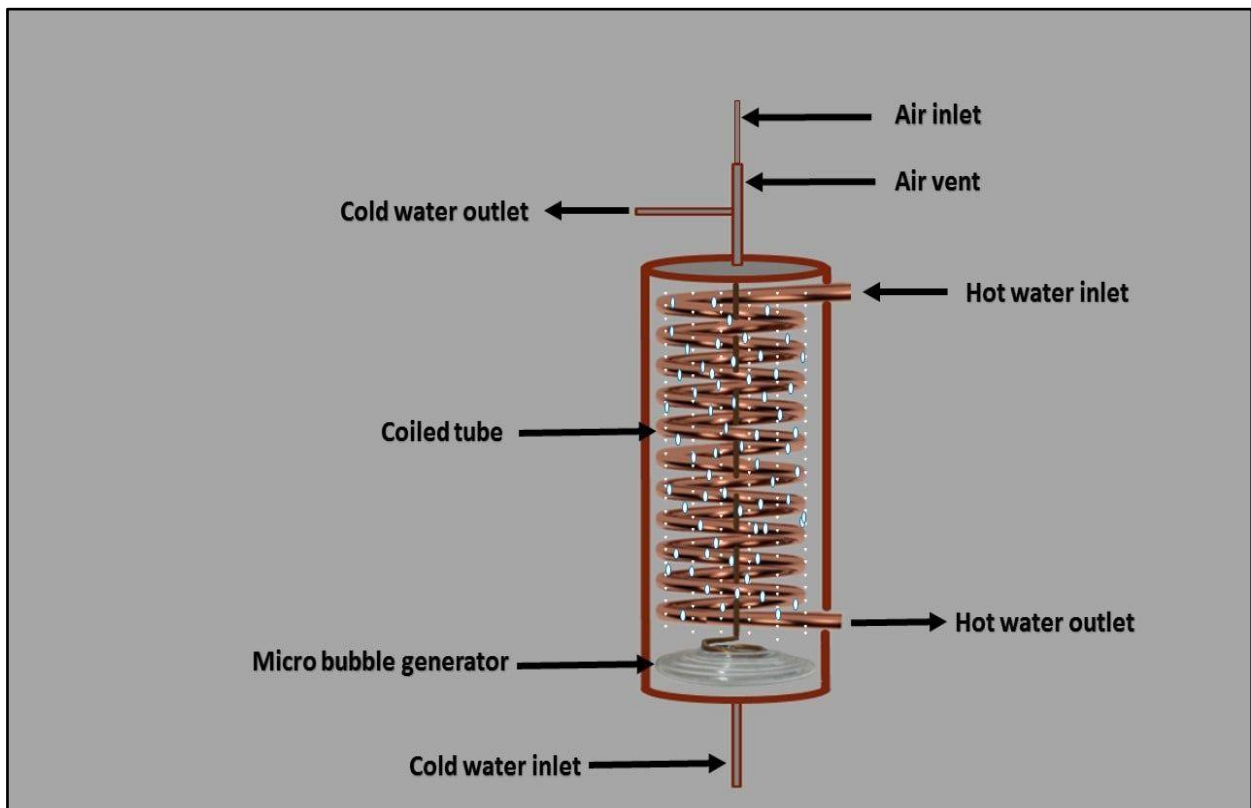
Figure 1.5: General view for a vertical shell and helically coiled tube heat exchanger with air bubble injection method.

1.5 Research Problem And Objectives Of The Thesis

According to the literature review, it has been seen that limited studies have been published on air injection as an enhancement technique. Besides, the previous experiments concentrated on a narrow variety of operational conditions, which are insufficient to explain the process by which the bubbles caused the improvement. However, the present work may be adopted as an expansion of the work in question on this methodology and to fill a void that exists in the literature with the following points:

1. Proposed a new strategy for injection air bubbles (plastic-spiral shape tube with 1400 holes per meter and three different diameters to explain the effect of bubble diameter on the thermal performance of heat exchangers.

2. Investigate the effect of injected air bubbles on the thermal performance of four shells and helically coiled tube heat exchange.

➤ Smooth coiled tube heat exchange.

➤ Finned Coiled tube with 5 mm pitch heat exchange.

➤ Finned Coiled tube with 8 mm pitch heat exchange.

➤ Finned Coiled tube with 10 mm pitch heat exchange.

3. Investigate a wide range of parameters that were non-investigated from before, such as different airflow rates with different pressure.

4. study the influence of variation in the injected air flow rate, air pressure, pitch of spiral fins, and bubble diameter on the thermal performance of a shell and helically coiled smooth and (internally – externally) finned tube heat exchanger.

5. Different heat transfer parameters are calculated depending on the measurement; these include:

➤ Overall heat transfer Coefficient.
➤ Effectiveness.
➤ The temperature distribution along with the heat exchanger height.
➤ The increment of the pressure drop is due to the air injection.

To achieved these objectives, an appropriate experimental set-up was designed and manufactured especially for this experimental study and equipped with the necessary measurement instruments for pressure, temperature, and flow rates.

1.6 Thesis Outline

The present thesis is divided into five chapters and four appendixes, as flowing:

➢ The current chapter [chapter one] is a general introduction to heat exchanger enhancement techniques, helically coiled (smooth and finned) tube heat exchangers, fluid flow mechanism inside the coiled tube, and finally, the air bubble injection technique.

➢ Chapter two presents a review of the literature that is relevant to the topic of the present thesis. These studies include the most popular enhancement techniques of the shell and helically coiled tube heat exchanger in chronological order. These include the surface modification technique, compound enhancement techniques, and more recent air bubble injection techniques.

➢ Chapter three describes the experimental work. A description of the experimental apparatus used to investigate the effect of air bubbles injection on heat transfer characteristics of the vertical shell and helical coiled (smooth and finned) tube heat exchanger is given. The procedure of the experiments performed and the physical properties of the working fluid are outlined in chapter three.

➢ Chapter four presents the discussion of the experimental results obtained for various parameters at different operational conditions.

➢ Chapter five is about the conclusions obtained from the experimental study and provides some recommendations for future work.

Chapter Two

Literature Review

CHAPTER TWO

LITERATURE REVIEW

INTRODUCTION

More recently, air bubble injection has been suggested as one of the promising enhancement methods of heat exchanger thermal performance**.**Upon air injected into a liquid, an air bubble will form within the liquid. However, these bubble's number, shape, size, and distribution rely on the injection technique and the fluid's properties. Once the bubbles form in the liquid, naturally, they float and move upward due to the buoyancy force, which initiates by the difference in the densities of the liquid and air. This random motion of bubbles will mix the liquid bulk and break down the hydrodynamic and thermal boundary layers, enhancing heat exchange in thermal systems, such as heat exchangers. However, the mixing level depends on many factors, such as the air bubbles flow rate, number of bubbles, size of bubbles, and heat exchanger design **[23-28]**

This chapter provides a review of the studies on a shell and helically coiled tube heat exchangers to improve their thermal performance through the use of heat transfer enhancement strategies (passive, active, and compound), with an emphasis on the air bubbles injection technique and helical fins coil as the topic of the current thesis.

2.1 Geometrical Surfaces Modification Techniques of Heat Exchanger

Manipulating the surface geometries of the coiled-tube heat exchanger such as curvature ratio, coil spacing and other dimensions are passive reinforcement techniques. In this context, **Kahani et al. [29]** Experimentally studied the effect of curvature ratio and coil spacing on heat transfer performance and pressure drop of a

coil heat exchanger operating under laminar flow conditions. The results confirmed a significant improvement in the heat transfer rate associated with the higher pressure drop in the helical coil than the straight tube. Moreover, the results showed that the heat transfer rate was enhanced by increasing the coil temperature and decreasing the bending ratio.

Austen and Soliman [30] investigated the influence of the coil pitch on the pressure drop experimentally, and the heat transfer rate of helical coil heat exchangers operates under uniform heat flux. Two pairs of coils were tested; each pair corresponds to the same diametric ratio but a substantially different pitch ratio. The working fluid was water. The results showed that the pitch was significantly affected the heat transfer rate at low Reynolds numbers. In order to increase the turbulent level of fluid flows in a helically coiled tube, **Yildiz et al. [31]** placed spring-shaped wires with different pitches inside the helically coiled tube and studied the influence of this mechanism on the heat transfer and pressure drop of the shell and helical pipe heat exchanger experimentally. The results demonstrated that the best increment in the heat transfer rate was with the smallest pitch/wire diameter ratio since it was accounted as much as five times compared to an empty pipe for the same Dean number. Although the inlet/outlet pressure drop was raised to 10 times with respect to the conventional empty helical case, the increase in Nusselt number reflects an increase of the effectiveness of the helically coiled tube heat exchanger by 30 %. Heat transfer coefficients for three different shell and helically coiled tube heat exchangers with different coil pitches and curvature ratios were investigated experimentally by **Shokouhmand and Salimpour [32]**. The results showed that the shell side heat transfer coefficient enhances with increasing coil pitch. Moreover, the results confirmed that the overall heat transfer coefficient in the counter flow was 40% more than those in parallel flow.Finally, **Jamshidi et al. [33]** experimentally studied the effects of geometrical parameters and fluid flow on the heat transfer rate in the shell and coil heat exchangers. Results showed that the larger coil diameter,

coil pitch, and mass flow rate could improve the heat transfer rate in these types of heat exchangers.

2.2 Finning Surface of helical coil heat exchanger

Tubes can be finned on both the interior and exterior. This is probably the oldest form of heat transfer enhancement. Finning is usually desirable when the fluid has a relatively low heat transfer film coefficient, as does a gas. The fin increases the film coefficient with added turbulence and increases the heat transfer surface area. This added performance results in a higher pressure drop. Recent papers also describe predicting finned tube performance[34].

LI Ya-xia et al. [35] used numerical simulation to evaluate the turbulent flow and temperature fields in helical tubes cooperating with spiral corrugation, as seen in Fig 2.1. In addition, the flow and heat transfer effects of spiral corrugation parameters and Reynolds number were investigated.
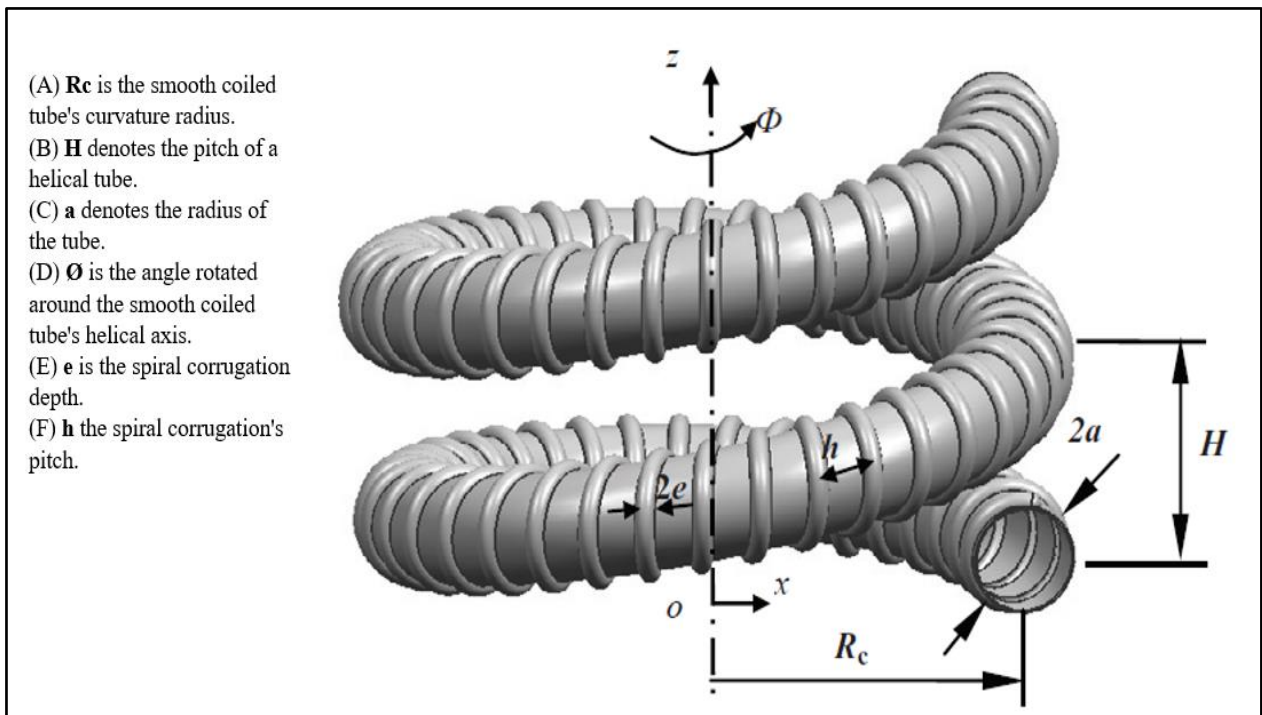
Figure 2.2: helical tube cooperating with spiral corrugation [35].

The findings showed that spiral corrugation could increase heat transfer in a smooth helical tube due to the additional swirling motion. In addition, the reduced

pitch of spiral corrugation will improve heat transfer in the tube due to increase secondary flow inside coil tube.Under the reporting framework, helical tubes cooperating with spiral corrugation improve heat transfer by 50-80 % while growing flow resistance by 50-300 % over smooth helical tubes.

Sivalakshmi et al. [36] studied the effect of helical fins on a double pipe heat exchanger's performance experimentally. The performance of a heat exchanger in a straight inner pipe in terms of average heat transfer rate, heat transfer coefficient, and effectiveness were analyzed and compared to a heat exchanger with helical fins mounted over the inner pipe, as shown in fig 2.2.

Figure 2.3: straight tube with Helical fins **[36]**.

The research shows that the addition of fins boosts the heat transfer coefficient. At higher flow rates, the average heat transfer rate and the heat exchangers effectiveness rise 38.46 % and 35 %, respectively.

2.3 Enhancement Heat Transfer of Heat Exchangers By Compound Methods Techniques

Several reports have discussed the use of combined enhancement, including both the effects of passive and active methods. However, the combination of passive methods is somewhat limited, with the most common being internal and external finned tubes. Other combinations may be nearly impossible because of the manufacturing techniques used in modifying the tube geometry **[37]**.

The most common passive techniques for improving heat transfer in tubes are rough surfaces, displaced enhancement systems, swirl-flow devices, curved geometries, spiral fins, and flow additives **[37-38]**. These techniques are typically used individually, although it is well understood that in some situations, two or three of the existing methods may be used concurrently to achieve an enhancement more significant than that achieved by using only one technique **[37]**.

Multiple compound techniques have been investigated to evaluate under what conditions can achieve an enhancement more significant than that provided by a single technique. For example, the helical coiling improves when the fluid experiences a centrifugal force, forcing fluid from the core region towards the outer wall and thinning the boundary layers **[39]**. The improvement effect associated with the walls (corrugation, fins, grooves, etc.) is due to the disruption of the growth of the boundary layers, an increase in heat transfer field, the production of swirling or secondary flows **[40]**.

Solano et al. [41] studied the thermal-hydraulic behavior of three types of improvement techniques based on artificial roughness: corrugated tubes, dimpled tubes, and wire coils, as shown in Fig 2.3. The comparison was carried out using the three best samples from the authors various geometries in previous works **[42]**.

p corrugation pitch.
h corrugation height.
p dimple pitch.
a length between dimples.
h dimple height
e diameter wire

a Wire Coil Insert

b Corrugated Tube

c Dimpled Tube
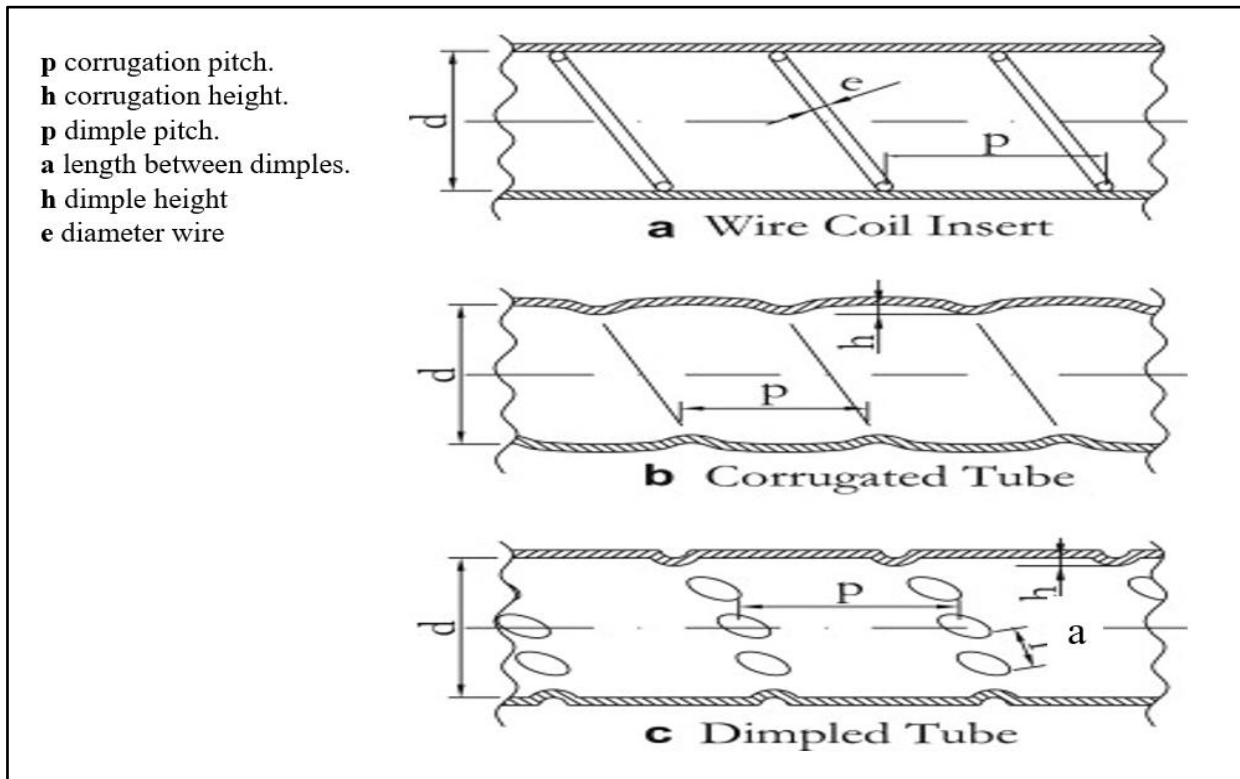
Figure 2.4: illustrates the different forms of surface roughness considered in this article **[41]**.

The findings demonstrated that artificial roughness has a more significant effect on pressure drop characteristics than heat transfer enhancement. Likewise, this shape strongly affects the advance of the transition to turbulence and its characteristics: smooth or sudden. According to the study, smooth tubes are recommended for Reynolds numbers less than 200. Wire coils are more advantageous for Reynolds numbers between 200 and 2000, while corrugated and dimpled tubes are preferred over wire coils for Reynolds numbers greater than 2000 due to lower pressure drop for equivalent heat transfer coefficient values.

Mehdi et al. [44] investigate the thermal performance of a helical shell and tube heat exchanger numerically without a fin, with circular fins, and with cut (V-shaped) circular fins (at an angle of 15°) attached to the coil, as shown in fig 2.4.
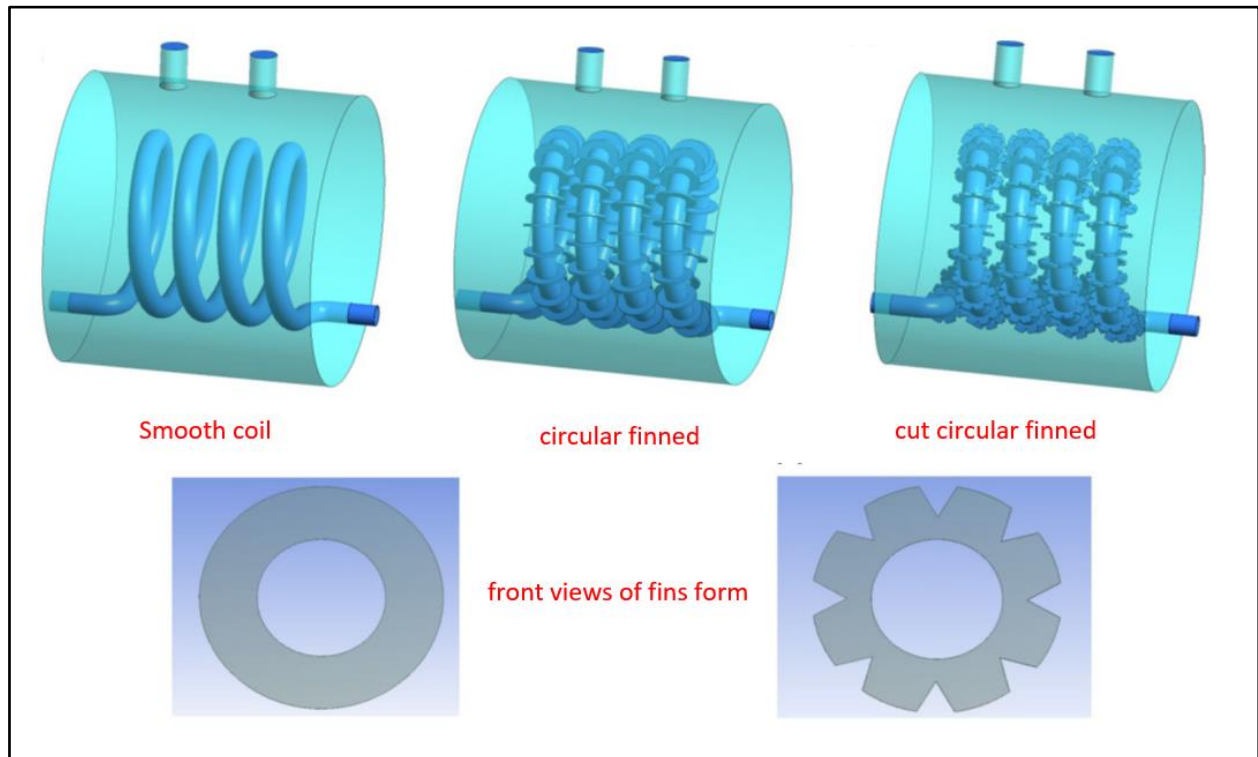
Figure 2.4: Diagram of the research geometry **[44]**.

The extracted results demonstrated that heat transfer increases in both simple and circular finned heat exchangers where the fluid velocity (both hot and cold) on the shell side is greater than the fluid velocity (both hot and cold) on the tube side. Finally, it is discovered that the results of cut circular fins on the helical shell and tube heat exchanger performance and heat transfer are minimal compared to the circular fins.

2.4 Enhancement Heat Transfer By Injection Air Bubbles of Heat Exchanger

Several academic studies have been conducted to understand the dynamic behaviour of bubbles within liquids. New strategies have been proposed to inject tiny air bubbles to improve heat exchangers thermal characteristics. The value of the airflow rate introduced into the heat exchanger is essential for improving the heat transfer phenomena in a heat exchanger. The higher the airflow rate (Q_a), we get the higher enhancement ratio due to increased (Re) and mix levels inside the shell. However, this dependency could be affected in some cases when the airflow rate reaches a specific value **[45-46]**.In this case, it can act as an insulator around the tubes due to the low air thermal conductivity. It is, therefore, necessary to produce a specific number of air bubbles of a specific size. The main achievements of improved heat exchangers by injection of air bubble heat exchangers are summarized as follows.

For the first time, the sub-millimeter air bubbles injection technique was suggested by **Dizaji et al. [23]** to improve the thermal performance of a shell and helically coiled tube heat exchanger in which a liquid (especially water) was used as a working fluid. However, they studied the influence of air bubbles injection on the number of thermal units (NTU) and effectiveness (ε) of the vertical shell and coiled tube heat exchanger's effectiveness.

The experiments were carried out with a volumetric flow rate and a steady temperature of the hot water (coiled side) of 3.8 LPM and 40 ^{o}C, respectively. The mass flow rates range was from 5 to 15 LPM, and the inlet temperature of cold water (shell side) was kept constant at 12 ^{o}C. The experiments were carried out with different air bubble injection conditions at a steady air flow rate of 1 LPM. The experimental setup and air injection process are depicted in Fig 2.5 and 2.6, respectively.
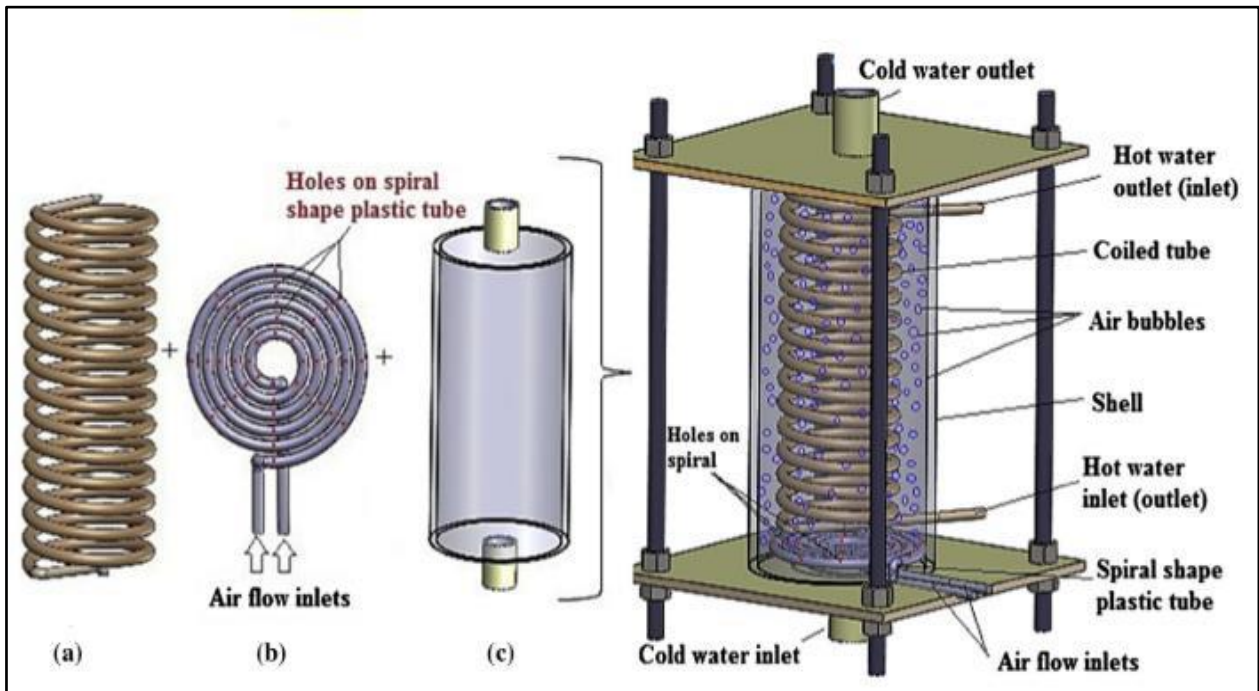
Figure 2.5: A general view of the test section, which contains the air bubble injection process **[23]**.
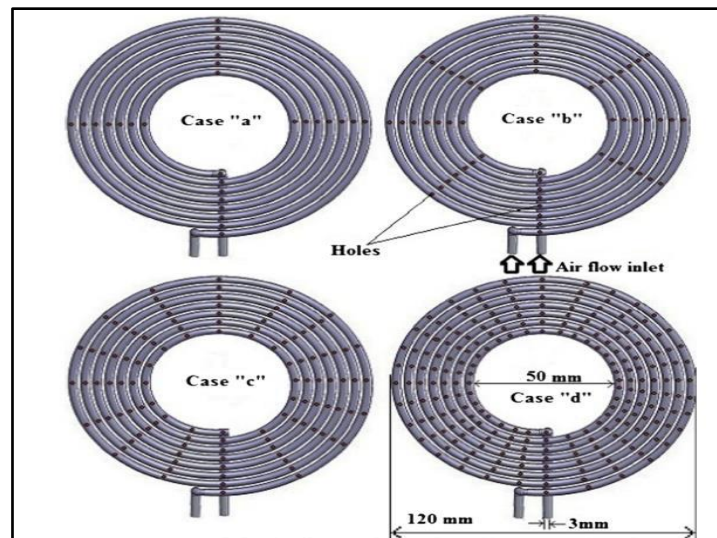
Figure 2.6: A general view of different number and hole locations on the air injection process **[23]**.

The findings showed that the number of thermal transfer units (NTU) and effectiveness were increased dramatically due to the air bubbles injection. The most significant improvement was achieved in case "d" Fig 2.6. Depending on the air injection state and cold-water mass flow rate (shell side), the NTU increased was

found to be up to 1.5–4.2 times, and the effectiveness increased 1.36–2.44 times compared to the case of no air bubbles injection (only water). Their experimental results concluded that the ratio (n/d) (the number of holes to the hole diameter) was the most influential parameter. The greater amount of (n/d), the more significant enhancement was.

The air injection technique's positive role on the helical coiled tube heat exchanger's thermal performance has encouraged researchers to examine it in other heat exchanger types. In this context, **Dizaji et al. [47]** clarify the effect of air bubbles injection on heat transfer rate, NTU, and effectiveness in a horizontal double pipe heat exchanger experimentally. The air injection method was based on creating tiny holes on a plastic tube to generate air bubbles along with the heat exchanger, as illustrated in Fig. 2.7. The mass flow rate and the inlet temperate of air through the plastic tube were 0.098×10^{-3} kg/s and 26°C, respectively. The flow rate and inlet temperature of cold water (outer pipe) were constant at 0.083 kg/s (Re=4000) and 25°C, respectively. Hot water (inner pipe) inlet temperature was kept constant at 40°C with mass flow rate variant from 0.0831 kg/s to 0.2495 kg/s (Re =5000 ~ 16000).
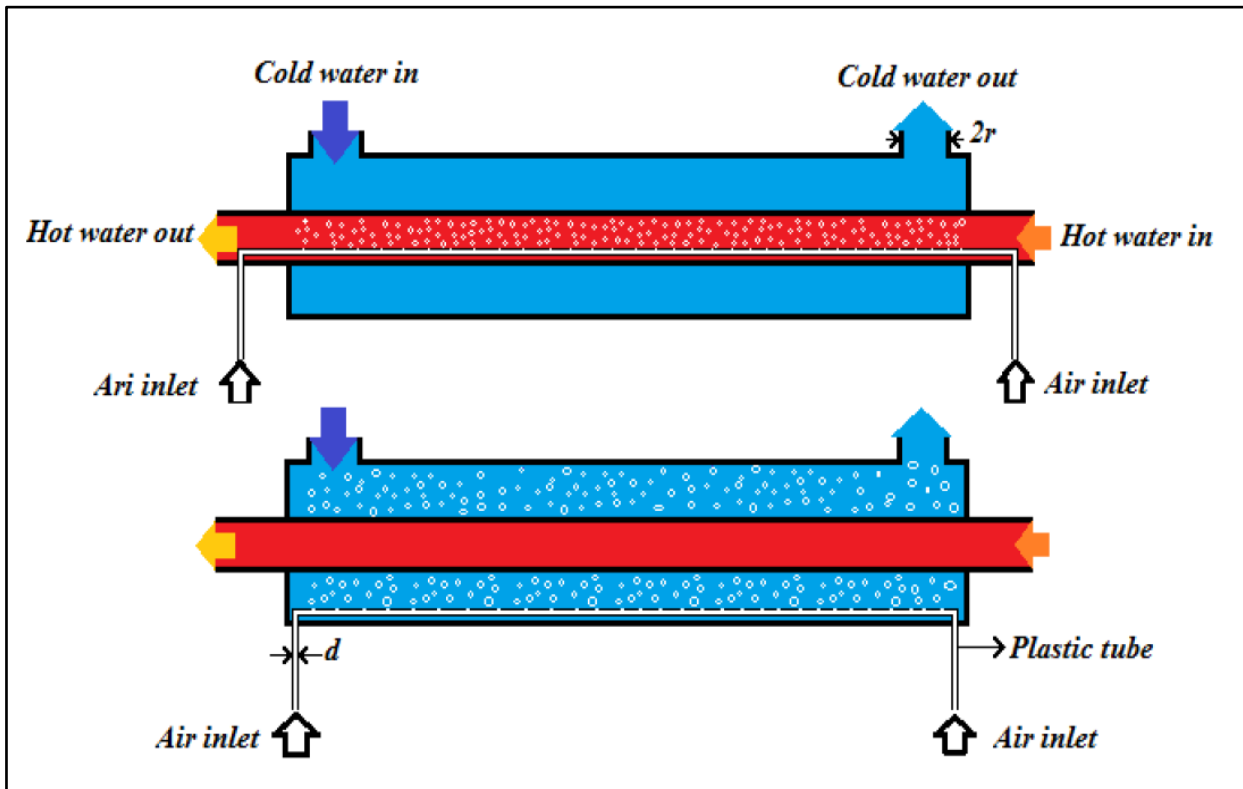
Figure 2.7: General view of air bubble injection methods **[47]**.

The results revealed that the Nusselt number was improved by about 6% - 35% based on the air injection conditions and Reynolds number of the shell side, and the effectiveness of the heat exchanger was increased by about 10% - 40%. Furthermore, the maximum effectiveness was achieved when air bubbles were injected into the annular space. Consequently, they concluded that the ratio of (n/d) is an essential parameter.

Moosavi et al. [24] proposed a steadily increasing airflow rate from 1 to 5 LPM to examine the effect on the thermal performance and pressure drop of a vertical shell and helically coiled tube heat exchanger. They used the same experimental set-up as **[47],**and **[23]** but with different operating parameters. Their results reveal that the airflow rate significantly impacts heat transfer enhancement in the heat exchanger. They discovered that increasing the airflow rate increased the overall heat transfer coefficient. Furthermore, their findings revealed that increasing the flow rate of air pumped into the shell side of the heat exchanger increased the overall heat

transfer coefficient by around 6-187 %. Depending on the shell side's water and airflow concentrations, the pressure drop increment ranged from 13% to 225 %.

Khorasani and Dadvand [48] used an injection mechanism to injection air bubbles into the horizontal shell and the helical coil heat exchanger in both (parallel flow and counter-flow) situations, as shown in Fig 2.8. Numerous airflow rates (1-5 LPM) and various shell-side water flow rates (1-5 LPM) have demonstrated that the NTU rises by (1.3–4.3) times by injecting air bubbles, with the most drastic increase occurring in the counter-flow case. It was also found that the maximum effectiveness value of 0.815 could be reached in the counter-flow situation.
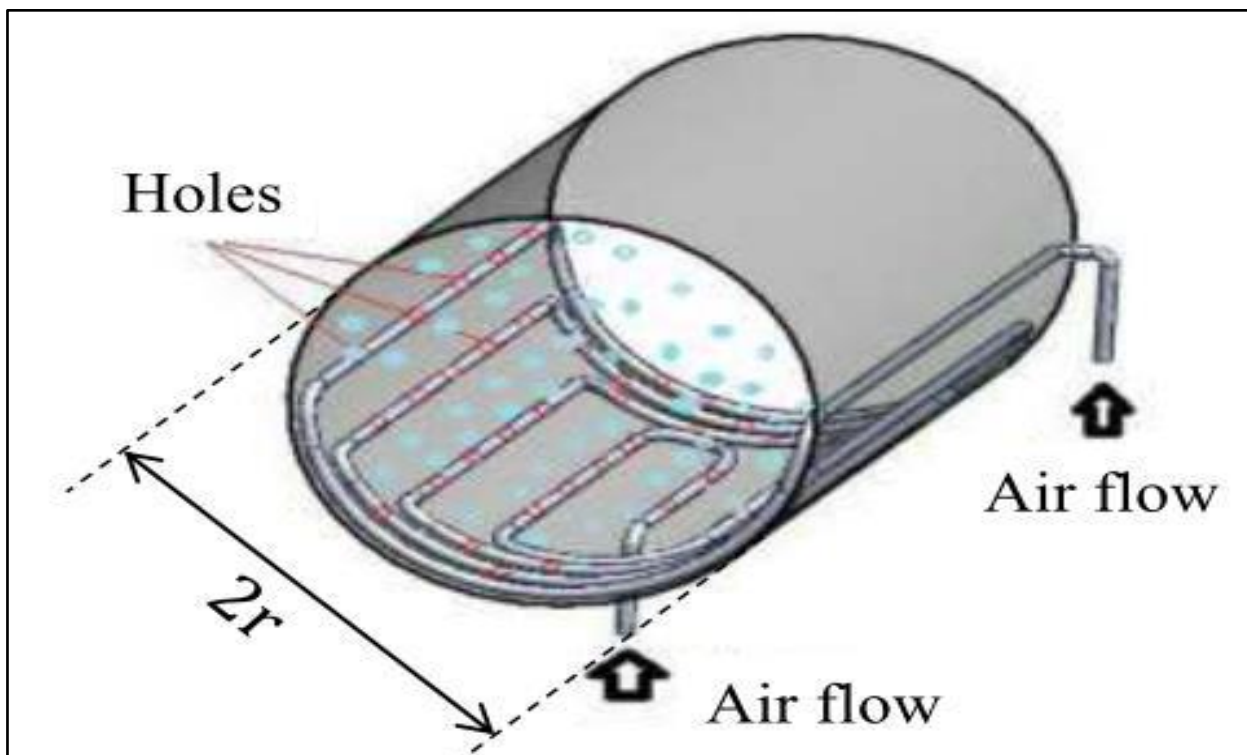
Figure 2.8: Schematic of shell and air bubbles injection mechanism **[48]**.

Heat transfer performance was carried out experimentally by **Nandan and Singh [49]** with various air injection sites. Four separate cases with and without air injection in the shell or tube side were considered, and the effects were compared. The study discovered that inserting air bubbles in the tube increases the heat transfer

rate by 25-40% at various Reynolds Number ranges. Furthermore, the air injection at various points also impacts on overall heat transfer coefficient.

El-Said and Alsood [50] have tested the possibility of enhancing the thermal performance of many tube heat exchangers by pumping the air as tiny bubbles using a cross-flow and parallel flow air injection technique, as illustrated in Fig 2.9. The air and shell side water flow rates were changed between 1 and 5 LPM and 12–21 LPM, respectively, with a constant tube side water flow rate.
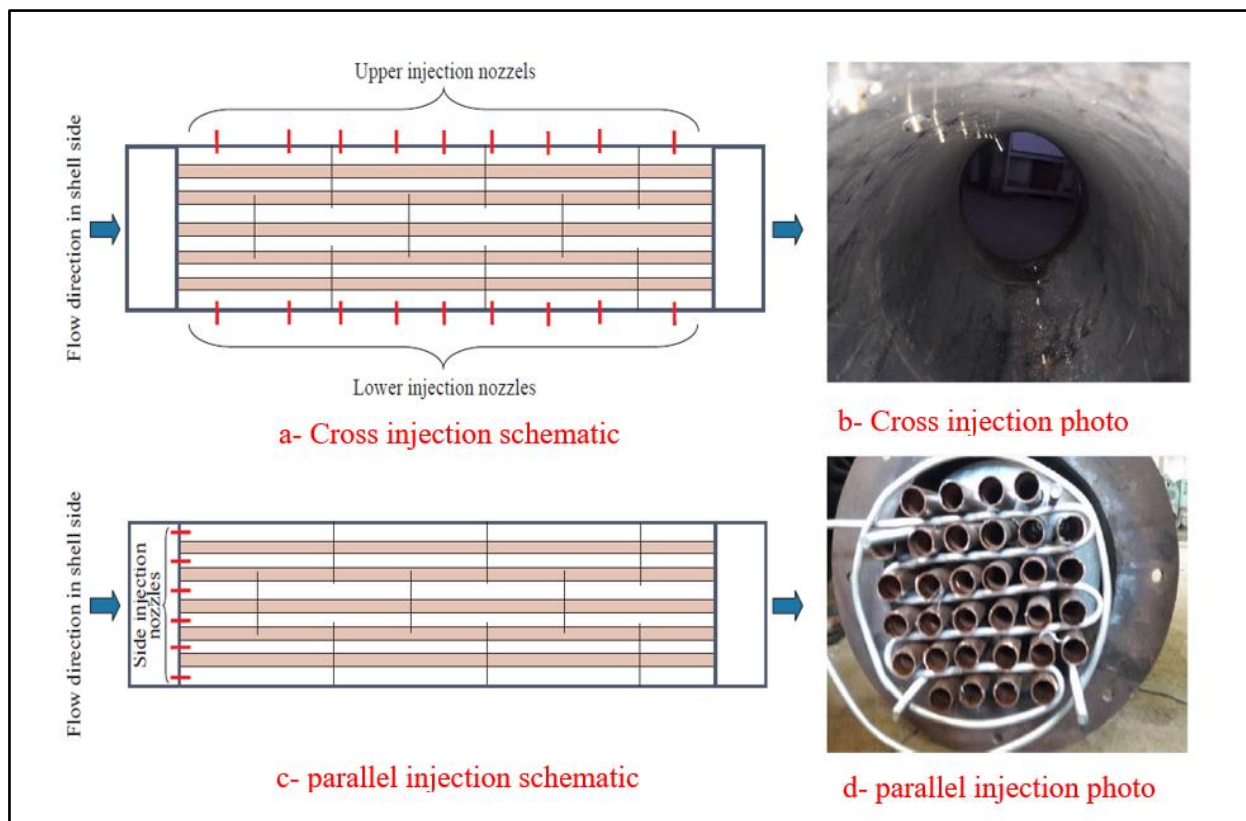
Figure 2.9: Injection holes layout **[50]**.

The study showed that the air bubble injection was significantly improved the heat exchangers performance and that the cross-flow injection method had a more significant benefit. Indeed, the augmentation on the U caused by cross-air injection into the heat exchanger shell was 131–176%, depending on air and shell side water flow rates. **Baqer et al. [51]** also examined the optimal operating conditions of injecting a sub-millimeter air bubble into the coil tube heat exchanger's shell side. The implemented shell-side flow, airflow, and coil-side flow rates were changed

from 2 LPM to 10 LPM, from 0 to 10 LPM, and 1 LPM to 2 LPM, respectively, with three temperature differences (20°C, 30°C, and 36°C). The results showed that the most effective shell-side flow rate was 6 LPM, and the effect of the air flow rate was more significant when it had a value greater than 6 LPM. The maximum augmentation in the NTU and the effectiveness were 1.93 and 0.83, correspondingly, while the minimum value of the NTU and the effectiveness were 0.66 and 0.63, respectively.Additional the experimental data showed that the temperature difference has a slight effect on the effectiveness, especially when the air flow rate over 6 LPM. . **Kreem et al. [52]** studied influence of tiny air bubbles injection on temperature distribution along a vertical shell and helical coiled tube of heat exchanger,indeed observed an intimate thermal mixing of bubbles in the heat exchanger shell and proposed that could be the main reason for improving the thermal performance ,through ahigh heat transfer was recorded and indicated by the sudden rasing of the temperature along the heat exchanger.furthermore,steady state can be achived faster as void fraction range is increased.

Subesh et al. [53] test two different air bubble injection techniques (parallel and cross-flow) on the shell side and heat exchanger tube by an applied wide range of injected airflow and cold water (1 to 6 LPM of airflow rates and 10 to 20 LPM shell side water flow rates with constant tube side hot water flow rate 1 LPM). They observed that the results of cross-injection of ε, NTU, and U of the heat exchanger were more significant than the parallel injection method for all experimental conditions. Furthermore, the pressure loss in the cross-injection method was higher than in the shell-side parallel injection method. **Ghashim et al. [54]** have been experimentally tested the effect of the injection of tiny air bubbles into the heat transfer and pressure drop of the helically coiled tube heat exchanger operating under turbulent flow conditions. The airflow rate was 1.5, 2.5, and 3.5 LPM, the constant mass flow rate of cold water 0.0331 kg/s, and the hot fluid (Re) were between 9000 and 50000. Research shows that the air injected led to a 64 – 126 % rise in Nu and

raised the pressure drop from 66 – 85 % for the entire range (Re) tested. **Sokhal et al. [55]** evaluate the thermal performance of a shell-and-tube heat exchanger with a new technique called air bubble injection. The study has been carried out with different parameters such as flow rate, fluid inlet temperature, and air injection techniques. The air has been injected at different locations such as the inlet of pipe, throughout the pipe, and in the outer pipe of the heat exchanger. The authors found that the increase of the air bubble flow rates increased the heat exchanger's performance, Contrary to no bubble injection.

Panahi [56] explored the influence of air bubble injection on the Nusselt number Nu during forced convection and the effectiveness of vertical shell and helically coiled tube heat exchanger. The tests were carried out using the same set-up and operating parameters of Dizaji et al. **[47]**. The study found that injecting air bubbles into the shell side improved Nusselt number (Nu) and effectiveness by 50 – 328 % and 53 – 127 %, respectively.

In internal combustion engines, energy conservation and thermal management play a significant role in overall performance, affecting engine exhaust emissions and total fuel consumption. As a result, **Zavaragh et al. [57]** optimized the heat transfer and exhaust emission experimentally by using air bubbles injection within the engine cooling system (water jackets) as a new method to increase cooling system output. The air injection technique has two significant benefits. In the warming state, air injection into the coolant fluid causes the engine components to heat up faster by forming air layers (heat insulation layer) around the cylinder. In the cooling condition, air injection is restricted to a certain degree to generate turbulence flow, which increases heat transfer by mixing boundary layers. The analysis indicated that injecting air bubbles regularly using the proper procedure would decrease fuel consumption by approximately 5.69 % while lowering engine pollutant emissions by approximately 16.93 %.

Pourhedayat et al. [58] studied the effect of air bubble injection on dimensionless exergy destruction, NTU, and the effectiveness of a vertical double-pipe heat exchanger experimentally. Since each type of heat exchanger needs a different injection system based on the heat exchanger configuration, the technique used here is to produce air bubbles by drilling small holes in a ring tube of varying amounts and diameter mounted in the annular space of the heat exchanger, as seen in Fig 2.10. The study was conducted out with hot water inlet temperature r of 40°C and constant Reynolds number (Re=5500 based on water flow rate), and cold-water inlet temperature and Reynolds number of 25°C with 5000 < Re < 16000, respectively. To inject air into both sides of the ring tube, an aquarium air pump was used.
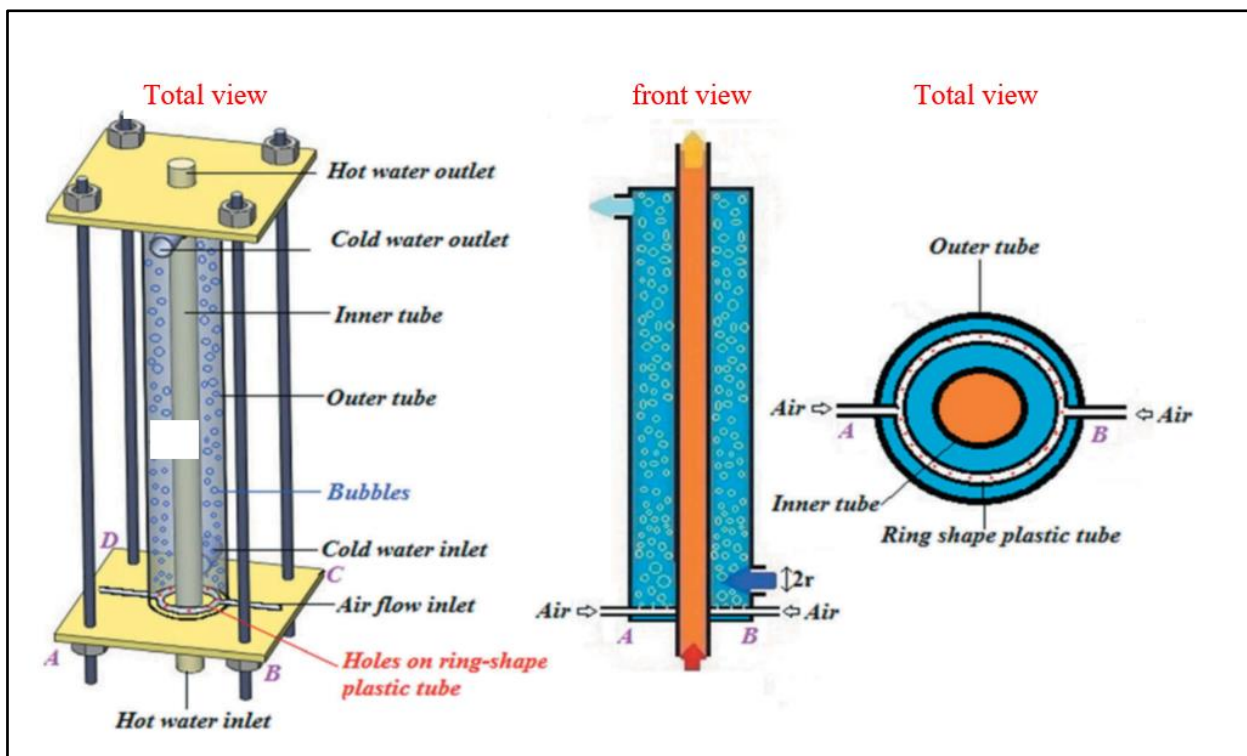
Figure 2.5: Test section and injection method **[58]**.

The results demonstrated that the injected bubbles cause additional exergy destruction, which is natural. However, the exergy destruction by bubbles was less than that of other hard turbulators that function as a wall against flow movement. With n=36 and d=0.3, the Nusselt number (Nu), dimensionless exergy destruction,

and effectiveness were improved by around 57 %, 30 %, and 45 %, respectively. The skilled construction of perforations on a plastic tube and the logical selection of their number and diameter will improve the performance of heat exchangers.

Finally, **Shukla and Yadav [59]** investigated the impact of air bubble diameter on the effectiveness, NTU, and overall heat transfer coefficient numerically of shell and helical coil heat exchangers using ANYSYS FLUENT 14.5 CFD software. Five different air bubble diameters (0.05, 0.1, 0.3, 0.5 and 0.7 mm) were tested. The CFD results revealed that air bubbles with a diameter of 0.7mm have the greatest heat transfer. Furthermore, the greatest increases in NTU, overall heat transfer coefficient, and effectiveness were 1.39, 1327, and 0.74, respectively.

Table 2.1: Summary of Important Investigations of literature review.

Authors	Year	Fluid	Type of investigation	method	Observation	results
Dizaji **[23]**	2015	water	experimentally	Injection air bubbles via plastic sparger inside vertical shell and helical coil of heat exchanger.	-number of holes (28-224). -diameter of bubbles (0.3mm). -both the parallel and counter flow were investigation.	- NTU/NTUa (1.5-4.2). - ε/εa (1.36-2.44).
Dizaji **[47]**	2016	water	experimentally	Injection air bubbles inside horizontal shell and helical coiled tube heat exchanger by two positions inside (tube and shell).	-diameter of holes (0.3 and 0.7mm). -number of holes (40-80). -counter flow. -maximum ε occur when air injection inside annular space.	-NU (6%-35%). -ε (10%-40%).
Nandan **[49]**	2016	water	experimentally	Injection air bubbles at (tube entrance, shell entrance, and throughout the tube section.	-heat transfer coefficient (h) increased with increased Re (6600-23000), where h is a function of Re.	-NU (15%-20%) when air injection at shell entrance. -NU (20%-35%) when air injection at tube entrance. NU (30%-45%) when air injection throughout the tube section.
Moosavi **[24]**	2016	water	Experimentally	Injection air bubbles into: -helical coil. -vertical shell.	-number of holes (224). -diameter of bubbles (0.3mm).	-maximum enhancement occur in case air injection to shell. -ε (3%-56%), and U (6%-187%). -ΔP coil (49%-370%), and ΔP shell (13%-225%).
khorasan **[48]**	2017	water	experimentally	Injection air bubbles via new method (plastic tube beside outer wall of shell).	-number of holes unknown. -diameter of holes (0.3mm). -counter and parallel flow.	-NTU (1.3-4.3), counter flow, Qs=1 Lpm, and Qa=5 Lpm. -ε max (0.815), counter flow, Qs=5Lpm, Qa=5Lpm.
Alsaid **[50]**	2018	water	experimentally	Injection air bubbles in parallel and cross flow into shell side and multi tube heat exchanger with baffles.	-for cross injection use 18 nozzle with diameter 0.7mm. -for parallel injection use bending tube with diameter holes (0.7mm).	-for cross flow ΔPmax (54.2mmbar), and for parallel flow ΔPmax (45.2 mmbar), -for crossflow U (131%-176%), ε (136%-173%).

Authors	Year	Fluid	Type of investigation	method	Observation	results
Ahmed [51]	2019	water	experimentally	Injection air bubbles via porous sparger inside vertical shell and helical coil tube of heat exchanger in parallel with cold water flow.	-unknown number of holes. -assume 100µ diameter of bubbles. - counter flow were investigation.	- Max NTU (1.93), and ε (0.83). - Min NTU (0.66), and ε (0.63).
Kareem [47]	2019	water	experimentally	Injection air bubbles via porous sparger inside vertical shell and helical coil tube of heat exchanger in parallel with cold water flow.	Study the influence of injection air bubbles on temperature distribution along the vertical shell and helical coil tube heat exchanger.	-high heat transfer was recorded that indicated through sudden rising of the temperature along the heat exchanger. -the study state can be achieved faster as the (Vd) increased.
Panahi [56]	2017	water	experimentally	Injection air bubbles inside vertical shell and helical coiled tube heat, and experiments were performed for both parallel- and counter-flow configurations.	-number of holes (28,56,112, and 224). -diameter of bubbles (0.3mm). -Re (1000-4000).	-NU (50%-328%), and ε (53%-127%) in counter flow.
zavaragh [57]	2017	water	Experimentally	Injection air bubbles inside water jacket of engine.	Air injection inside water jacket has two significant advantages: a- in warm up stage, air bubbles cause rapid heating of engine components. b- In cooling stage will generate vortices that will destroy boundary layer to decrease heat resistance, whereas increase heat transfer rate.	The fuel consumption will decrease by approximately 5.69%, while engine pollutant emission lowering to approximately 16.93.
shukla [59]	2019	water	numerically	Using ANYSYS FLUENT 14.5 CFD software.	Five different air bubble diameters (0.05,0.1,0.3,0.5, and 0.7mm) were tested.	-The air bubbles with diameter 0.7mm have the greatest heat transfer rate. -Maximum NTU 1.39, U 1327, and ε 0.74.

30

Authors	Year	Fluid	Type of investigation	method	Observation	results
Li Ya [35]	2012	water	numerically	using helical coil tube cooperating with spiral corrugation and studied effect on heat transfer rate.	-using different spiral pitch.	-finding showed that, decreasing spiral pitch will increase heat transfer, and increasing pressure drop. -heat transfer rate (50%-80%), pressure drop (50%-300%).
sivala [36]	2021	water	experimentally	Using helical fin over the inner pipe of double pipe heat exchanger.	-compare the thermal performance of smooth tube heat exchanger with finned tube heat exchanger.	-the heat transfer rate enhancement (38.46%), and effectiveness (35%) at higher flow rate.
Solano [41]	2012	water	experimentally	Using corrugated tube, dimpled tube, and wire coils to study the effect of artificial roughness on thermal performance of heat exchanger.	the comparison was carried out using the three best samples from the various geometries in previous work [41].	Results show that the shape of the artificial roughness exerts a greater influence on the pressure drop characteristics than on the heat transfer augmentation.
Wongchar r [43]	2012	water	experimentally	Using Cuo/water nanofluid in corrugated tube fitted with twisted tape.	The nanofluid and twisted tape results are compared with those obtained from nanofluid alone and twisted tape alone.	The finding showed that the thermal performance associated with the combination of Cuo/water nanofluid and twisted tape were higher than those associated with the individual techniques under identical operating conditions.

2.5 Scope of The Present Work

From a survey of the literature, it can be summarized as follows:

1. According to the literature review, the air injection technique seems one of the most promising techniques for improving the thermal performance of a shell and helically coiled tube heat exchangers. Nonetheless, further laboratory experiments and theoretical (analytical, numerical) studies are needed to fully comprehend these essential enhancement techniques.

2. Hard turbulators enhancement techniques mentioned in the literature survey, such as wire coiled, twisted tape, corrugated tubes, wavy stripes, barbed wires, and springs, require additional materials, increasing the heat exchanger's cost, increased pressure drop, and weight.

3. There is a shortage of experimental data and designable correlations concerning the air injection method. However, investigate the effect of the inlet temperature difference between hot and cold fluid, the abundant numbers of tiny air bubbles rather than countable bubbles, the implementation of bubbles with micro-scale rather than the submillimeter scale on the thermal performance of the helically coiled tube heat exchanger are critical. In addition, studying the temperature distribution along the shell side and optimizing the shell side and air flow rates are essential for the heat exchanger working with this enhancement technique.

As clearly demonstrated by the literature review, although a relatively good number of studies have been carried out regarding the implementation of the air injection technique to enhance the thermal performance of heat exchangers, there was no attention focused on the injected air bubble diameter. therefore, the present study aims to fill this gap by investigating the effect of bubble diameter on the augmentation of the thermal performance of a vertical shell and helical coil (smooth and finned) tube heat exchanger. To do so, different operational conditions, such as

the shell side, coil side flow rates, and the injected air bubble diameters (0.1,0.8, and 1.5mm), were experimentally tested.

In addition to novelty in the current study by combining more than one improvement technique represented by using helical coil finned tubes with variable spiral pitch (pf) 5,8, and 10mm together with injection air bubble technique with variable bubble diameter 0.1,0.8, and 1.5mm, constant numbers of bubbles (1400) per meter, through studying its effect on improving heat transfer in heat exchangers.

Chapter Three

Experimental Work

CHAPTER THREE

EXPERIMENTAL WORK

INTRODUCTION

The previous studies, as mentioned in the literature review, gives a clear indication of the possibility to improving the thermal performance of a shell and helically coiled tube heat exchanger by using air bubbles injection technique. The following sections will describe, in detail, the experimental apparatus, procedure, and experimental conditions used in work.

3.1 Experimental Apparatus

A general view and a schematic layout of the experimental test rig are illustrated in Fig 3.1 and 3.2. In general, the main parts of test rig can be classified into three main units, briefly defined as follows:

3.1.1 Heating Unit: The hot water supply system was constructed to supply hot water to the coiled side of the test section. The heating unit includes a water storage tank, pump, rotameter, valves, variac, a wattmeter, electrical heater, and connection tubes, as shown in Figures 3.1 and 3.2.

3.1.2 Cooling Unit: The cold-water supply system constructed to supply cold water to the shell side of the test section. The cooling unit includes a cold-water reservoir, pump, rotary compressor, evaporator, condenser, expansion valve, and thermostat, as shown in Figures 3.1 and 3.2.

3.1.3 Test Section: The test section was manufactured from three parts, as explained in the following suction:
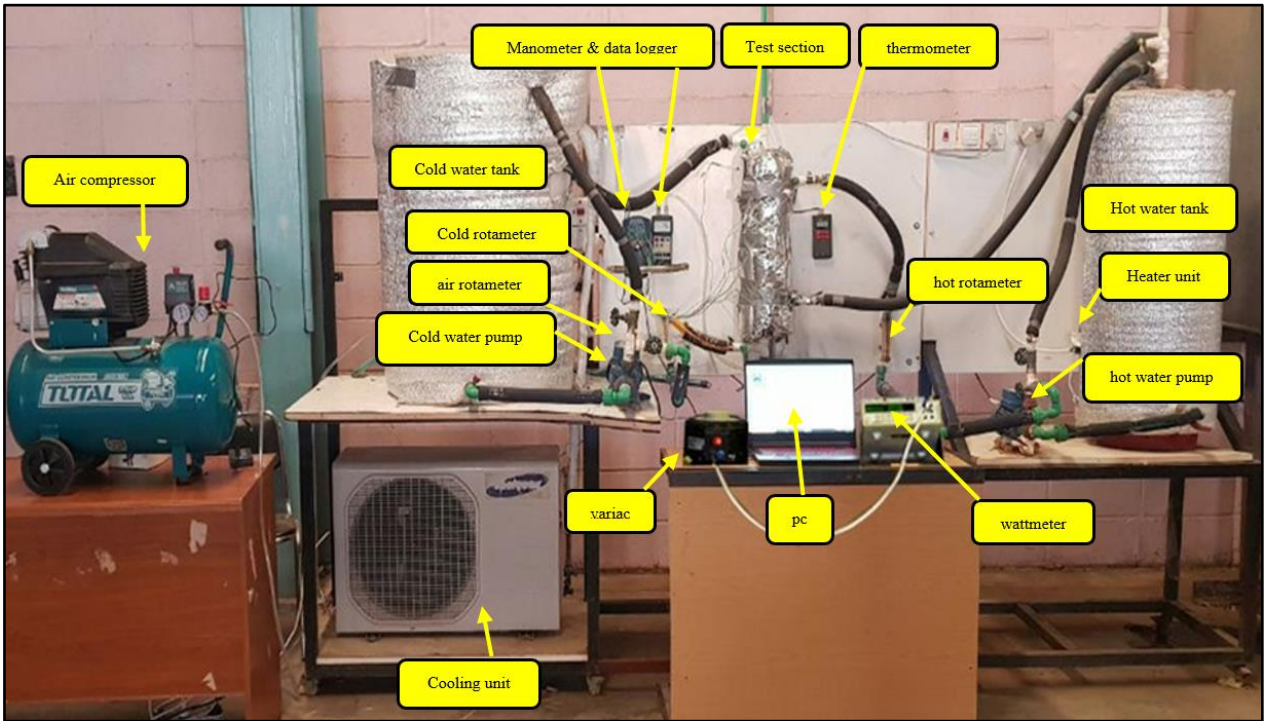
Figure 3.1: Experimental Apparatus; a photographic image of the general arrangement.
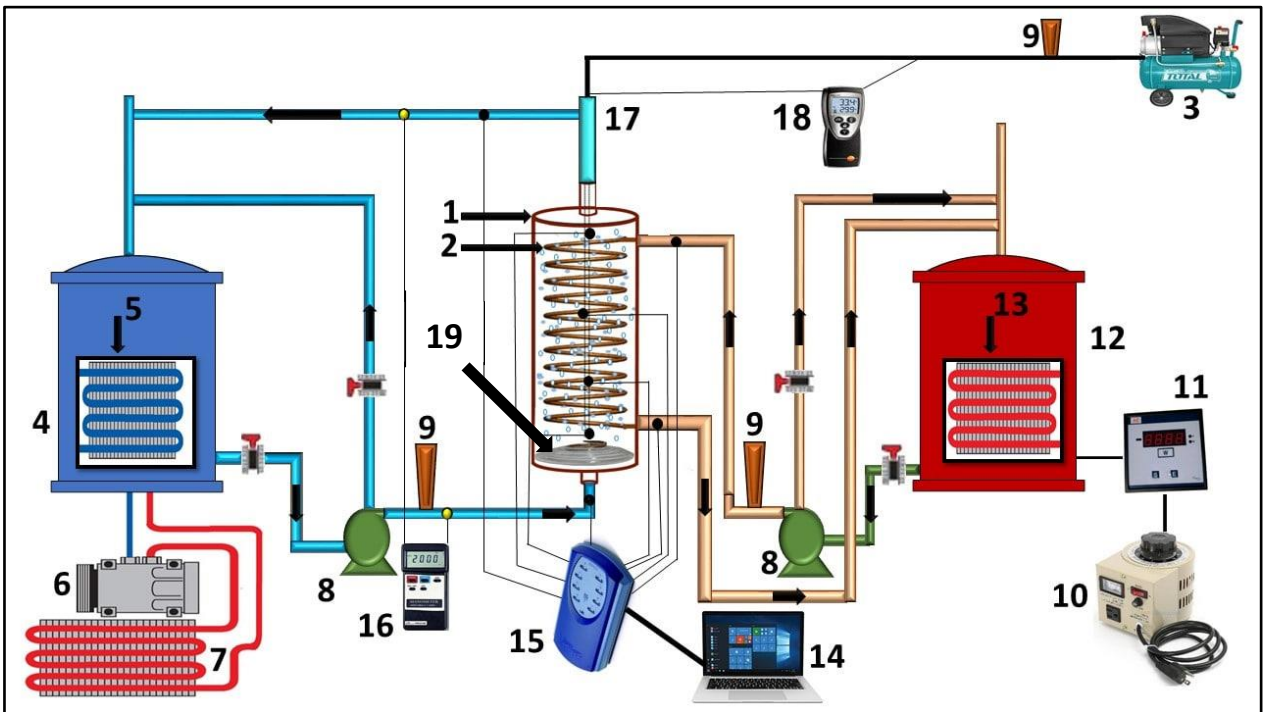
Figure 3.2: a schematic illustration of the tests set-up: 1. housing tube, 2. helically smooth coiled tube, 3. air pump, 4. a cold storage tank, 5. evaporator, 6. compressor, 7. Condensor,8. water pump, 9. rotameter, 10. variac, 11. wattmeter, 12. a hot storage tank, 13. heater. 14. pc, 15. recorder of data, 16. manometer, 17. a slit of air, 18. air temperature thermometer.19.sparger.

3.1.3.1 cold-water section: It consists of a PVC column with a total height of 50 cm, an outer diameter of 15 cm, and a thickness of 0.025 cm. It is connected from below to the cold-water supply line and from the top to the water return line of the cold-water tank. It has four ports, two for hot water in and out and two for cold water. In addition, it has four evenly spaced holes along with its height that are used to install temperature gauges (thermocouples). These thermocouples are connected to an eight-channel data logger and a computer to read and record them. The distance between the thermocouples along the shell is 9 cm, as shown in Fig 3.3 and 3.4.
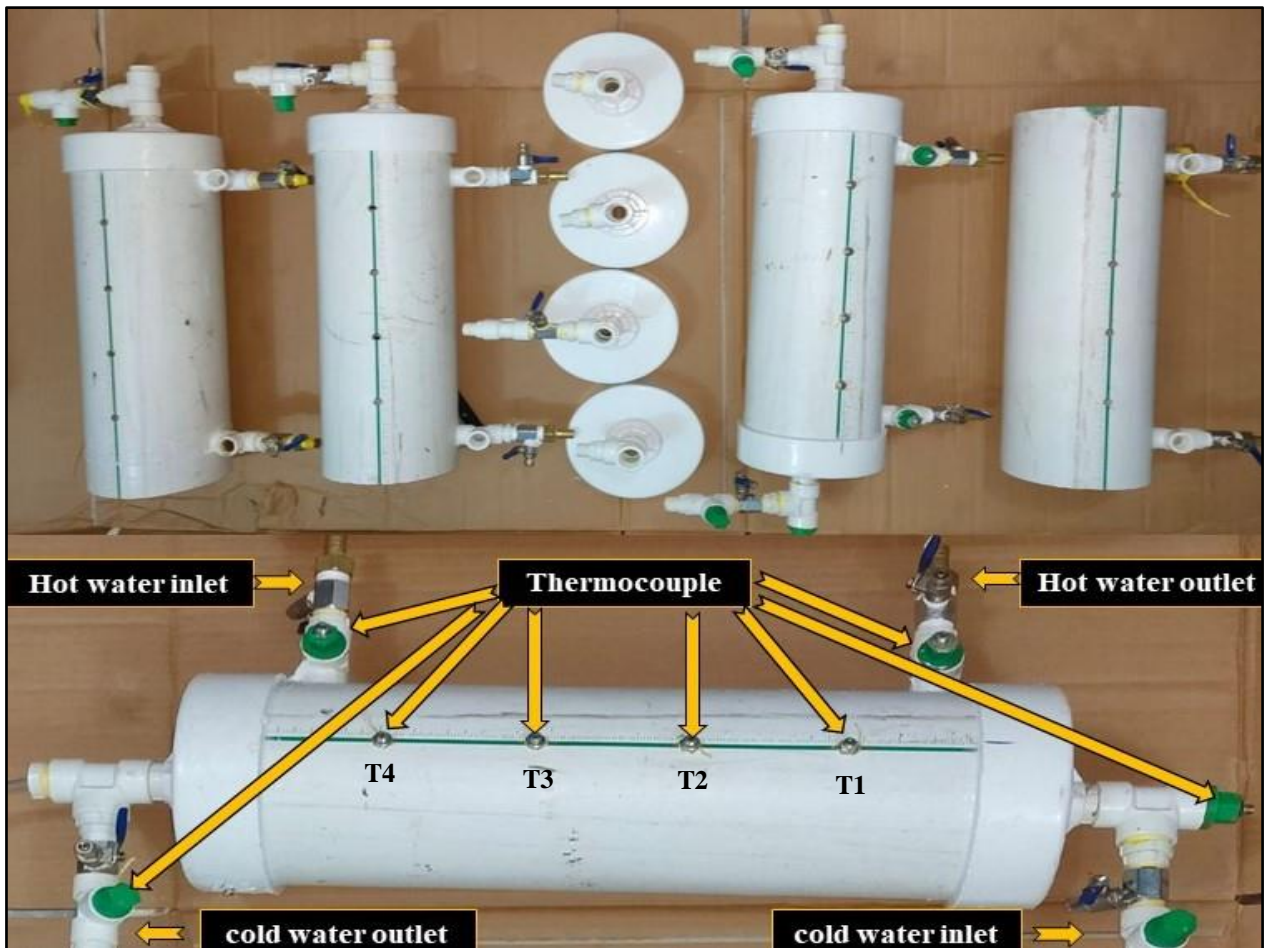
Figure 3.3: The cold-water section and thermocouples positions.
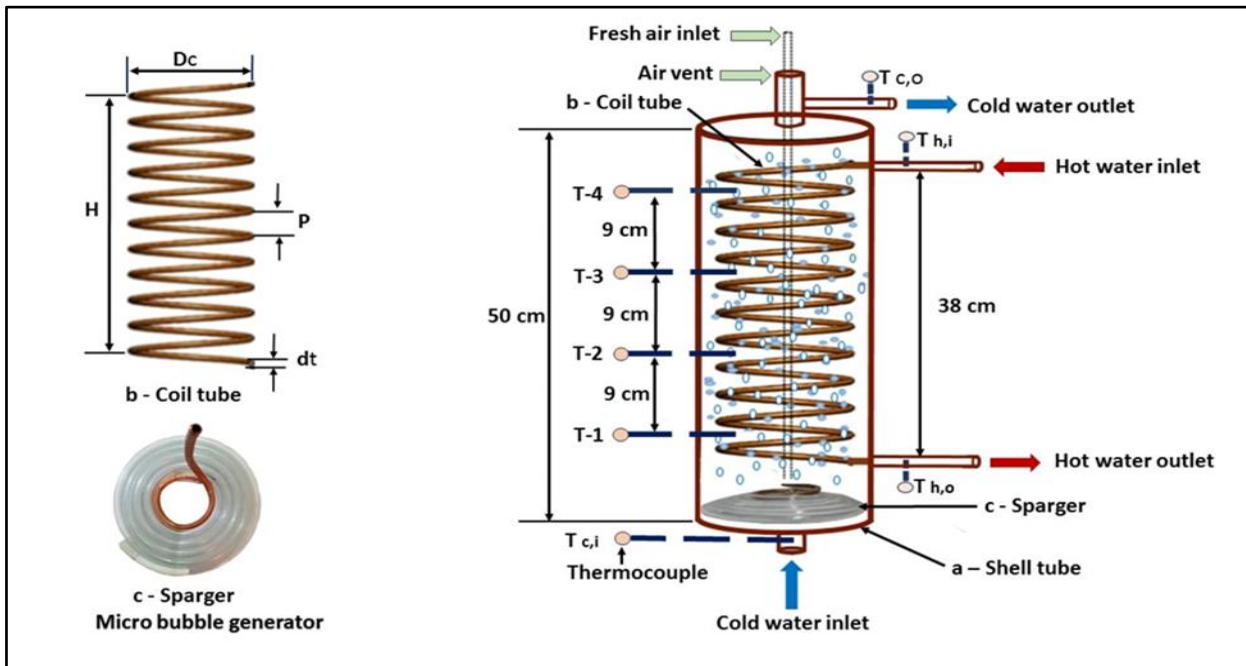
Figure 3.4: Test section.

3.1.3.2 Hot Water Section: consists of four samples of tubes with a length of 393.9 cm and 0.6 cm outer diameter that have been wrapped in a helical shape with regular dimensions. One of samples has a smooth surface, and the three others have been formed to have internal and external fins in a spiral shape and different pitch (5,8, and10mm). The process of manufacturing fins took place in Baghdad, the Bab al-Sheikh region, with special moulds. As well as the helically coiling process was done accurately due to the difficulty of winding the tubes that contain fins; and a small piece of the finned tubes was also sent to a laboratory in Iran via an office in Baghdad to clarify the dimensions and shape of the inner and outer fins, as shown in fig (3.5), and appendix (B). The coil is immersed entirely in water, and the first end of the coil (at the top of the shell) is connected to the inlet hot water tube, while the second end (at the bottom of the shell) is connected to the return line of hot water tube that connected with hot water storage tank, as illustrated in fig 3.1 and 3.2.
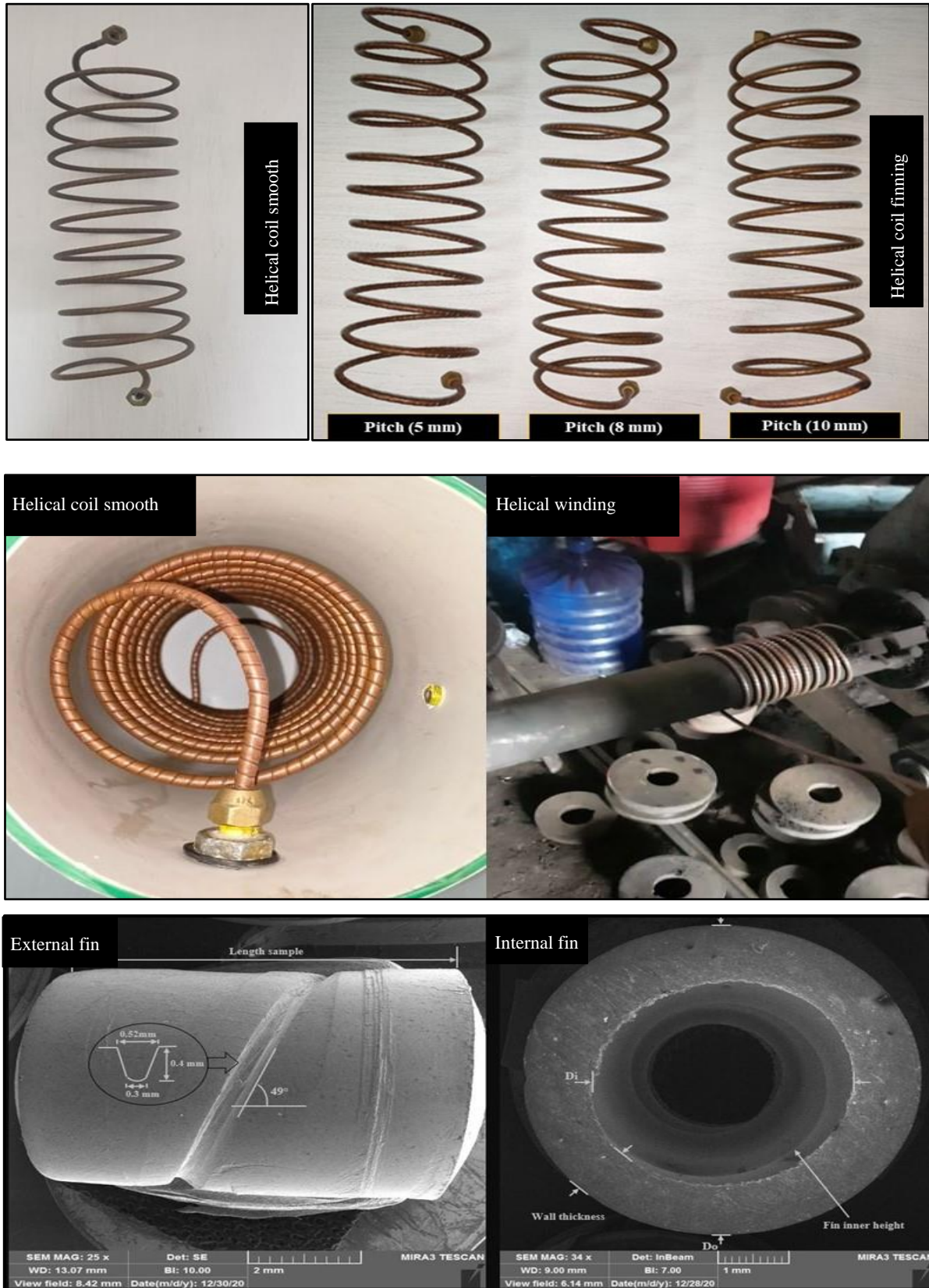
Figure 3.5: Manufacture of some practical parts.

3 bar,0.1mm diameter   3 bar,0.8mm diameter   3 bar,1.5mm diameter

Inlet air

1400 holes per meter

Ø 14.5 cm

Ø 2.5 cm
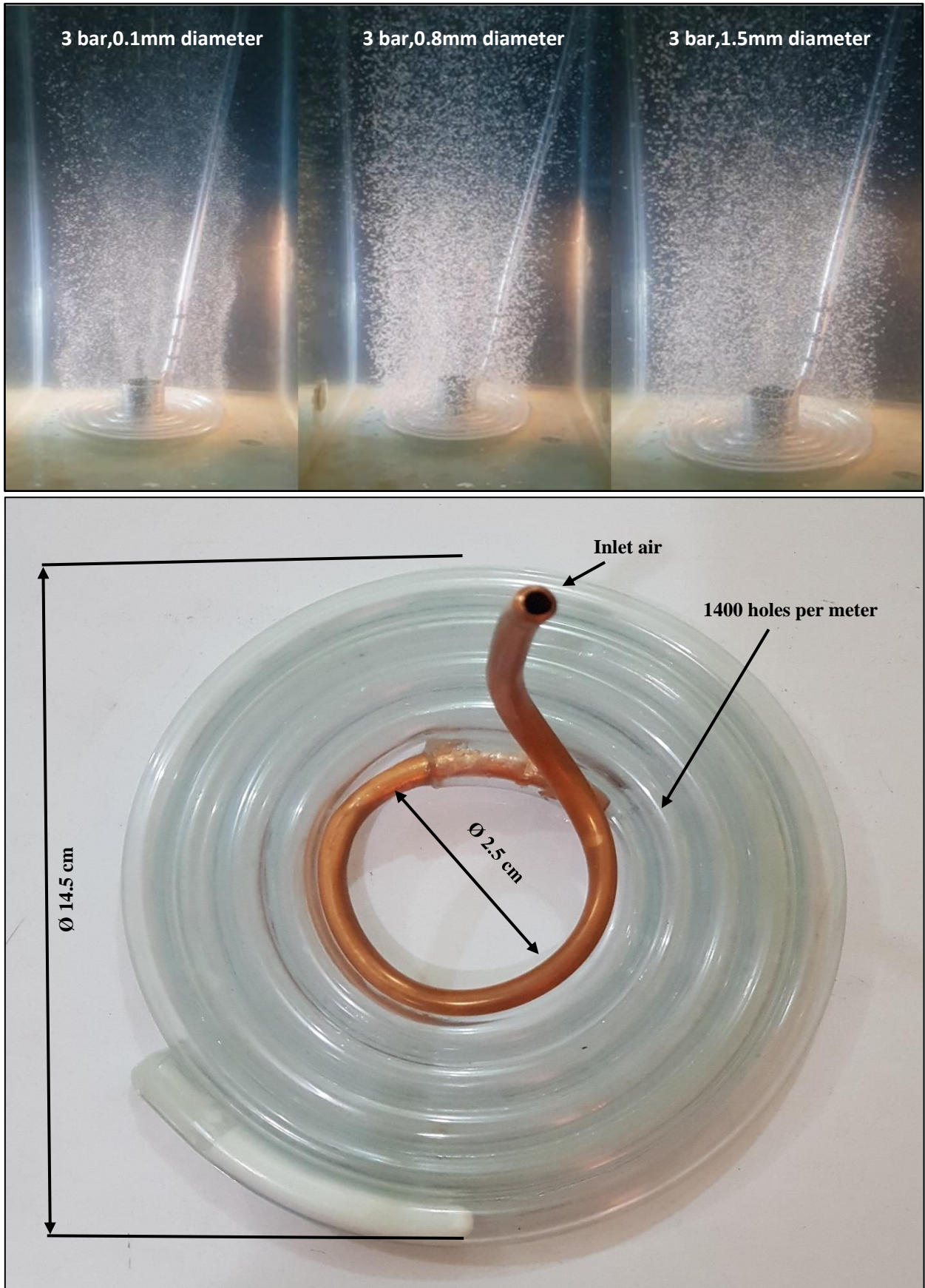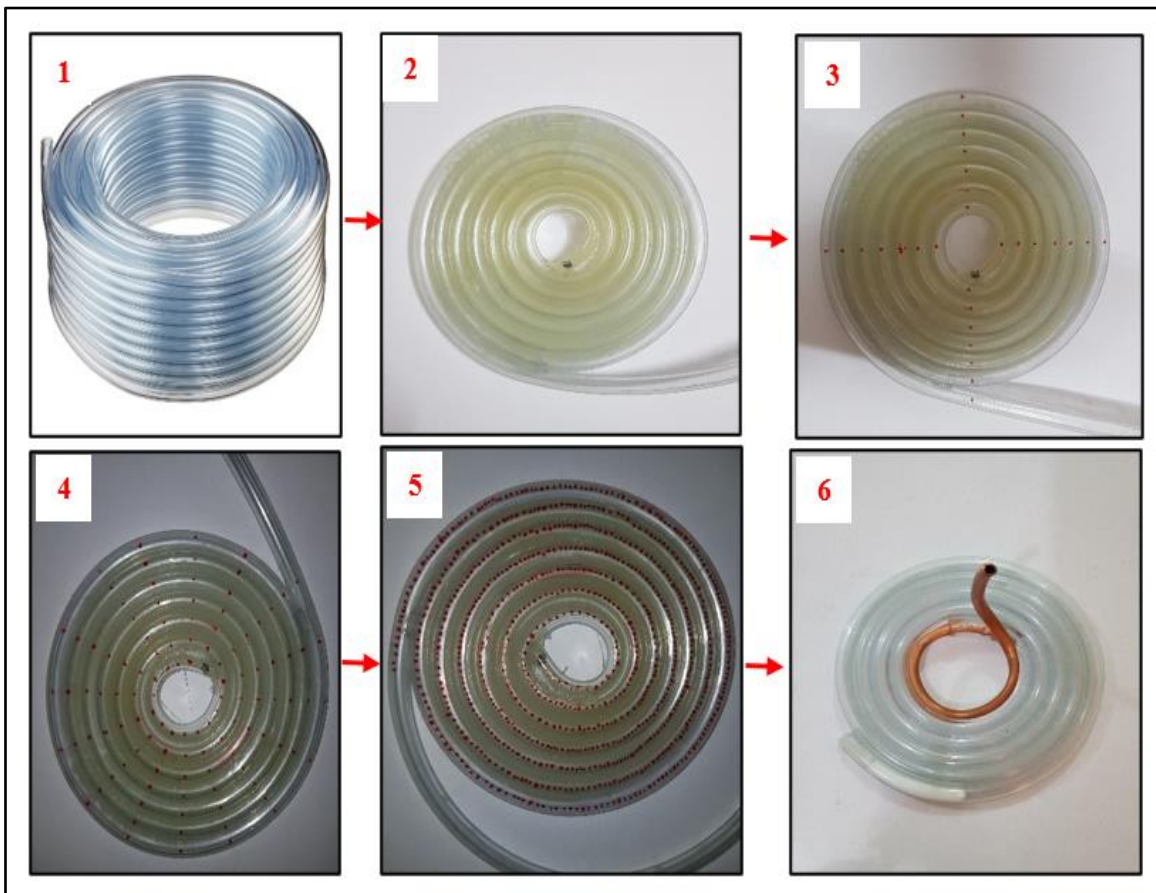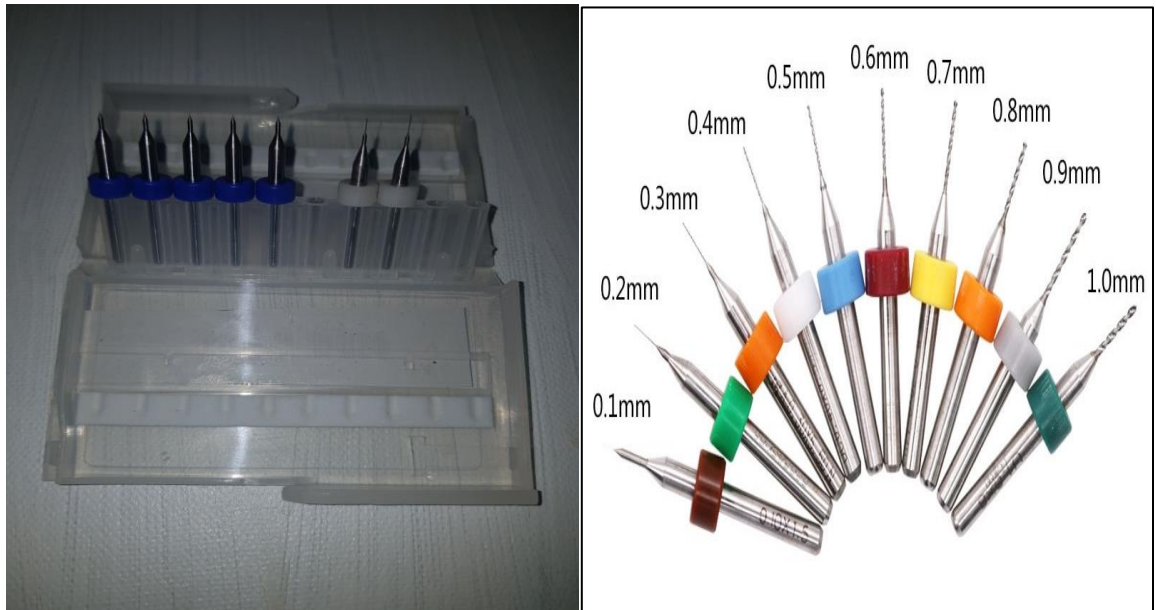
Figure 3.6:sparger

Figure 3.7: drill bits and manufacturing process of sparger.

3.2 Experimental Equipment

The details of the important experimental equipment are given in the following sections.

3.2.1 Shell and Helical Coils (Smooth and Finned) Tube Heat Exchanger

Traditional shell and helical coil tube heat exchangers are used in the experiments. Hot water flows through the coils (smooth and finned) tube side of copper, whereas cold water flows through the shell side of PVC in a counter-current configuration. The shell has an internal diameter of 14.5 cm, a thickness of 0.025 cm, and a total height of 50 cm. furthermore, the coil construction from 11 rings with an external diameter of 11cm is mounted inside the shell. The pitch between the rings (p) of 3cm, and the coils overall height is 38cm. Further details are given in Table 3.1 and fig 3.4. The outer surface of the shell is insulated using polyolefin foam insulation layer Expanded polyethylene foam (EPE) with a very low thermal conductivity (0.002 W/m. K) of 8 mm thick for use as a thermal insulator around the hot water tank, the cold-water tank, pipes, and the test section to minimize environmental heat losses.

Table 3.1: an overview of the dimensions of the heat exchanger in (mm).

Tube	D_o	t	H	L	D_c	d_i	N	p	p_f
shell	150	2.5	500	-	-	-	-	-	-
Coiled tube	6	1.6	380	3939	110	4.4	11	30	5,8,10

3.2.2 Loop of Water

There are two water loops; a hot water loop and a cold-water loop, as seen in fig 3.2. The hot water loop consists of a water storage tank (120 L) with an electrical water heater with a capacity of 3 kW, a variac, wattmeter, and centrifugal pump with a capacity of 30 LPM for hot water pumping from/to heaters and a heat exchanger tube side(see Fig 3.1 & 3.2), variac was used as a voltage controller sine the variac and wattmeter were helped together to keep the inlet water of coiled tube at a constant

temperature which allows to perform all experiments under the same temperatures and to avoid or reduce the uncertainty among them. Therefore, the electric source was supplied to variac firstly, then to the wattmeter, and finally to the electric heater. Furthermore, the cold-water loop consists of a water storage tank (250 L), a rotary compressor, an expansion valve, an evaporator, a refrigerant R-22, a condenser, and a thermostat to hold the shell side of the inlet water at a specific temperature, as well as a centrifugal pump with a capacity of 30 LPM for cold water pumping from/to the cooler and the heat exchanger side. Both pumps have the same technical data as tabulated in table 3.2. Additionally, the pumps mass flow rate was high compared to the experiments flow rate range; therefore, each pump has a recirculation loop to controlled manually on the water flow rate, as shown in fig 3.8.
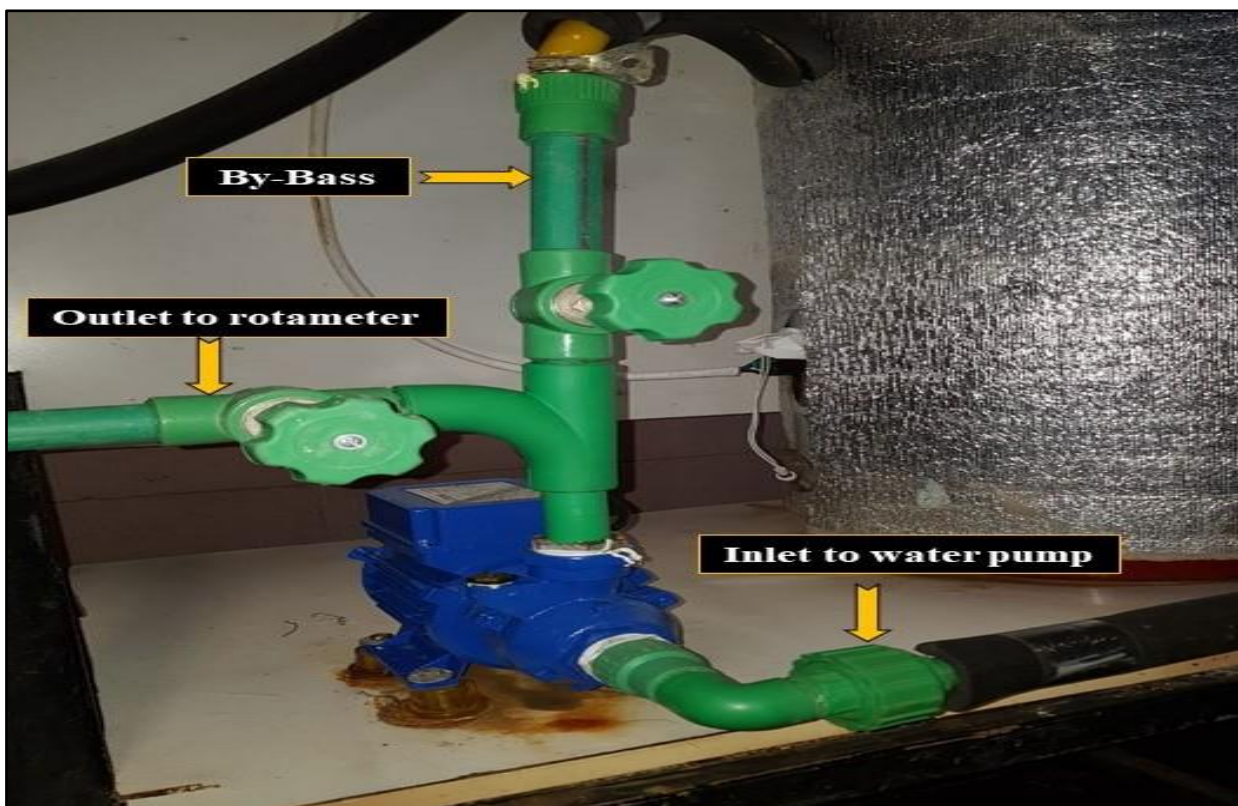
Figure 3.8: water pump.

Table 3.2: water pump technical data

Parameter	Comment
Type	KF/0
Max. fluid temperature	80 ºC
Power	0.372 KW
Voltage	220 V
Frequency	50 Hz
Pressure	3 bar
Max. head	30 m
Flow rate	30 LPM

3.2.3 Measurement Devices

Inlet and outlet temperatures of hot water, cold water, and temperature distribution along the shell tube were assessed using K-Type (Nickel Chromium, fig. 3.9) calibrated thermocouples with extension wires (RS Component Ltd, Nothants, UK). These thermocouples are linked to a data logger that directly shows their readings on a PC, except the inlet and outlet air temperature is connected to a digital thermometer, as seen in fig. 3.1 and 3.2. The thermocouple accuracy is seen in Table 3.3. Simultaneously, the calibration curve of the thermocouples is given in Appendix (A). The type K thermocouple is used in most thermal applications because it has good corrosion resistance. In addition, it has a wide operational temperature range. The specifications of this thermocouple type are below:

Temperature Range:

- ➢ Thermocouple grade wire, −270 to 1260 °C.
- ➢ Extension grade wire, 0 to 200 °C.
- ➢ Melting Point, 1400 °C.
- ➢ Special Limits of Error: ± 1.1°C or 0.4%.

Table 3.3: Error of temperature measurement in thermocouples.

Parameters	unit	error
The temperature of the hot water outlet	°C	±0.4
The temperature of the hot water inlet	°C	±0.4
The temperature of the cold water outlet	°C	±0.4
The temperature of the cold-water inlet	°C	±0.5
Cold water along column side T1	°C	±0.4
Cold water along column side T2	°C	±0.4
Cold water along column side T3	°C	±0.4
Cold water along column side T4	°C	±0.5
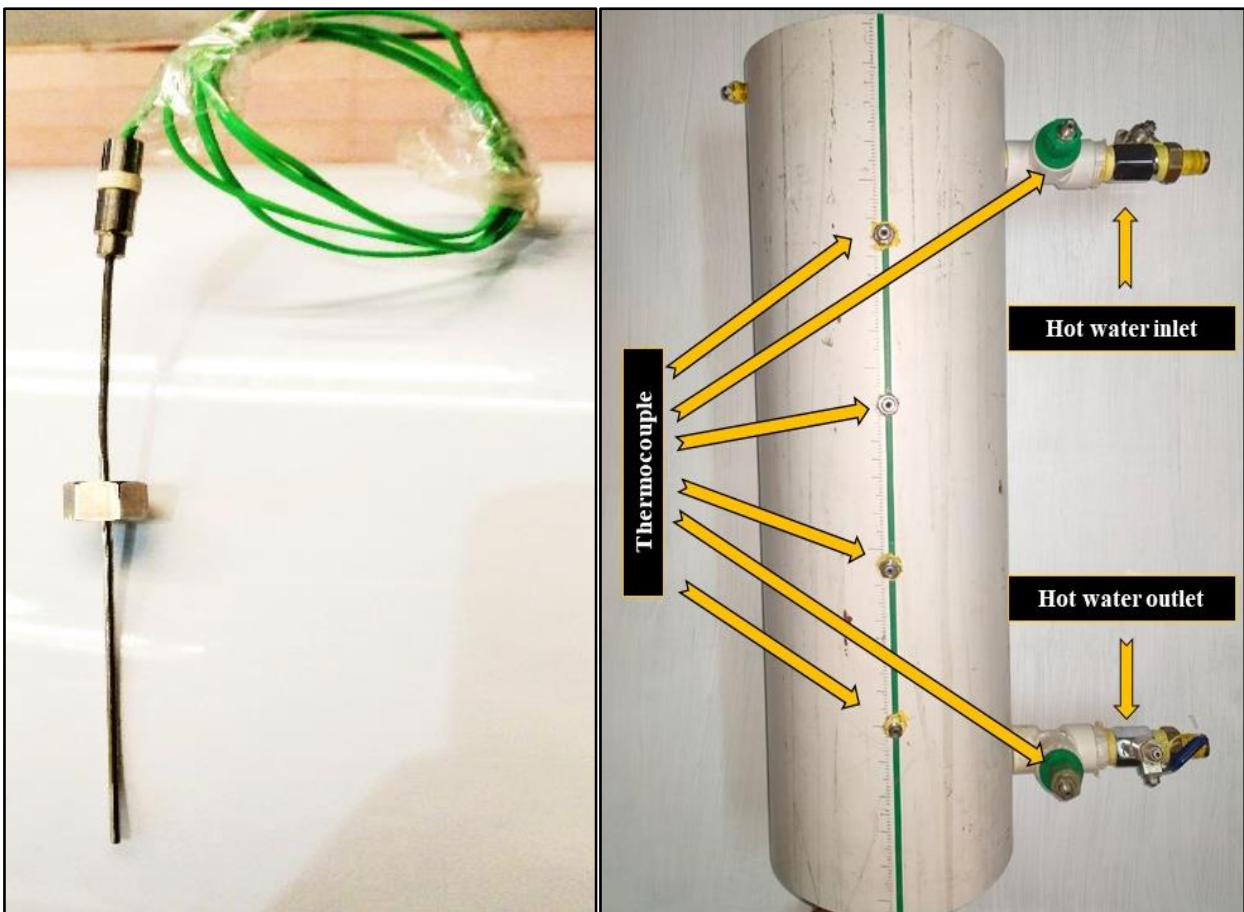
Figure 3.9: k-type, Nickel-Chromium thermocouple.

Besides, the pressure is determined using an analogue pressure gauge. Volumetric flow rates for both hot and cold water are determined by rotameters (panel type). Rota-meters with 18 LPM and 4 LPM maximum flow rates for cold and hot water and roto-meters (Key Instruments Model FR2000 ±5 % Full Scale) were used to quantify airflow. In addition, it was calibrated before starting the experiments to determine the water mass flow rate accurately for each experiment (see Appendix (A)).

3.2.4 Air Supply Unit

A total Air Compressor (50 L) air compressor made in China (see fig. 3.10) was used to supply fresh air to the sparger unit. Technical data of the air compressor are tabulated in Table 3.4.

Figure 3.10: air compressor.

Table 3.4: air compressor specifications.

Parameter	comment
Voltage	220-240V,50Hz
Input power	1.8Kw(2.5HP)
Speed	2850rpm
Tank capacity	50L(13.2Gal)
Operating pressure	max.8bar
Air displacement	119L/min
Pump lubricated	Oil
Noise:	96db

3.2.5 Data Logger

The 8-channel data logger (fig 3.11), with the following parameters, was used:

1- Eight-channel data loggers for thermocouples.

2- Supports all common forms of thermocouples.

3- Measures from-270 to +1820 °C.

4- High resolution and accuracy (For common type K thermocouples, the TC-08 can sustain a resolution of 0.025°C, over a range of –250 to +1370 °C).

5- Fast sampling rate up to 10 measurements per second.

6- The USB interfaces.

7- Pico Log is used for Windows data logging applications.

The data logger is directly attached to the pc with a USB link, where the thermocouple reads directly on the pc.

Figure 3.11: Picolog-6 data logger with 8-thermocouples.

3.2.6 Digital Thermometer

Inlet and outlet air temperatures were determined using a digital thermometer of type Digitron 3208. fig 3.12. The general characteristics of the thermometer are displayed in table 3.5.

Figure 3.12: Digital Thermometer.

Table 3. 5: Digital thermometer specifications.

Parameter	comment
Absolute Maximum Temperature Measurement	+950°C
Calibrated	SYSCAL
Thermometer Type	Handheld
Probe Type	K
Application	Industrial
Best Accuracy	±0.2 %
Number of Temperature Inputs	1
Resolution	0.1 °C
Length	140mm
Width	70mm
Height	26mm
Dimensions	140 x 70 x 26mm
Intrinsically Safe	Yes
Model Number p	3208IS
Weight	250g
Hazardous Area Certification	ATEX
Temperature Scale	Centigrade
Battery Type	9V
Absolute Maximum Temperature Measurement	+950°C

3.2.7 Manometer

The PCE-917 digital manometer was developed to measure the pressure of gasses and liquids under extreme environmental conditions. Therefore, the manometer has two connections to the upper end of the tube. One for the inlet (P1) and the other for the outlet (P2), as seen in fig. (3.13). The manometers measurement

range is approximately ($\pm$ 101.50) psi with a resolution of (0.05/0.1) and an accuracy of ± 2 percent (full range), as shown in Table 3.6 below.
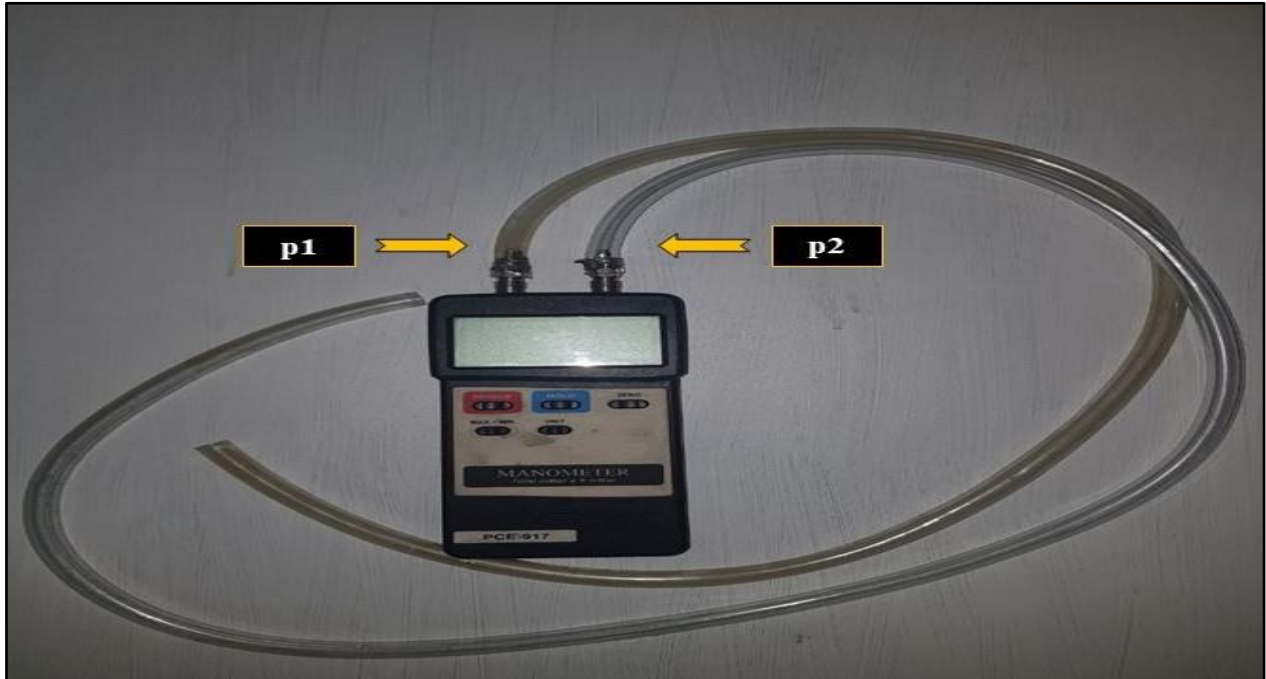
Figure 3.13: PCE-917 digital manometer.

Table 3.6: manometer (PCE-917) specifications.

Model	PCE-917
PSI	Range ($\pm$ 101.50) psi
	Resolution (0.05 / 0.1)
Accuracy	± 2 % (full range)
Reproducibility	± 1 %
Measurement sequence	0.8 s
Min- Max- Peak- Hold	Yes
Interface	RS-232
Power supply	1 x 9 V battery PP3
Material of case	plastic
Dimensions of case	180 x 72 x 32 mm
Weight	210 g

3.3 Experimental Procedure

The experiments were carried out in the laboratories of the technical collage engineering/najaf,extended from december to february ,during the offical working hours of collage,under the enviroment temperature range nearly (18-22°C).To fill out this section, the procedure of the first five experiments will be discussed first as the following:

1. First of all preparing the experimental set-up and checking all the instruments and connections if have leakages, additional to check the electrical power supply.

2. Circulate the hot water (coil side) and the cold water (shell side) by running the pumps and choosing a specific flow rate. This stages objective to maintain a consistent temperature in the experimental system.

3. Prepare hot water and cold water in storage tanks by running the heat and cooling systems and selecting the temperature difference ($\Delta T=20$ °C). Then specified the hot and cold water flow rates. Firstly the test section is operated without air bubbles injection, and heat is exchanged between hot and cold fluids until reaching a steady-state that is achieved after (20 25 min) according to the type of coil that used.

4. After reaching steady-state, measurement of flow meters by rotometer of hot and cold water, and temperatures through thermocouples by reading them directly on the PC through the data logger. These readings are the first heat exchanger measurement experiment to run without air injection. This process is repeated for each side of the shell, and the side flow rate of the coil.

5. Select the (air flow rate and pressure values) and Repeat the same value of cold and hot water flow rate after that start injecting air into the shell side after reaching to steady-state of injection bubbles case (2-5min) according to type of coil that is used. The test section temperatures are recorded automatically by the data logger.

The experiments were carried out on finned, and smooth coil tubes with different operation parameters as shown in tables (3.10,3.11, and 3.12).

Figure 3.14 represent the screen capture of the measured temperatures along with the heat exchanger.

Table 3.7 Test conditions for the experiments

Smooth helical coil tube for sparger hole (0.1,0.8,1.5mm) - 360 runs			
pressure(bar)	hot water (L/min)	cold water (L/min)	air flow rate (L/min)
2,3,4,5	1,1.5,2	2,4,6,8	0,0.5,1,1.5,2
Finned helical coil tube, pitch (5,8,10mm) for sparger hole (0.1,0.8,1.5 mm) – 360 runs			
pressure(bar)	hot water (L/min)	cold water (L/min)	air flow rate (L/min)
3	1,1.5	2,4,6,8	0,0.5,1,1.5,2

3.4 Comparison Between Porous Sparger [51] and Sparger (Spiral- Shape Plastic Tube in The Presented Study).
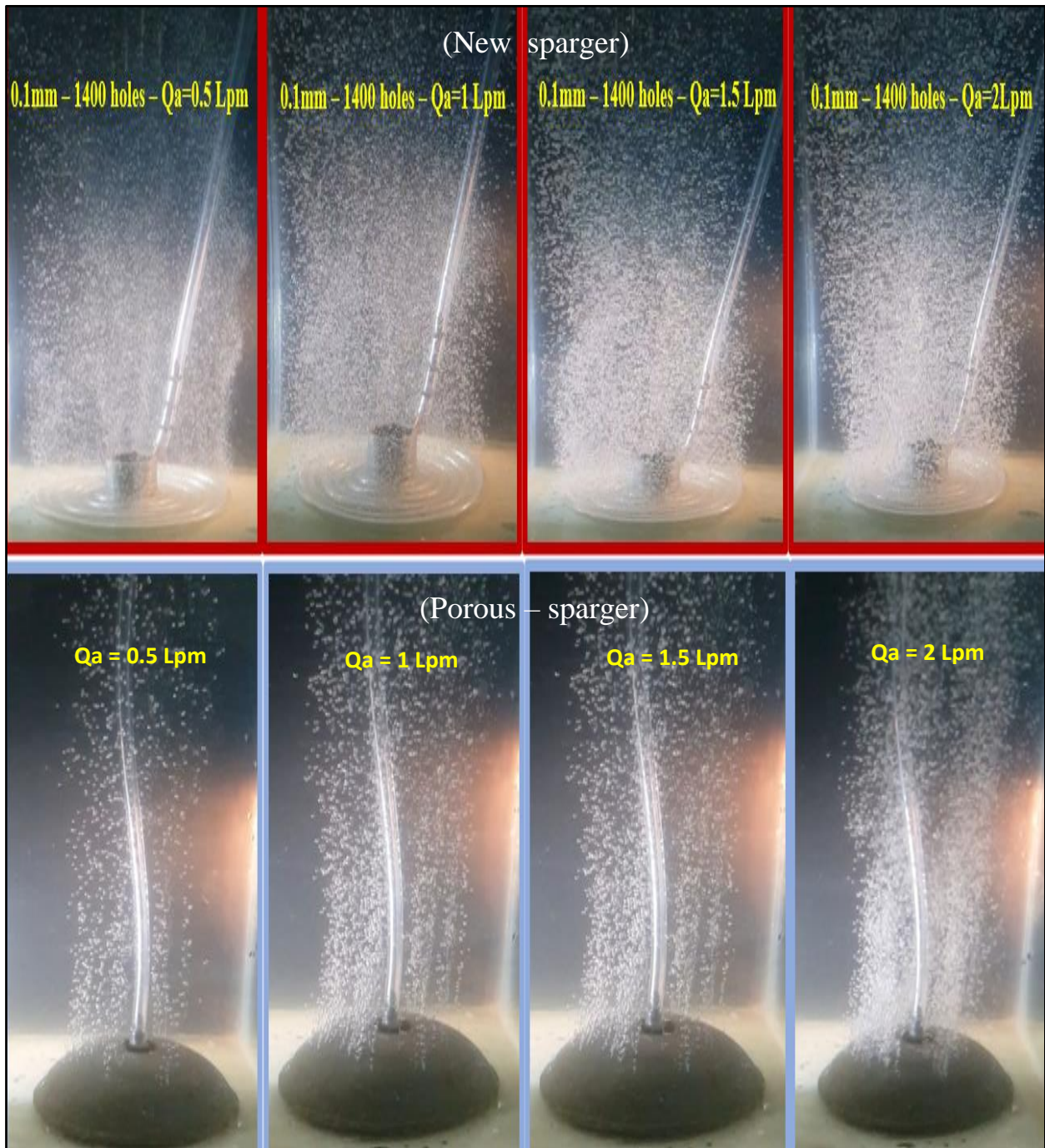
Figure 3.14: Comparison between porous sparger **[51]** and sparger (spiral-shape plastic tube) at air pressure (3 bar).

Table 3.8: Comparison between sparger (spiral- shape plastic tube) and porous sparger [51].

sparger (spiral- shape plastic tube)	Porous sparger [51]
It was practically synthesized.	It was bought from the market.
It is made of plastic.	It is made of stone.
known number and diameter of holes (1400) (0.1mm, 0.8mm, and 1.5mm).	The number and diameter of the bubbles are unknown.
Cost is lower; almost no more than $ 1.5 per sparger	Higher cost Approximately 15$ per sparger
Air bubbles cover all sparger area at any airflow rate	None
Given the possibility of studying the effect of number and bubbles diameter on the rate of heat transfer.	None

3.5 Calculation Equations of Experimental Work.
3.5.1 overall heat transfer coefficient

The overall heat transfer coefficient can be calculated using the equation shown below **[24]**.

$$U_s = \frac{q}{A_s \cdot \Delta T_{LMTD}} \tag{3.1}$$

Where q, A_s and ΔT_{LMTD} represent the heat transfer rate, surface area of heat transfer, and the log-mean temperature difference, respectively.

As a consequence, using energy balance, the heat transfer rate (q) can be calculated as follows:

$$q = \dot{m}_h C_{p,h}\left(T_{h,i} - T_{h,o}\right) = \dot{m}_c C_{p,c}\left(T_{c,o} - T_{c,i}\right) \tag{3.2}$$

The log-mean temperature difference for counter flow can be calculated from the equation below [24]:

$$\Delta T_{LMDT} = \frac{(T_{h,i} - T_{c,o}) - (T_{h,o} - T_{c,i})}{\ln\left(\frac{T_{h,i} - T_{c,o}}{T_{h,o} - T_{c,i}}\right)} \tag{3.3}$$

$$Re_{shell} = \frac{v \cdot d}{\upsilon} \tag{3.4}$$

$$v = \frac{Q}{\frac{\pi}{4} D_h^2} \tag{3.5}$$

$$, D_h = \frac{4\left(\frac{\pi D^2}{4}\right)}{\pi D} = D$$

Where Q, Re, v, D_h and υ represent the water flow rate through the shell side of the heat exchanger, Reynold number of shells, shell velocity, shell hydraulic diameter, and kinematic viscosity, respectively.

3.5.2 Volume Fraction (VF)

$$VF = \frac{\text{airflow rate}}{\text{airflow rate + water flow rate}} \tag{3.6}$$

3.5.3 effectiveness (ε)

The effectiveness of a heat exchanger explains the ratio of the actual to maximum possible heat transfer [24]:

$$\varepsilon_s = \frac{\text{actual heat transfer in a heat exchanger}}{\text{maximum possible heat transfer in a heat exchanger}} = \frac{q}{C_{min} (T_{h,i} - T_{c,i})} \tag{3.7}$$

Where q, C_{min}, T_{hi}, and T_{ho} represent the heat transfer,thermal capacity, temperature of coil inlet,and temperature of coil outlet.

3.6 Uncertainty Calculations

The following equation can be used to calculate the uncertainty of experimental data [61]:

$$W_R = \sqrt{\sum_0^i \left(\frac{\partial R}{\partial X_i} \cdot W_{X_i}\right)^2} \tag{3.8}$$

Moreover, the result is given as:

$$R = f(X_1, X_2, \ldots, X_n) \tag{3.9}$$

Where:

W_R: Uncertainty in the result

$X_1, X_2, \ldots, X_n$: Independent variables, and

$W_1, W_2, \ldots\ldots, W_n$: Uncertainty in the corresponding variables.

The uncertainty of the performance parameters that have been experimentally obtained in the present study will calculate sequentially in the following sections using the general formula (3.8).

3.6.1 Overall Heat Transfer Coefficient (U)

W_{A_S}=constant

$$W_U = \sqrt{\left(\frac{W_q}{A_s \cdot \Delta T_{LMTD}}\right)^2 + \left(-\frac{q \cdot W_{\Delta T_{LMTD}}}{A_s \cdot (\Delta T_{LMTD})^2}\right)^2 + \left(-\frac{q \cdot W_{A_S}}{A_s^2 \cdot \Delta T_{LMTD}}\right)^2} \tag{3.10}$$

$$W_{\Delta T_{LMTD}} = \frac{\sqrt{\left(\left\{\left(\frac{[(T_{h,i}-T_{c,o})-(T_{h,o}-T_{c,i})]}{(T_{h,i}-T_{c,o})}\right)-\ln\left(\frac{(T_{h,i}-T_{c,o})}{(T_{h,o}-T_{c,i})}\right)\right\}^2 \left[W_{T_{h,i}}^2 - W_{T_{c,o}}^2\right]\right)+ \left(\left\{\left(\frac{[(T_{h,i}-T_{c,o})-(T_{h,o}-T_{c,i})]}{(T_{h,o}-T_{c,i})}\right)-\ln\left(\frac{(T_{h,i}-T_{c,o})}{(T_{h,o}-T_{c,i})}\right)\right\}^2 \left[W_{T_{h,o}}^2 - W_{T_{c,i}}^2\right]\right)}}{\left(\ln\left[\frac{(T_{h,i}-T_{c,o})}{(T_{h,o}-T_{c,i})}\right]\right)^2} \tag{3.11}$$

$$W_q = q\sqrt{\left[\frac{W_{m_h}}{m_h}\right]^2 + \left[\frac{W_{C_{p_h}}}{C_{p_h}}\right]^2 + \left[\frac{W_{T_{h,i}}}{T_{h,i}-T_{h,o}}\right]^2 + \left[-\frac{W_{T_{h,o}}}{T_{h,i}-T_{h,o}}\right]^2} \tag{3.12}$$

Sub equations (3.11) and (3.12) in equation (3.10) to get on W_U

∴ Average $W_U = 13.23\%$

3.6.2 effectiveness (ε)

$$W_\varepsilon = \sqrt{\left(\frac{\partial \varepsilon}{\partial q} W_q\right)^2 + \left(\frac{\partial \varepsilon}{\partial Q_{.max.}} W_{Q.max}\right)^2} \tag{3.13}$$

$$W_q = q\sqrt{\left[\frac{W_{m_h}}{m_h}\right]^2 + \left[\frac{W_{Cp_h}}{Cp_h}\right]^2 + \left[\frac{W_{T_{h,i}}}{T_{h,i}-T_{h,o}}\right]^2 + \left[-\frac{W_{T_{h,o}}}{T_{h,i}-T_{h,o}}\right]^2} \tag{3.14}$$

$$\boxed{W_{Cp_h}=\text{constant}}$$

$$W_{Q.max.} = Q_{.max}\sqrt{\left[\frac{W_{m_h}}{m_h}\right]^2 + \left[\frac{W_{Cp_h}}{Cp_h}\right]^2 + \left[\frac{W_{T_{h,i}}}{T_{h,i}-T_{c,i}}\right]^2 + \left[-\frac{W_{T_{c,i}}}{T_{h,i}-T_{c,i}}\right]^2} \tag{3.15}$$

Sub equations (3.14) and (3.15) in equation (3.13) to get on W_ε

∴ Average $W_\varepsilon = 9.52\%$

Table 3.9: Average uncertainties of the performance parameters

Parameters	Uncertainty
Overall heat transfer coefficient	±13.23%
Effectiveness	±9.52 %

Table 3.10: calculations of uncertainty.

	Run No.	mass flow rate (l/m)			uncertainty calculation											
		hot water	cold water	air	LMTD	WLMTD	Qhot	WQhot	U	Wu	U %	QMAX	WQMAX	EFF	W EFF	EFF %
finned coil pitch 5mm	1	1.5	2	0	10.62	1.42	786.70	102.60	1101.41	186.73	16.70%	2089.50	131.93	0.38	0.05	14%
	2	1.5	2	0.5	10.78	0.59	1207.73	108.08	1510.50	158.73	10.51%	2089.50	131.24	0.58	0.06	10%
	3	1.5	2	1	10.70	0.80	1256.83	108.96	1583.08	182.19	11.51%	2089.50	131.45	0.60	0.06	10%
	4	1.5	2	1.5	10.48	0.86	1302.80	109.29	1675.42	197.50	11.79%	2089.50	130.85	0.62	0.06	9%
	5	1.5	2	2	10.27	0.86	1294.45	108.70	1699.25	201.90	11.88%	2089.50	131.41	0.62	0.06	9%
	7	1.5	4	0	12.21	0.13	916.25	103.46	1011.31	115.03	11.37%	2089.50	131.67	0.44	0.05	12%
	8	1.5	4	0.5	10.67	0.80	1303.85	110.50	1646.75	186.87	11.35%	2089.50	130.64	0.62	0.06	9%
	9	1.5	4	1	10.52	0.93	1333.10	110.84	1708.31	208.24	12.19%	2089.50	130.98	0.64	0.06	9%
	10	1.5	4	1.5	10.30	1.00	1336.24	110.28	1748.84	223.91	12.80%	2089.50	131.65	0.64	0.06	9%
	11	1.5	4	2	9.93	1.05	1374.89	110.82	1865.80	248.46	13.32%	2089.50	131.95	0.66	0.06	9%
	13	1.5	6	0	12.06	0.45	1054.15	105.58	1178.02	126.33	10.72%	2089.50	130.92	0.50	0.05	11%
	14	1.5	6	0.5	10.51	1.04	1314.30	109.79	1686.02	218.76	12.97%	2089.50	131.81	0.63	0.06	9%
	15	1.5	6	1	10.19	1.14	1380.11	110.85	1825.84	252.12	13.81%	2089.50	131.61	0.66	0.06	9%
	16	1.5	6	1.5	10.14	1.21	1438.62	112.57	1911.67	273.61	14.31%	2089.50	131.07	0.69	0.06	9%
	17	1.5	6	2	9.77	1.28	1543.10	115.82	2129.37	322.31	15.14%	2089.50	131.02	0.74	0.06	8%
	18	1.5	8	0	12.46	1.06	1125.20	106.90	1217.23	155.77	12.80%	2089.50	131.47	0.54	0.06	10%
	19	1.5	8	0.5	10.75	1.37	1410.41	112.31	1768.83	267.21	15.11%	2089.50	131.31	0.68	0.06	9%
	20	1.5	8	1	10.17	1.33	1456.38	112.72	1930.74	295.05	15.28%	2089.50	131.61	0.70	0.06	9%
	21	1.5	8	1.5	9.91	1.32	1484.59	113.35	2018.27	311.19	15.42%	2089.50	131.85	0.71	0.06	8%
	22	1.5	8	2	9.26	1.25	1608.92	117.06	2342.73	359.87	15.36%	2089.50	131.63	0.77	0.06	8%

$$\boxed{\text{Ave } W_U = 13.23\%} \qquad \boxed{\text{Ave } W_\varepsilon = 9.52\%}$$

Chapter Four

Results and Discussion

CHAPTER FOUR

EXPERIMENTAL RESULTS

INTRODUCTION

This chapter describes and analyzes the research findings for heat transfer characteristics such as the overall heat transfer coefficient (U), effectiveness (ε), pressure drop (Δp), and temperature distribution in the vertical shell and helical coiled (smooth and finned) tube heat exchanger with air injection bubbles inside cold water (air/water ,two phase flow).

As previously shown in studies **[23, 24, 50]**, the injection of air bubbles significantly increases the thermal performance of heat exchangers. As a result, it is expected to reduce the size of heat exchangers required to do the same purpose when used without air injection.

The shell side flow rate was ($Q_s = $ 2,4,6 and 8 L/min) , $\Delta T = 20$ °C, four different airflow rates ($Q_a = $ 0.5, 1, 1.5 and 2 L/min) , air pressure (2,3,4,and5 bar), diameter bubbles (0.1,0.8,and 1.5mm), number of bubbles =1400 per meter,spiral pitch ($p_f = $ 5,8, and 10mm) , under laminar flow ($316 \leq$ Re $\leq$ 1223),and three different coil side (hot fluid) flow rate ($Q_h = $ 1,1.5and 2 L/min) in addition to the control case without air injection.

4.1 Smooth Surface Helical Coil Tube Heat Exchanger

4.1.1 Overall Heat Transfer Coefficient (U_s)

The overall heat transfer coefficient (U_s)is investigated and optimized in this analysis as it represents a significant measure of how effective the thermal process is. The heat transfer rate (q) that appeared in Eq. (3.1) is based on the assumption that the water in the shell side is fully absorbed by the heat provided by the coil side (hot fluid). Many scholars have used this assumption **[23, 24, 56]**, and it is intended to remove all doubt about how much heat can inevitably be lost to the atmosphere.

Figure 4.1 depicts the variation of the overall heat transfer coefficient U_s with the shell side flow rate . In all cases, the injection of air bubbles within the shell side of the heat exchanger raises the overall heat transfer coefficient. As shown in Fig. 4.1, air bubble injection led to a significant enhancement in heat exchanger performance. The maximum value of the overall heat transfer coefficient (U_s)due to air injection was (1476 W/m². °C) when the water flow rate 8 L/M, hot water flow rate 2 LPM, and an airflow rate of 2 L/min,see fig (4.1C). in contrast, the minimum value was (850 W/m². °C) when water flow rate 2L/min, hot water flow rate1 L/min and airflow rate 0.5 L/min, see fig (4.1A).

This enhancement in heat transfer can easily be attributed to the influence of the bubbles that are injected. Due to the density difference between the air bubbles and water in the shell, the bubbles are driven vertically through the bulk of water under the effect of buoyancy force. As a result, the bubble plume will entrain fluid from the shell side and therefore increase its Reynold number (Re) and the turbulence level. Beyond this, the motion of the entrained fluid within a closed vessel, such as the shell, will also induce secondary flows, improving the mixing. Consequently, the boundary layer which forms on the outer surface of the coil will be disrupted. This is particularly important when the fluid layers' temperature in the

coil's vicinity is significantly higher than the temperature of the rest of bulk of the fluid in the shell.

Finally, the poor thermal conductivity of air could also decrease the rate of heat loss to the surroundings. It should be remembered that the shell side Reynolds number can be calculated using the correlations depending on the water flow rate as shown in equations (3.4) and (3.5).

Moreover, it should be remembered that the actual water velocity within the shell side is greater than the water velocity measured from Eq (3.5) since more fluid flow (water flow + airflow) can travel through the same shell after the airflow injection within the shell side of the heat exchanger. Furthermore, inevitably, the combined fluid would travel at a faster rate than pure water. As a result, the real water velocity and the actual shell side Reynolds number are greater than the Reynolds number calculated from Eq (3.4). As a result, this additional Reynolds number can be added as another positive action of air injection that increases the heat transfer rate of the heat exchanger.

In general, the overall heat transfer coefficient (U_s) increases significantly when air bubbles are injected into the shell side while the flow rates of the working fluids are kept constant. It is evident that the enhancement of the overall heat transfer coefficient continues to improve with increasing shell-side flow rate. Interestingly, (U_s) augmentation seems to have a maximum value depending mainly on the air injection flow rate. Thus, airflow rates of 2 L/min can be represented as the flow rate required to produce the maximum improvement in (U_s) within the study range for the three hot coil flow rates (1,1.5 and 2 L/min).

Additionally, we notice from fig 4.1 that the value of (U_s) increases with the coil side flow rate increase due to increasing thermal capacity (hot fluid) for the same heat process time. Finally, the average uncertainty of the overall heat transfer coefficient (U) was calculated (see Appendix C) and given in table 3.12.
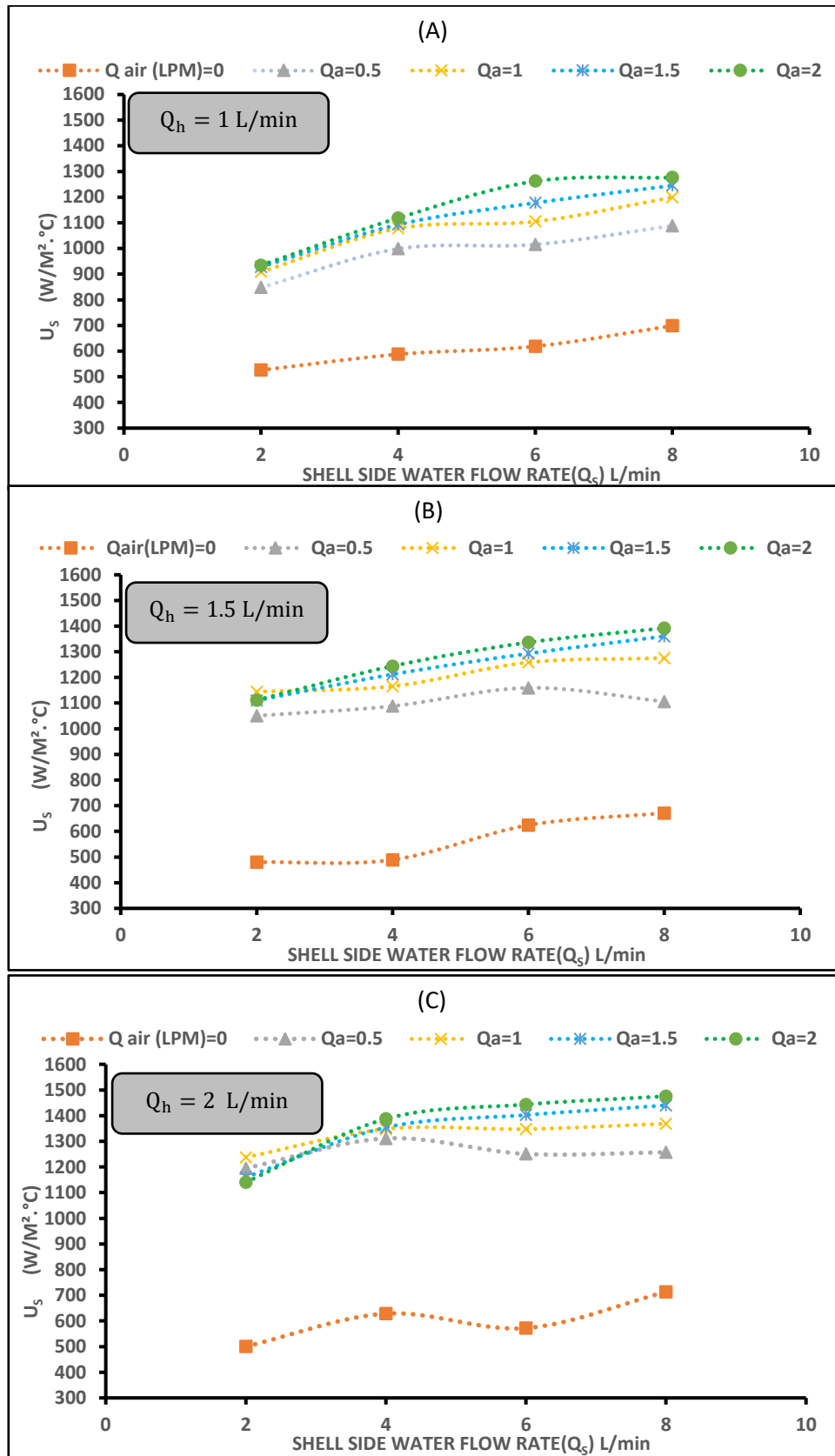
Figure 4.1:Effect of air bubbles injection on (U_s) of a smooth helical coiled tube heat exchanger P_a= 3 bar,Db =1.5mm.

Figure 4.2 clarifies the variation of the enhancement ratio of the overall heat transfer coefficient (U_{sa}/U_s) with the shell side flow rate. The enhancement ratio of the overall heat transfer coefficient with air injection bubble to overall heat transfer coefficient in a simple case (pure water) is (U_{sa}/U_s). As seen in Fig. 4.2, the slope of (U_{sa}/U_s) is reduced with an increased water flow rate. It is noted that the reduction of (U_{sa}/U_s) or its slope does not mean the decline of (U_s). It just means that the amount of positive effect of air bubble injection on (U_s) has been reduced compared to the increased water flow rate. Nevertheless, the overall heat transfer coefficient is yet increased.

Meanwhile, as shown in fig 4.2, the shell side flow rate of 6 LPM results in more improvement (U_s). However, these findings could lead to conclude that $Qa = 2\,L/min$ and $Qs = 6\,L/min$ are the optimum flow rates under the current experimental conditions.

The results reveal that the maximum enhancement ratios of (U_{sa}/U_s) was 2.52 at $Q_s = 6\,L/min$, $Q_a = 2\,L/min$, and $Q_h = 2\,L/min$. Furthermore, the minimum (U_{sa}/U_s) was 1.56 at $Q_s = 8\,L/min$, $Q_a = 0.5\,L/min$, and $Q_h = 1\,L/min$.
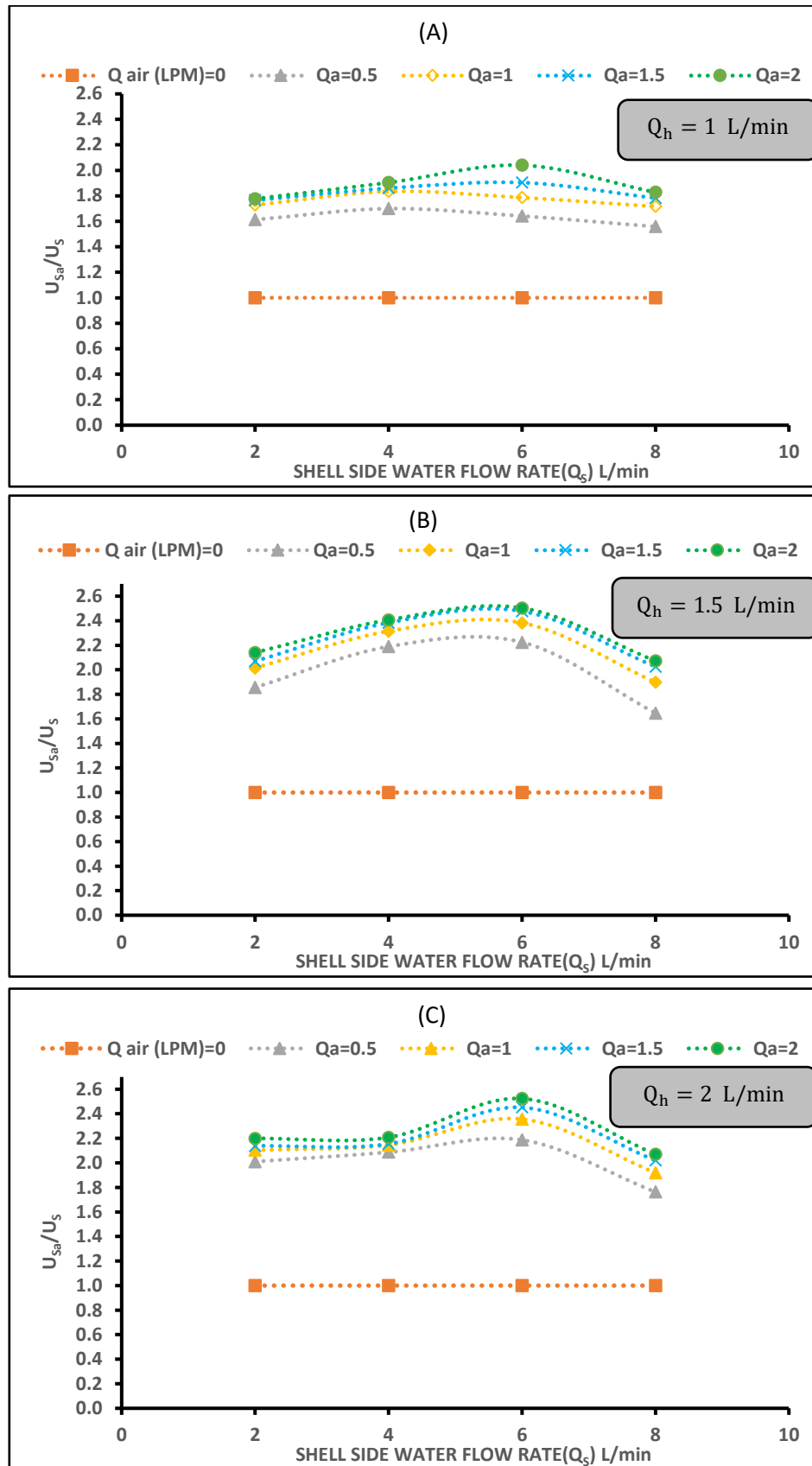
Figure 4.2: Effect of air bubbles injection on the (U_{sa}/U_s) With the shell side flow rate of a smooth helically coiled tube heat exchanger P_a= 3 bar,Db =1.5mm.

4.1.2 Volume Fraction (VF)

volume fraction (VF) is one of the most important parameters used to characterize two-phase fluid flow, especially the gas-liquid flow. Furthermore, air injection must be controlled because if air quantity increase, will work as an insulator layer on the coil due to increased (VF), which leads to reduced heat transfer. This phenomenon can also be explained using the definition of volume fraction as shown in equation (3.6) **[51]**.

Figure 4.3 illustrates the variation of the enhancement ratio of the overall heat transfer coefficient (U_{sa}/U_s) with volume fraction (VF).Increased water flow rate decreases the amount of volume fraction. Moreover, lowering the volume fraction means reducing airflow contribution (air bubbles) to overall fluid flow. Obviously, with a variable airflow rate in Fig 4.3, the increase in volume fraction is attributed to decreased water flow rate rather than an increase in air flow rate. However, for a given volume fraction, increasing the airflow rate raises the (U_{sa}/U_s). As a result, the amount of (U_{sa}/U_s) It decreases as the volume fraction increases.

So, as seen in fig 4.3, void fraction 0.25 at ($Q_s = 6$ L/min, and $Q_a = 2$ L/min) represents an optimal value for improving the heat exchanger's thermal performance. At the same time, the maximum enhancement ratio occurred when void fraction between 0.2 and 0.3 ($Q_s = 6$ L/min and $Q_a = 2$ L/min) for any (Q_h) On the other hand, the minimum enhancement ratio occurred when the void fraction value is 0.05 ($Q_s = 8$ L/min and $Q_a = 0.5$ L/min) for any (Q_h).
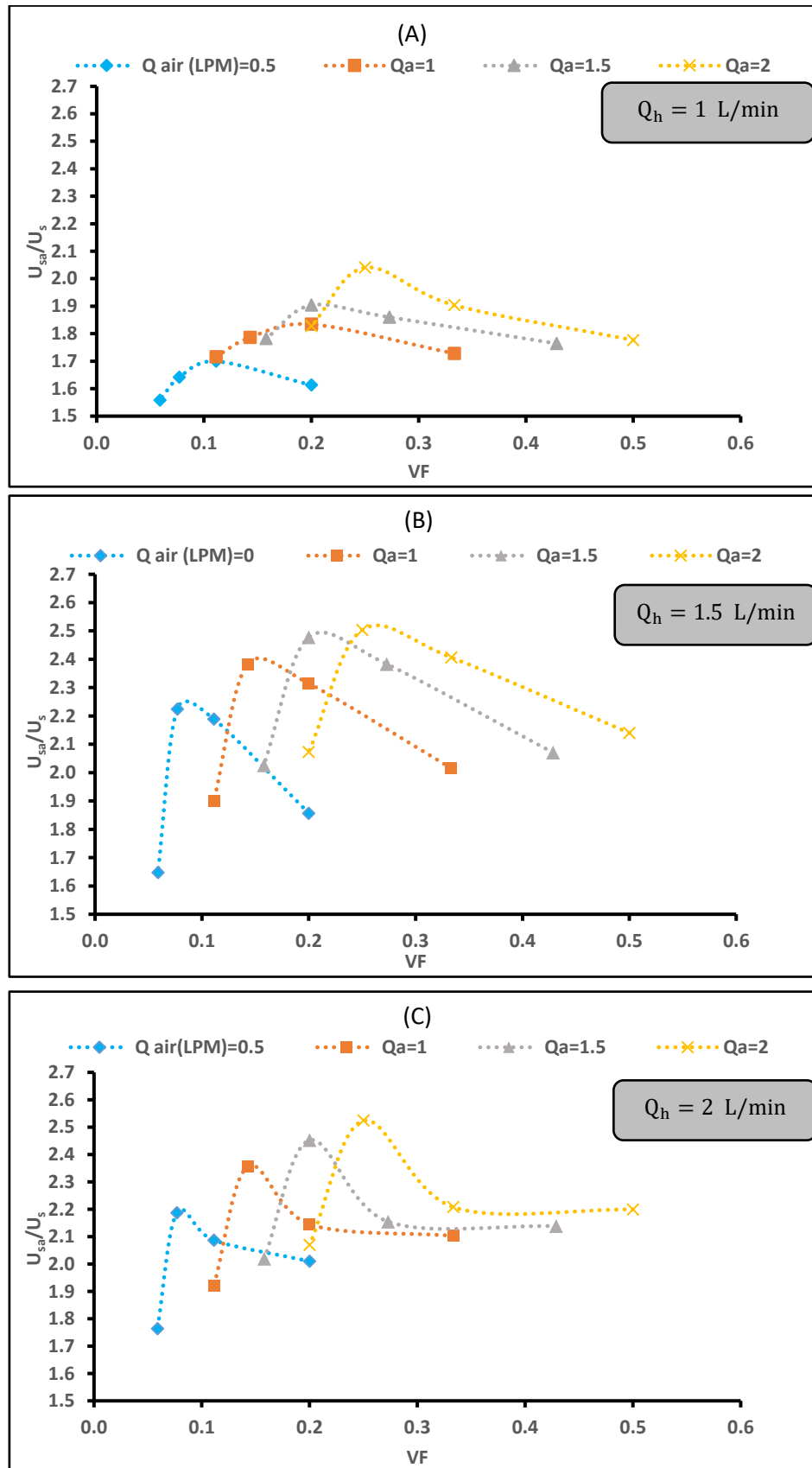
Figure 4.3: variation the ratio of (U_{sa}/U_s) with volume fraction for different airflow rates P_a= 3 bar, D_b =1.5mm.

4.1.3 Effectiveness (ε_s)

Figure 4.4 demonstrates the variance in thermal effectiveness with the shell side flow rate.The sudden improvement in effectiveness caused by air injection is noticeable, demonstrating the important role of air bubbles in improving heat transfer. The duty of the injected air on the effectiveness is continuing active for all shell-side flow rates. Further, Fig 4.4 illustrates that the maximum value of the effectiveness is 0.71 achieved when ($Q_h = 1$ L/min) at the shell-side flow rate of 8 L/min and the injected airflow rate of 2 L/M. Furthermore, the minimum value is 0.38 at $Q_h = 2$ L/min, the shell-side flow rate of 2 L/min, and the injected airflow rate of 0.5 L/min. In addition, the average uncertainty of the effectiveness (U) was calculated (see Appendix C) and given in table 3.12.

Lastly, the figure clearly shows that the effectiveness value decreases with the coil side flow rate increase due to increasing thermal capacity (hot fluid) for the same heat process time.
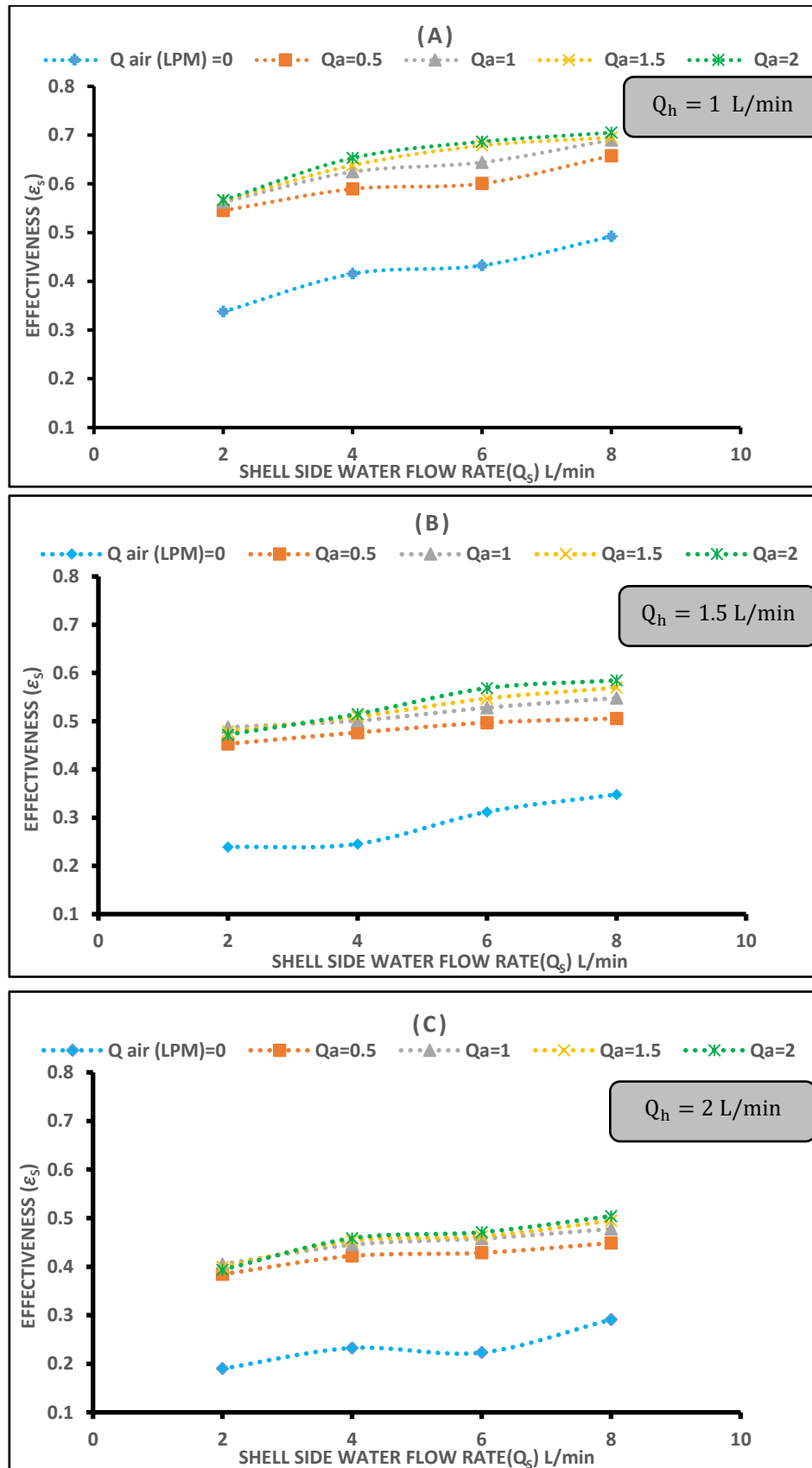
Figure 4.4: Variation of effectiveness (ε_s) with shell side flow rate at P_a = 3 bar, D_b = 1.5mm.

Finally, fig 4.5 demonstrates the relationship between the enhancement ratio of the effectiveness ($\varepsilon_{sa}/\varepsilon_s$) and the shell side flow rate .The improvement ratio develops from its minimum value by increasing the airflow rate reaching its maximum value and decreasing or continuing steadily with the airflow rate depending on the shell side flow rate. According to Fig 4.5, the $Q_s = 6$ L/min and ($Q_a = $ L/min) are the optimal value to enhance the effectiveness of the heat exchanger.

In addition, in fig 4.5, the slope of ($\varepsilon_{sa}/\varepsilon_s$) decreases as the water flow rate increases. It should be remembered that a decrease in ($\varepsilon_{sa}/\varepsilon_s$) or its slope does not imply a decrease in effectiveness. It simply means that the beneficial impact of air bubble injection on (ε_s) has been decreased due to the increased water flow rate. Nevertheless, the effectiveness is yet increased. Meanwhile, as seen in fig 4.5, the shell side flow rate of 6 L/min results in more improvement in effectiveness. However, these findings could lead to conclude that $Q_a = 2$ L/min and $Q_s = 6$ L/min are the optimum flow rates under the current experimental conditions.

The results reported that the maximum percentage enhancement ratios of ($\varepsilon_{sa}/\varepsilon_s$) was 2.11 at $Q_s = 6$ L/min , $Q_a = 2$ L/min , and $Q_h = 2$ L/min , furthermore, the minimum ($\varepsilon_{sa}/\varepsilon_s$) was 1.34 at $Q_s = 8$ L/min , $Q_a = 0.5$ L/min , and $Q_h = 1$L/min .
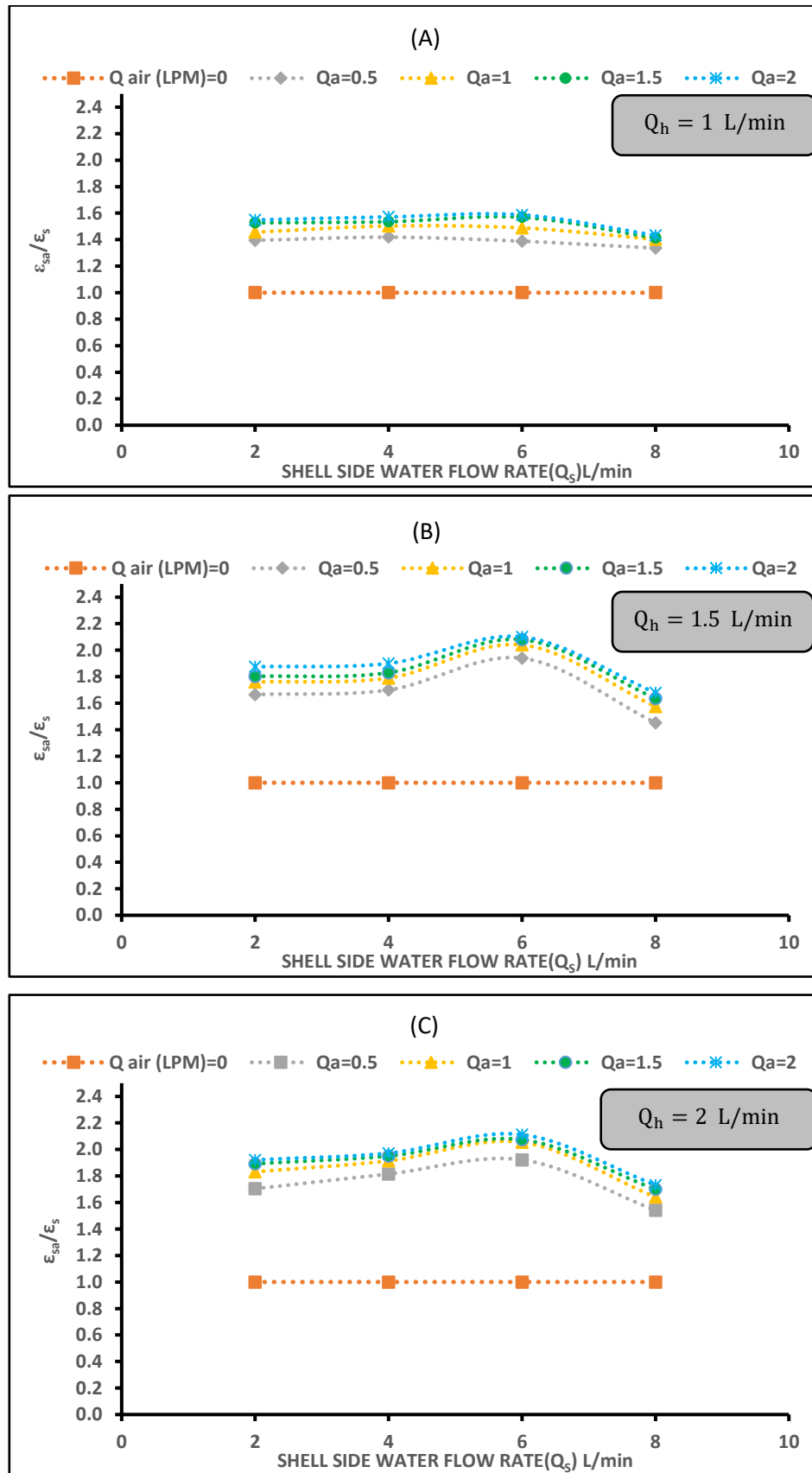
Figure 4.5: Variation of $(\varepsilon_{sa}/\varepsilon_s)$ with shell side flow rate at $P_a= 3$ bar, $D_b =1.5$ mm.

4.1.4 Pressure Drop (Δp_{ss})

Any attempt to enhance the thermal performance of a heat exchanger by using, for example, twisted tape, corrugated tubing, finned tubes, wavy stripes, barbed wires, or springs results in additional pressure drop as well as an increase in cost, energy, material, and weight.Tiny air bubble injection has been shown to be a promising strategy for heat transfer enhancement with the lowest possible pressure drop compared to the most common enhancement techniques such as nanofluid techniques and surface modification techniques **[23]**.

Figure 4.6, show the effect of increase shell-side flow rate on pressure drop (Δp_{ss}) .Obviously, the increased bubble diameter led to a development in pressure drop along the heat exchanger shell side. This could be mainly due to the increase in the shell side Re with increasing the size of bubbles.

Indeed, the experimental results showed that the maximum increment in pressure drop due to the air bubbles injection was 1.7 psi when $Q_a = 2$ L/min at $Q_s = 8$ L/min and bubble diameter $= 1.5$ mm. On the other hand, the minimum value of the pressure drop due to the air bubbles injection was 0.5 psi when $Q_a = 0.5$ L/min at water flow rate, $Q_s = 2$ L/min, and bubble diameter $= 0.1$ mm.
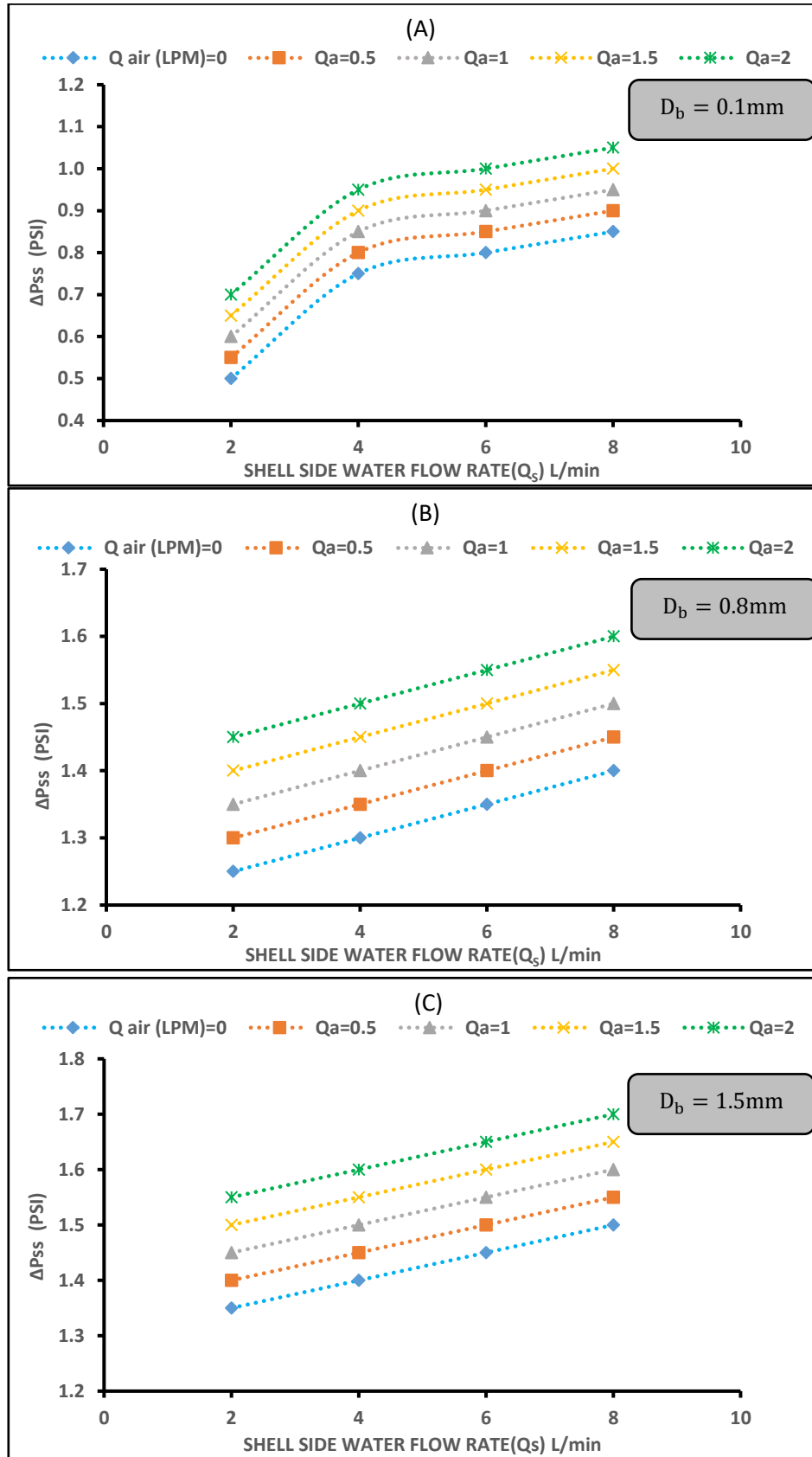
Figure 4.6: explain the varation of shell side pressure drop (Δp_{ss})with and without air injection,at $Q_h = 2$ L/M, air pressure =3 bar.

4.1.5 Influence Air Pressure (p_a) on Thermal Performance of Heat Exchanger

Figure 4.7 demonstrates the impact of varation air pressure value on coil outlet temperature.It was evident from fig 4.7 that the change in the air value has an apparent effect on the temperature of the hot water coming out of the coil; The higher value of the injected air, the lower the temperature of the hot water coming out of the coil. It is also noticeable that it has a more significant effect when it is (0.5 L/min) Because the process of optimizing the hot water coming out the temperature of the coil was done by using the compound technique (smooth helical coil tube plus air injection bubbles) instead of the helical smooth coil tube only. In addition, we note that in the case of ($Q_a = 1,1.5$ and 2 L/min), hot water coming out of the temperature of the coil will decrease by a lower value compared to ($Q_a = 0.5$ L/min) because the optimization process will be calculated compared to the value of the improvement obtained from (compound technique) using the first value of air represented by ($Q_a = 0.5$ L/min). Moreover, air injection pressure appears to have only a minor impact on improving heat transfer.
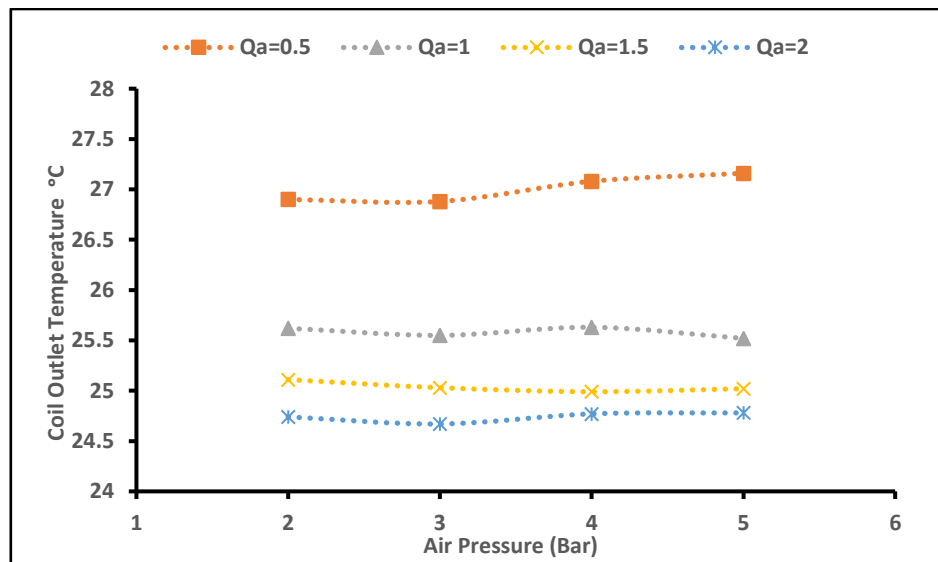
Figure 4.7: effect of variation air pressure on coil outlet temperature,at bubble diameter =1.5 mm$Q_s = 6$ L/min, and $Q_h = 1.5$ L/min.

4.2 Finned Surface Helical Coil Tube Heat Exchanger

4.2.1 Overall Heat Transfer Coefficient (U_f)

Figure 4.8 demonstrates the variation of the overall heat transfer coefficient U_f with the shell side flow rate .Similarly, two other figures (Figs. 4.9 and 4.10) are presented for a different pitch of spiral fins (p_f) (8 and 10 mm) and the same operating conditions in fig 4.8.

The value of (U_f) increases with increasing the Q_s reaches its maximum value at approximately $Q_s = 8$ L/min.at the same time, the overall heat transfer coefficient develops with increasing the injected air flow rate.

Moreover, we concluded from figs 4.8, 4.9, and 4.10 that the value of the overall heat transfer coefficient increases as the bubble diameter increases and decreases the pitch of the spiral fin (p_f), as shown in the following comparison paragraphs 4.4 and 4.5. The reason for this is that when the bubble diameter increases, it will lead to a greater displacement of the fluid than the smaller diameter bubble, leading to an increase in the Reynolds number. the movement of the larger bubble diameter could lead to more diffusion and perfect thermal mixing. So, from all the above reasons, the heat transfer rate increases. Moreover, the results show that the inner coil fins could enhance the heat transfer compared to the smooth spiral tube due to the additional rotational movement (secondary flow). Meanwhile, reducing the distance between the fins will lead to higher heat transfer due to the increase in the number of fins, increasing the surface area of heat transfer. In turn, the outer helical fins destroy the thermal boundary layer formed on the surface of the tube, which increases the heat transfer from the hot to the cold liquid. So,

(U_f) D bubble 0.1 mm < (U_f) D bubble 0.8 mm < (U_f) D bubble 1.5 mm

(U_f) pitch 10 mm < (U_f) pitch 8 mm < (U_f) pitch 5 mm

Indeed, the highest value of (U_f) was 2343 W/m².°C obtained at $Q_a = 2$ L/min, $Q_s = 8$ L/min,(p_f) $=$ (5mm), and bubble diameter (1.5 mm), while

the lowest value of (U_f) Was 1275 W/m².°C obtained at Q_a = 0.5 L/min, Q_s = 2 L/min, (p_f) = (10mm), and bubble diameter (0.1 mm).
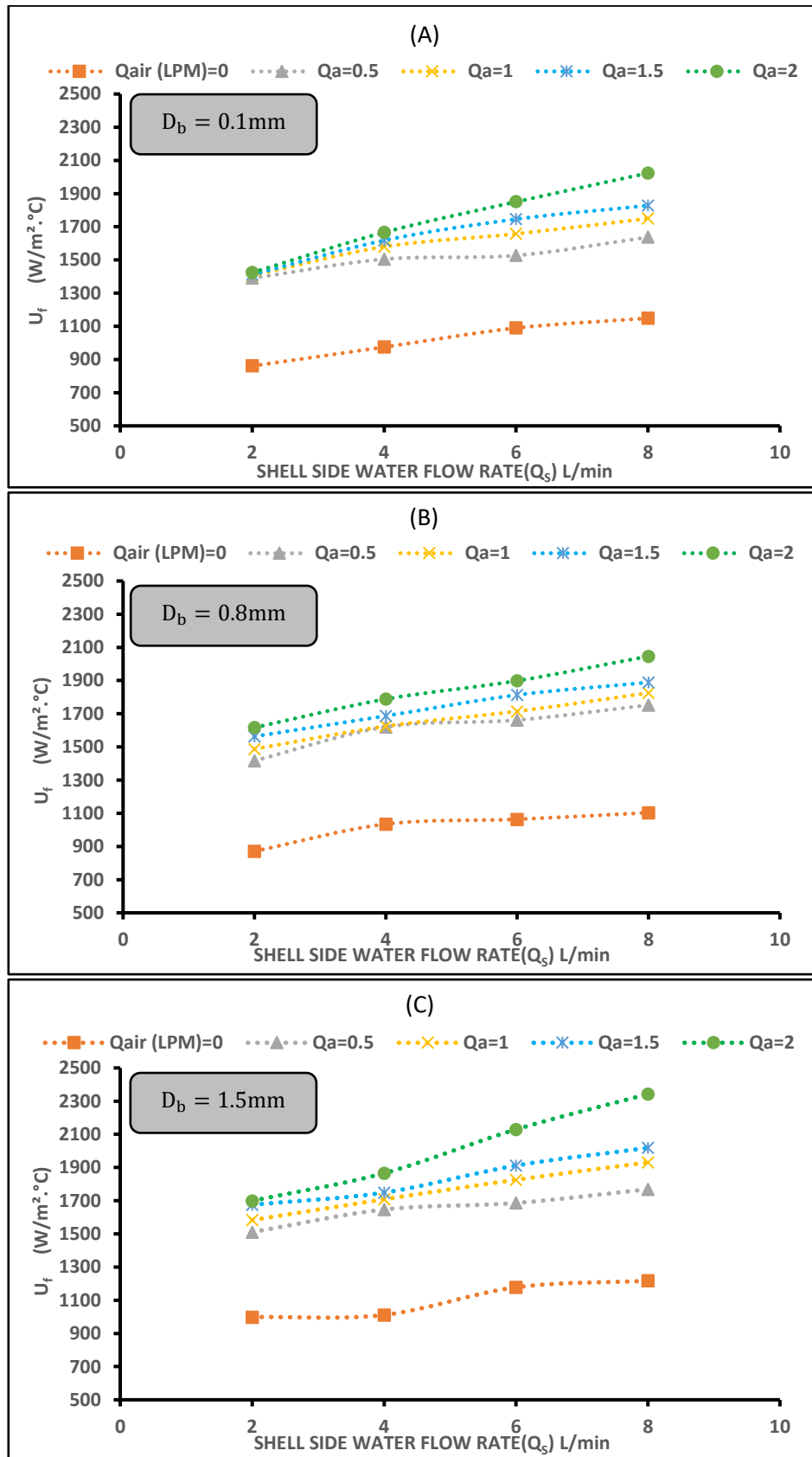
Figure 4.8: Effect of air bubbles injection on the overall heat transfer coefficient (U_f) , $(p_f = 5mm)$, and $p_a = 3$ bar, $Q_h = 1.5$ L/min.

(A)

(B)

(C)
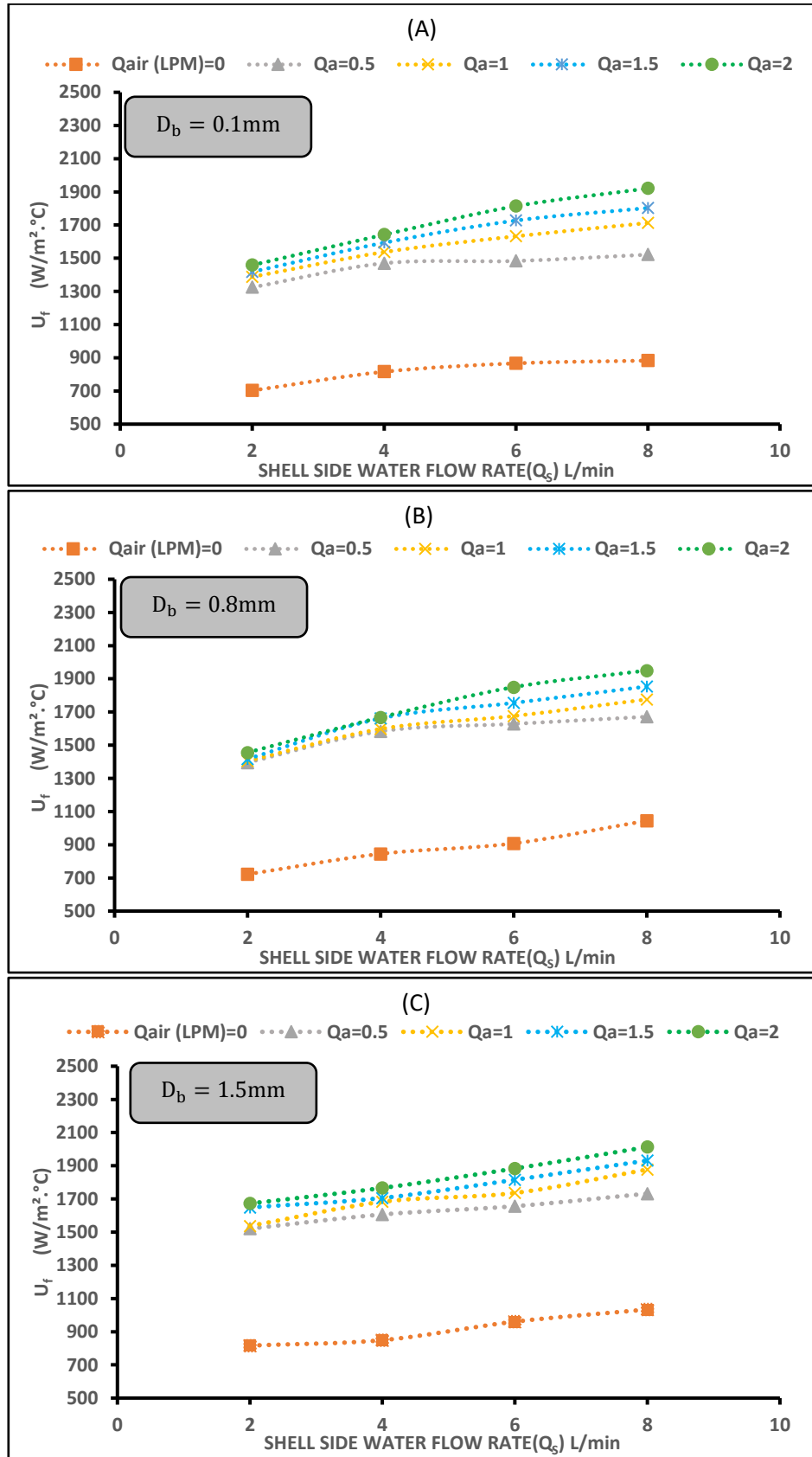
Figure 4.9: Effect of air bubbles injection on the overall heat transfer coefficient (U_f), $(p_f = 8mm)$, and $p_a = 3$ bar, $Q_h = 1.5$ L/min.
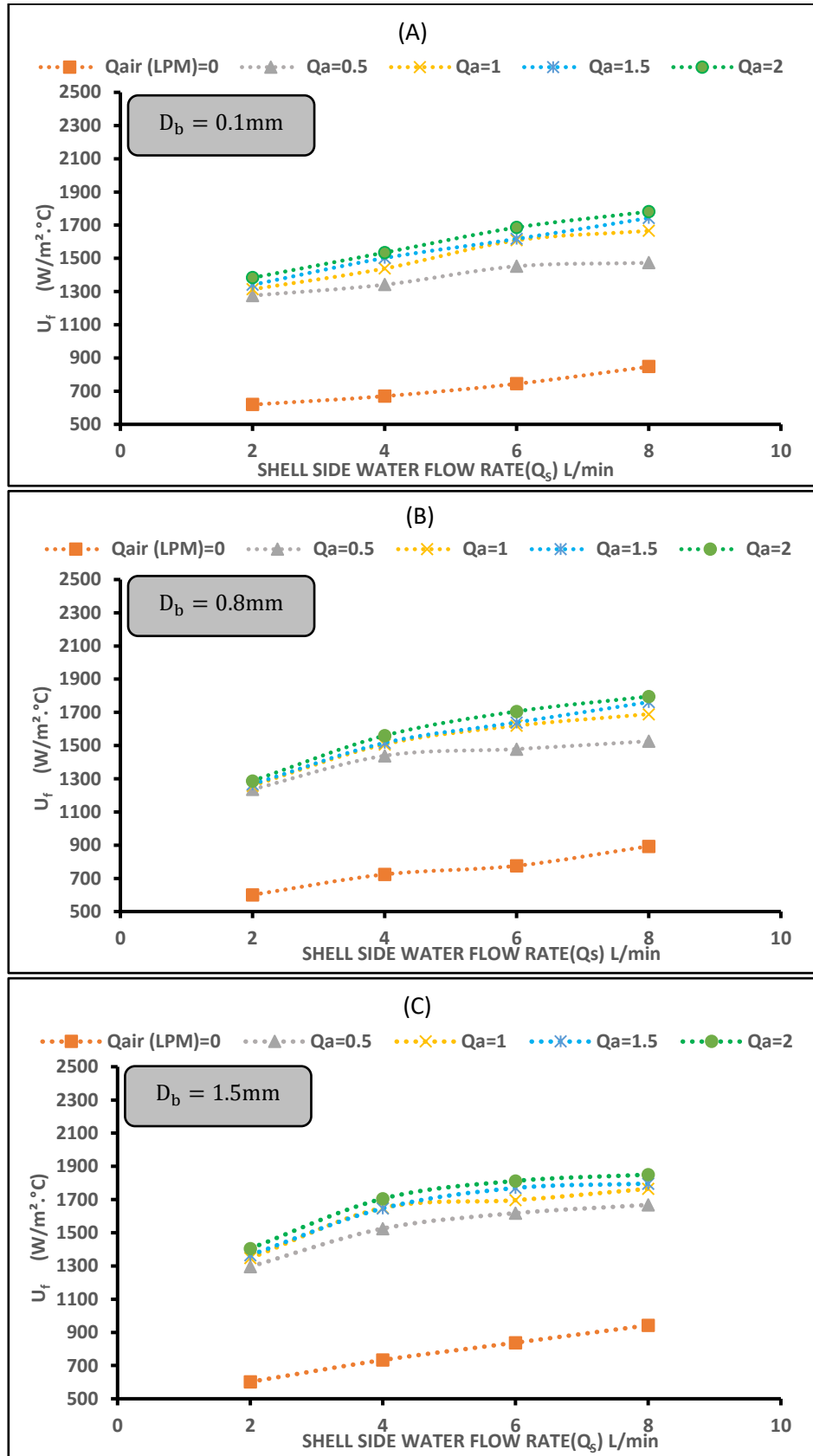
Figure 4.10: Effect of air bubbles injection on the overall heat transfer coefficient (U_f) , $(p_f = 10mm)$, and $p_a = 3$ bar, $Q_h = 1.5$ L/min.

As well as looking at the impact on the measured values of (U_f), it is instructive also to investigate the dimensionless improvement in heat exchanger performance. This is done by considering the enhancement ratio (U_{fa}/U_f) Where (U_f) represents the value of the overall heat transfer coefficient for finned tube in the case without air injection while (U_{fa}) represents the value of the overall heat transfer coefficient for finned tube in the case with air injection.

Figure 4.11 shows the variation of (U_{fa}/U_f) with the shell side flow rate. For all cases measured here, the ratio of (U_{fa}/U_f) Initially increases as the shell side flow rate increases. There is then a clear maximum value at $(Q_s = 4 \text{ L/min})$ and then the enhancement ratio gradually decreases with any subsequent increase of Q_s, as mentioned in paragraph (4.2.1). Nevertheless, even at the highest shell-side flow considered, the ratio (U_{fa}/U_f) It is still significantly greater than one, implying that the performance of the heat exchanger is still superior to the case without air injection.

Additionally, Fig 4.11 shows that (U_{fa}/U_f) Increases with an increase in the airflow rate. Still, in all cases, the maximum enhancement ratio of (U_{fa}/U_f) is clearly obtained at $Q_s = 4 \text{ L/min}, Q_a = 2 \text{ L/min}$, and bubble diameter $= 1.5$mm is 92 %. while the minimum enhancement of (U_{fa}/U_f) is clearly obtained at $Q_s = 8 \text{ L/min}$, $Q_a = 0.5 \text{ L/min}$, and bubble diameter $= 0.1$mm is 38 %. therefore, according to fig 4.11, $(Q_s = 4\text{L/min})$ and $(Q_a = 2 \text{ L/min})$ are the optimal value to enhance the overall heat transfer coefficient of the heat exchanger.

(U_{fa}/U_f) D bubble 0.1 mm $< (U_{fa}/U_f)$ D bubble 0.8 mm $< (U_{fa}/\varepsilon U_f)$ D bubble 1.5 mm
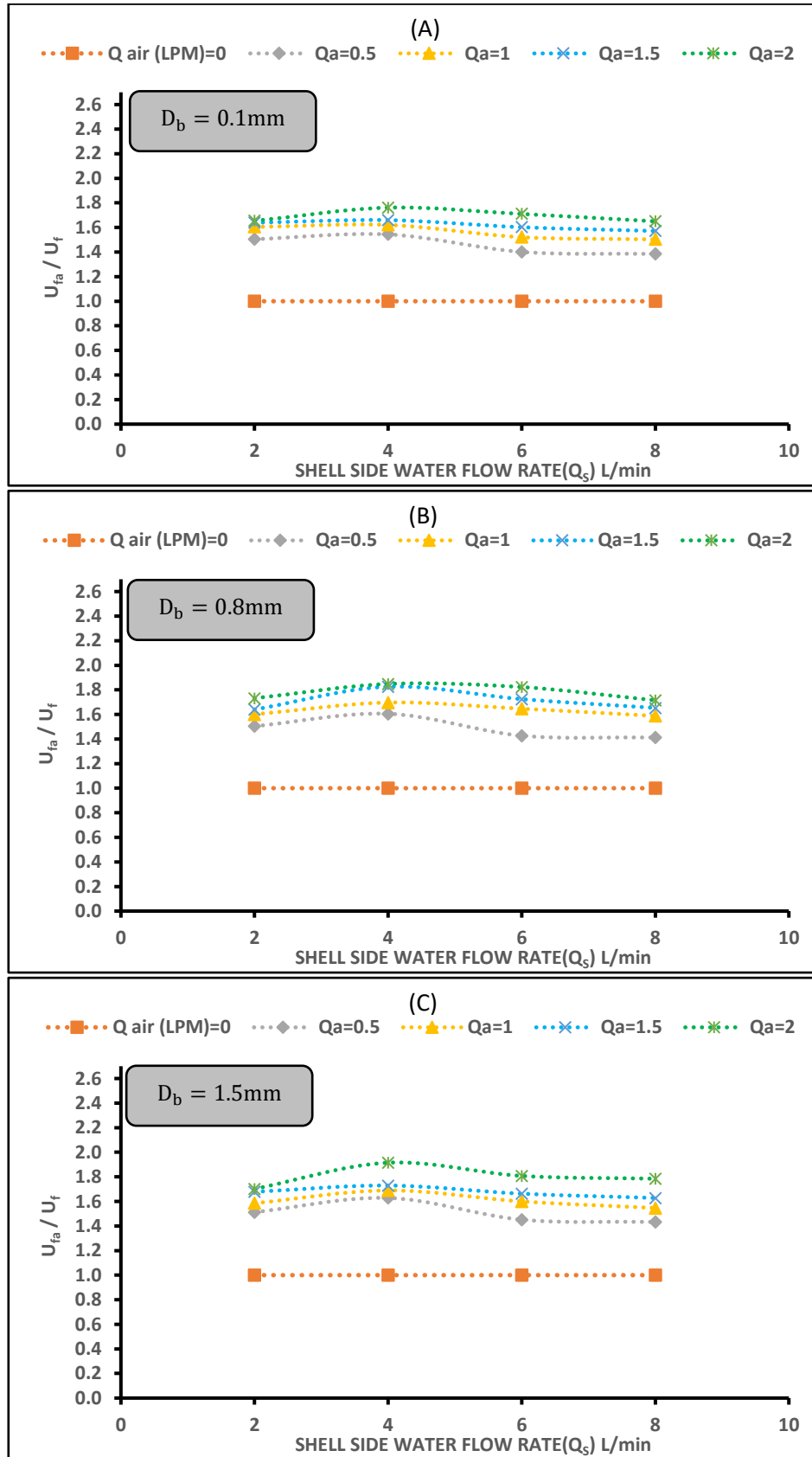
Figure 4.11: Effect of air bubbles injection on the (U_{fa}/U_f) rate, $Q_h = 1.5$ L/min, $(p_f = 5mm)$, and $p_a = 3$ bar.

4.2.2 Effectiveness (ε_f)

Figure 4.12 illustrates the variation of the effectiveness (ε_f) with the shell side flow rate.Similarly, two other figures (Figs. 4.13 and 4.14) are presented for different pitches of spiral fins (8 and 10 mm) and the same operating conditions in fig 4.12.

The value of (ε_f) Increases with increasing the Q_s and reaches its maximum value at approximately $Q_s = 8$ L/min. At the same time, the effectiveness develops by increasing the injected air flow rate. obviously, the value of the injected air seems to give the maximum value at $Q_a = 2$ L/min when $Q_s = 8$ L/min.

We conclude from figs 4.12, 4.13, and 4.14 that the (ε_f) Increases with the bubble diameter increase and decrease the distance between spiral fins, as shown in the following comparison paragraphs (4.4 and 4.5). So,

$$(\mathbf{\varepsilon_f}) \text{ D bubble } 0.1 \text{ mm} < (\mathbf{\varepsilon_f}) \text{ D bubble } 0.8 \text{ mm} < (\mathbf{\varepsilon_f}) \text{ D bubble } 1.5 \text{ mm}$$

$$(\mathbf{\varepsilon_f}) \text{ pitch } 10 \text{ mm} < (\mathbf{\varepsilon_f}) \text{ pitch } 8 \text{ mm} < (\mathbf{\varepsilon_f}) \text{ pitch } 5 \text{ mm}$$

The minimum obtained value of (ε_f) was 0.53 at $Q_a = 0.5$ L/min, $Q_h = 1.5$ L/min,$Qs = 2$ L/min, ($p_f = 10$mm) , and bubble diameter (0.1 mm) .On the other hand, the maximum value of the (ε_f)was 0.77 at $Q_a = 2$ L/min, $Q_h = 1.5$ L/min,$Q_s = 8$ L/min,($p_f = 5$mm), and bubble diameter (1.5 mm).
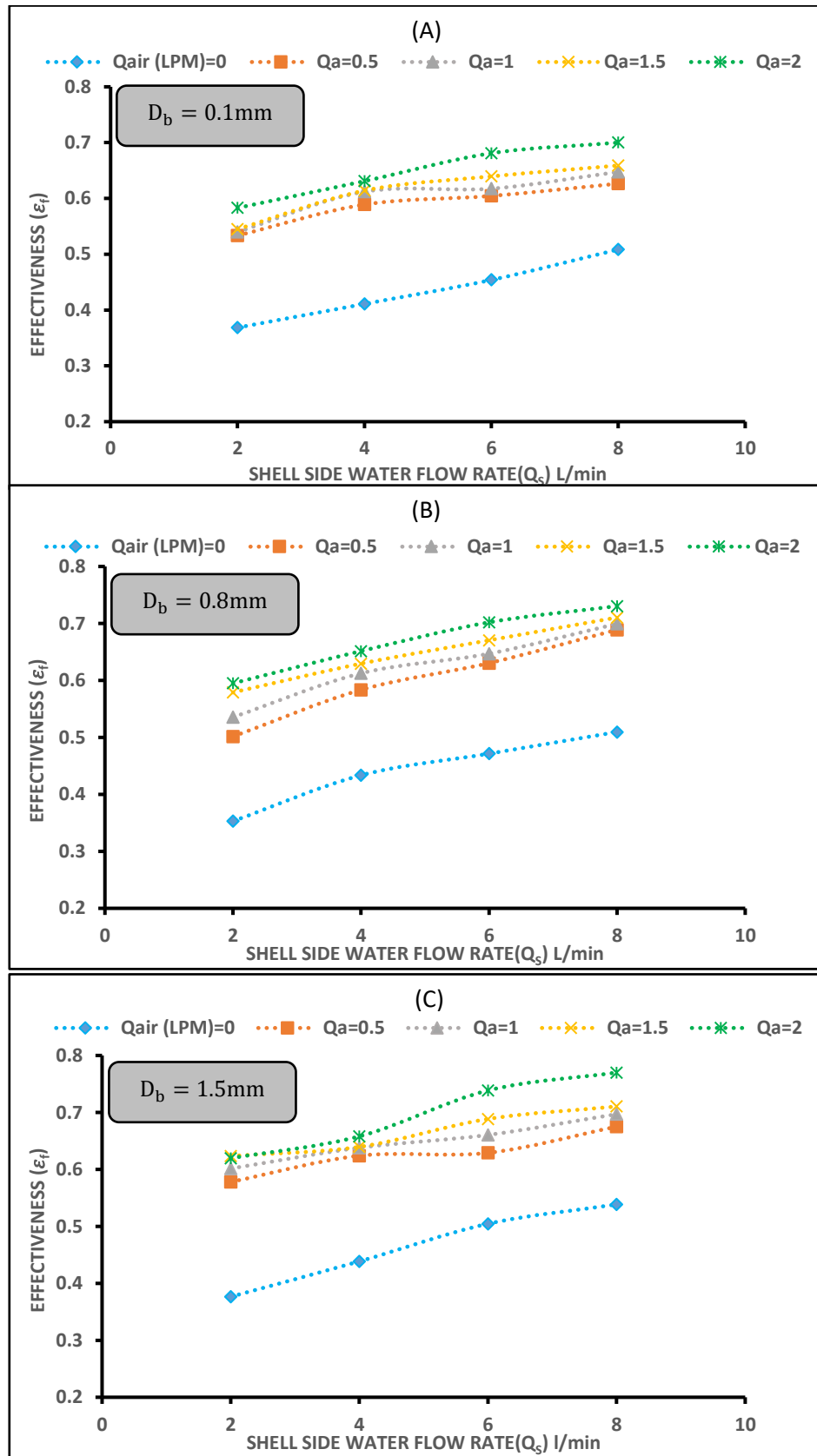
Figure 4.12: Effect of air bubbles injection on (ε_f) at $(p_f = 5mm)$, $Q_h = 1.5$ L/min, and $p_a = 3$ bar).
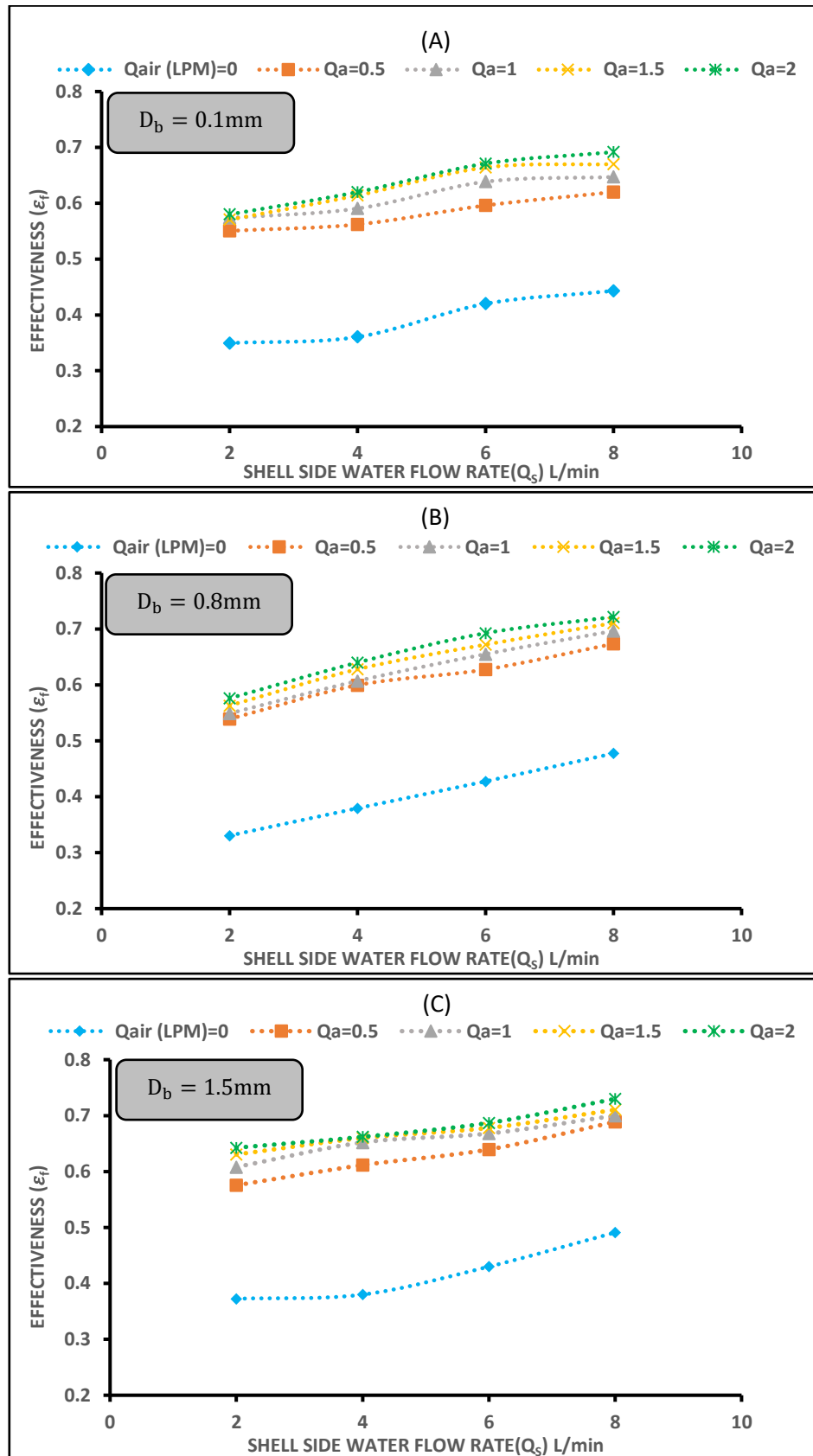
Figure 4.13: Effect of air bubbles injection on (ε_f) at ($p_f = 8$mm), $Q_h = 1.5$ L/min, and $p_a = 3$ bar).
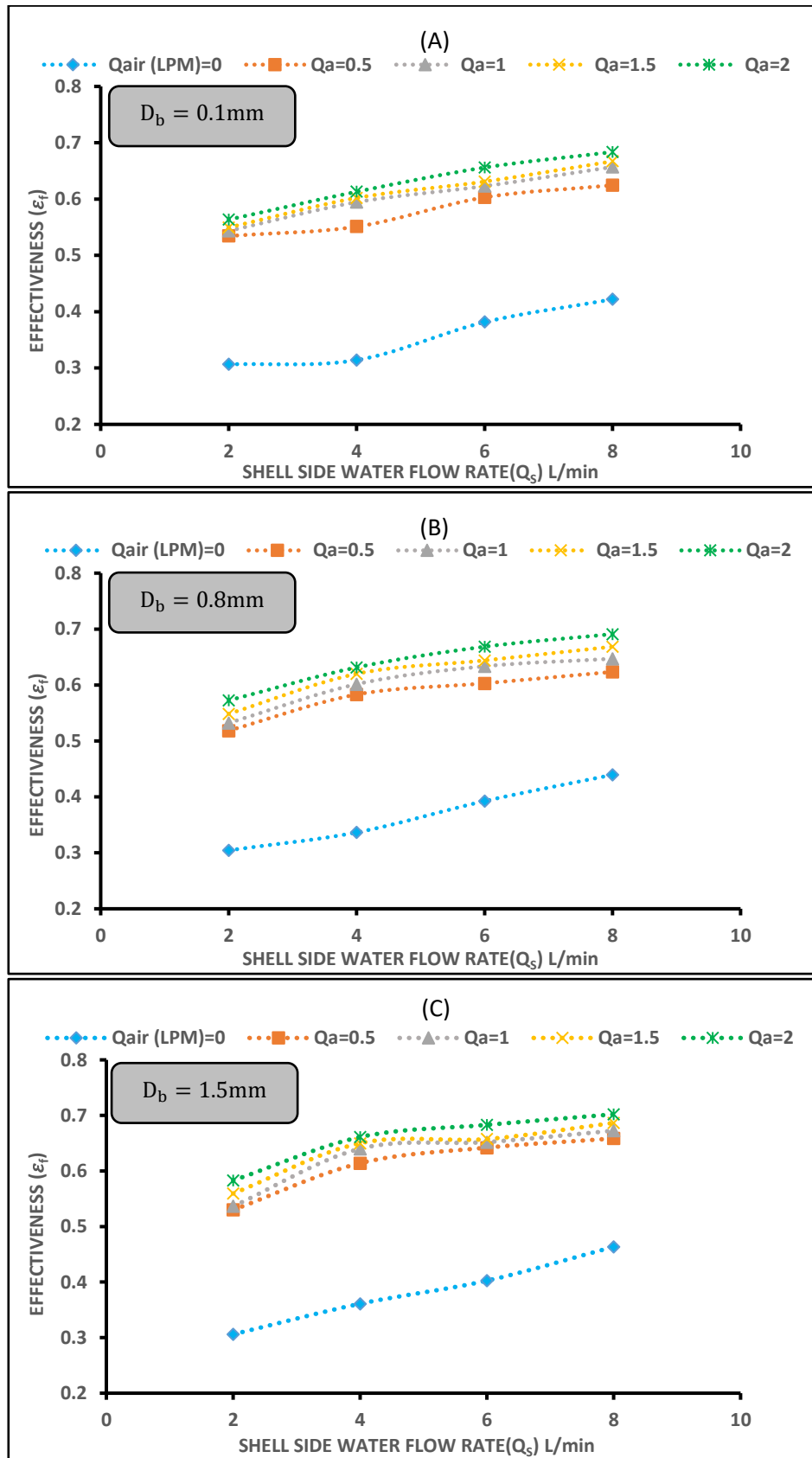
Figure 4.14:Effect of air bubbles injection on (ε_f) at $(p_f = 10mm)$, $Q_h = 1.5$ L/min, and $p_a = 3$ bar).

Lastly, fig. 4.15 demonstrates the relationship between the enhancement ratio of the effectiveness $(\varepsilon_{fa}/\varepsilon_{f})$ and the shell-side flow rate.As seen in fig. 4.15, the slope of $(\varepsilon_{fa}/\varepsilon_{f})$ Is reduced with the increase of the water flow rate. It is noted that the reduction or slope of $(\varepsilon_{fa}/\varepsilon_{f})$ Does not mean the reduction of effectiveness. It just means that the positive effect of air bubble injection on effectiveness has been reduced compared to the increased water flow rate. However, the effectiveness is yet increased. So,

$(\boldsymbol{\varepsilon_{fa}/\varepsilon_{f}})$ D bubble 0.1 mm $< (\boldsymbol{\varepsilon_{fa}/\varepsilon_{f}})$ D bubble 0.8 mm $< (\boldsymbol{\varepsilon_{fa}/\varepsilon_{f}})$ D bubble 1.5 mm

The minimum enhancement obtained value of $(\varepsilon_{fa}/\varepsilon_{f})$ was 1.23 at $Q_a = 0.5$ L/min, $Q_s = 8$ L/min , and bubble diameter (0.1 mm).On the other hand,the maximum value of the $(\varepsilon_{fa}/\varepsilon_{f})$ was 1.71 at $Q_a = 2$ L/min, $Q_s = 4$ L/min, and bubble diameter (1.5 mm).therefore,according to Fig 4.15, $(Q_s = 4$ L/min) and $(Q_a = 2$ L/min) are the optimal value to enhance the effectiveness of the heat exchanger.
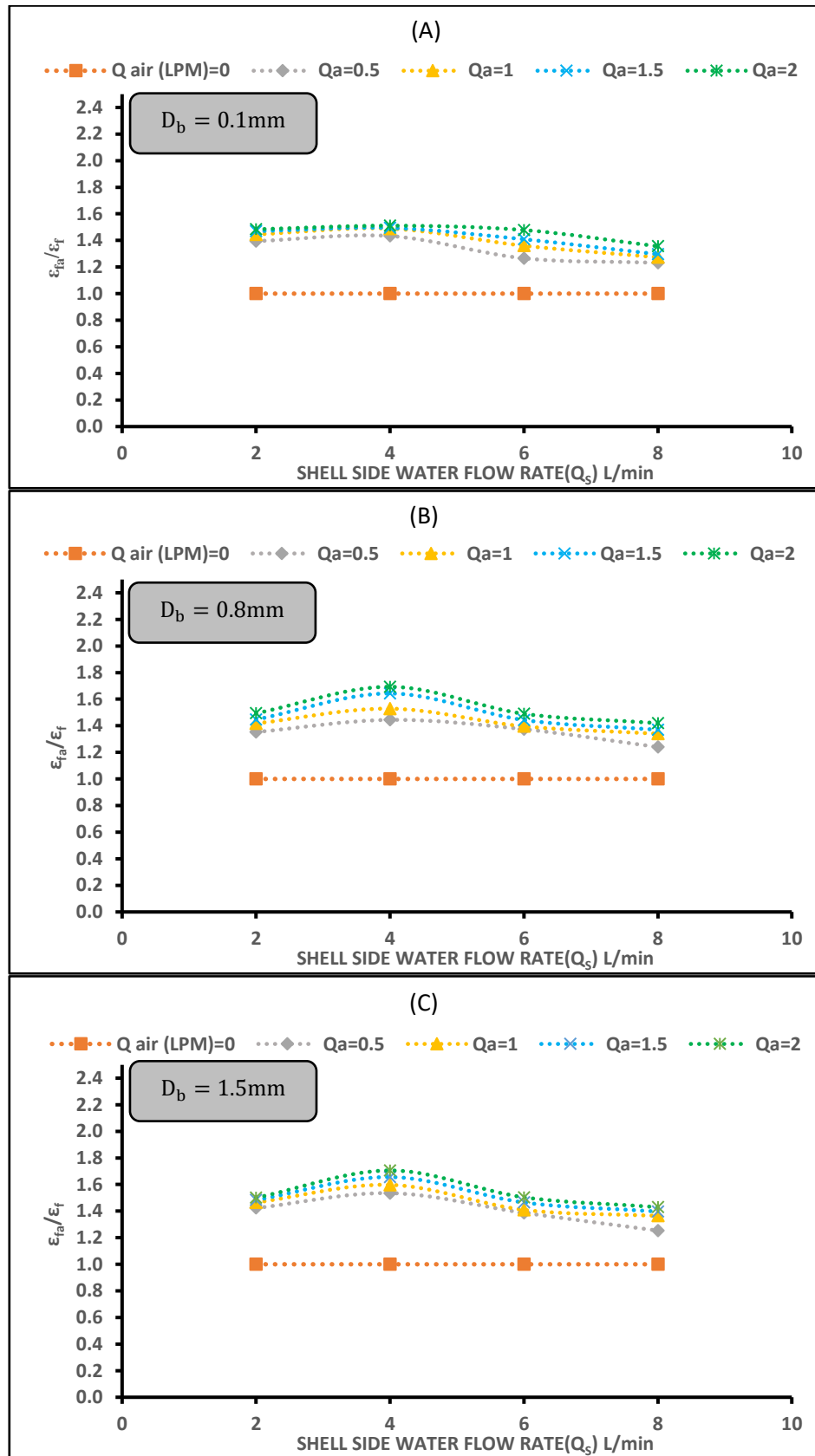
Figure 4.15: Effect of air bubbles injection on the $(\varepsilon_{fa}/\varepsilon_{f)}$ at , $Q_h = 1.5$ L/min, (p_f = 5 mm),and $p_a = 3$ bar.

4.2.3 Pressure Drop (Δp_{sf})

Figure 4.16 illustrates the effect of bubble diameter on the pressure drop (Δp_{sf}) .Evidently, the bigger bubble diameter led to a rise in pressure drop along the heat exchanger's shell side. Therefore, this may be attributed to an increase in the shell side Re as the diameter of the bubble increases. In addition, the fins added to the surface of the helical coil tube will obstruct the flow of water inside the shell, added to the effect of bubbles on pressure drop, which leads to an increase in pressure drop more than in the case of a smooth coil (Δp_{ss}).

Moreover, the experimental findings revealed that the highest increase in pressure drop caused by the injection of air bubbles was 1.85 psi when $Q_a =$ 2 L/min at the water flow rate, $Q_s = 8$ L/min, and bubble diameter=1.5 mm. on the other hand, the minimum value of the pressure drop due to the injection of air bubbles, was 0.75 psi as $Q_a = 0.5$ L/min at the water flow rate, $Q_s = 2$ L/min, and bubble diameter $= 0.1$ mm.
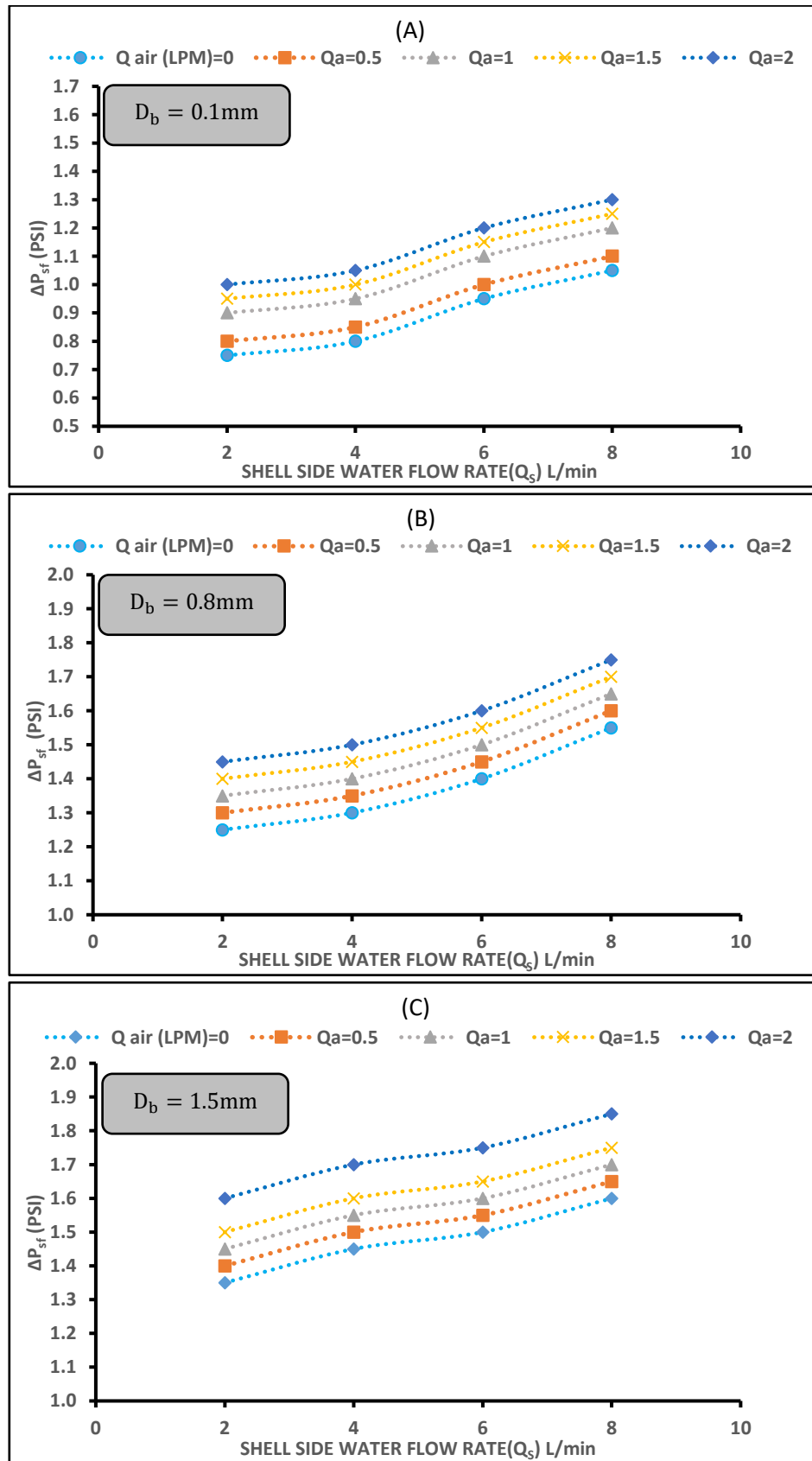
Figure 4.16: effect shell side water flow rate on pressure drop (Δp_{sf}) at $Q_h = 1.5$ L/min, $P_f = 5$ mm, and $P_a = 3$ bar.

4.3 Effect Bubble Diameter (D_b) on Thermal Performance of Heat Exchanger in Smooth and Finned Tube helical coil

As mentioned earlier, one of the main aims of the present study is to investigate, for the first time, the effect of air bubble diameter on the thermal performance of the helical coiled (smooth and finned) tube heat exchanger. To do so, three different bubble diameters were tested (0.1 mm, 0.8 mm, and 1.5 mm) at the same operational conditions.

4.3.1 Effect of Bubble Diameter (D_b) On (U) In Smooth and Finned Helical Coil Tube Heat Exchanger

Figure 4.17 demonstrates the variation of U with the shell side flow rate of (smooth and finned p_f = 5 mm) tube.Obviously, the bubble diameter has contributed to improving the heat exchanger thermal performance. The larger bubble diameter, the higher the thermal efficiency was. This is agreed with the CFD results of **[59]**. However, one can justify the current behavior by increasing the shell side Re, which is an essential and more effective parameter for the overall heat transfer process. The contribution of thermal mixing due to the bubble motion in the overall thermal enhancement is only minor as the size of the water bulk in the shell is much larger than the heat source (coil). That means the larger bubble diameter can push or displace more liquid than the small ones, which results in a more significant increase in the shell side Re, leading to more heat transfer enhancement.
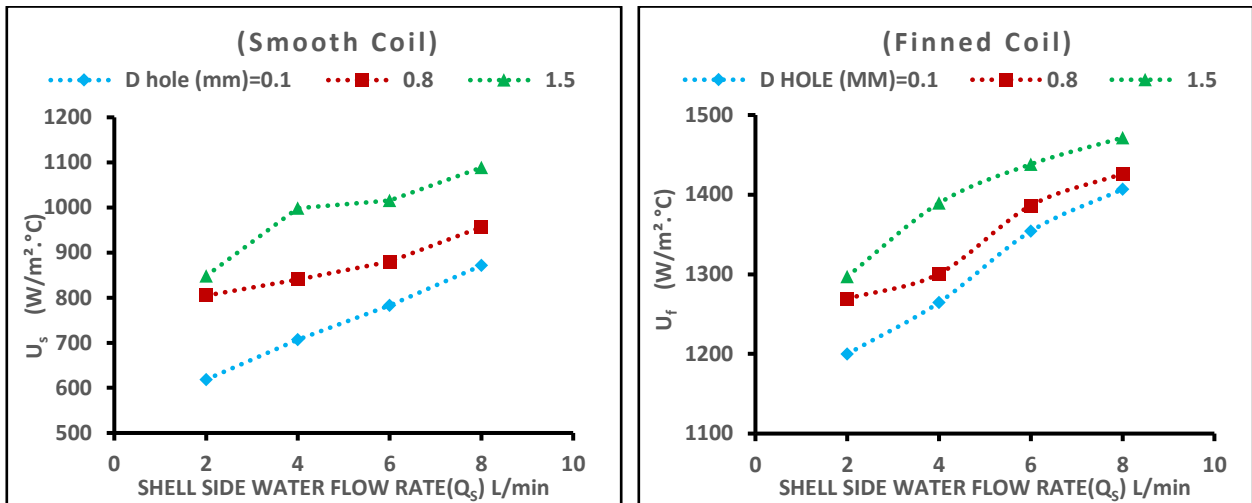
Figure 4.17: Effect of bubble diameter on (U_s, U_f) at $Q_a = 0.5$ L/min, $Q_{ah} = 1$ L/min,and $P_a= 3$bar.

4.3.2 Effect of Bubble Diameter (D_b) On (ε) In Smooth and Finned Helical Coil Tube Heat Exchanger

Figure 4.18 illustrates the effectiveness varies with the shell side flow rate of the three different bubble diameters (0.1,0.8 and 1.5 mm) and the same operational conditions of fig.4.17. Similar to the variation of U (see fig 4.17) appears in fig. 4.18. The improvement of effectiveness is evident with increasing the shell side flow rate and with increasing bubble diameter. This is consistent with our justification above.
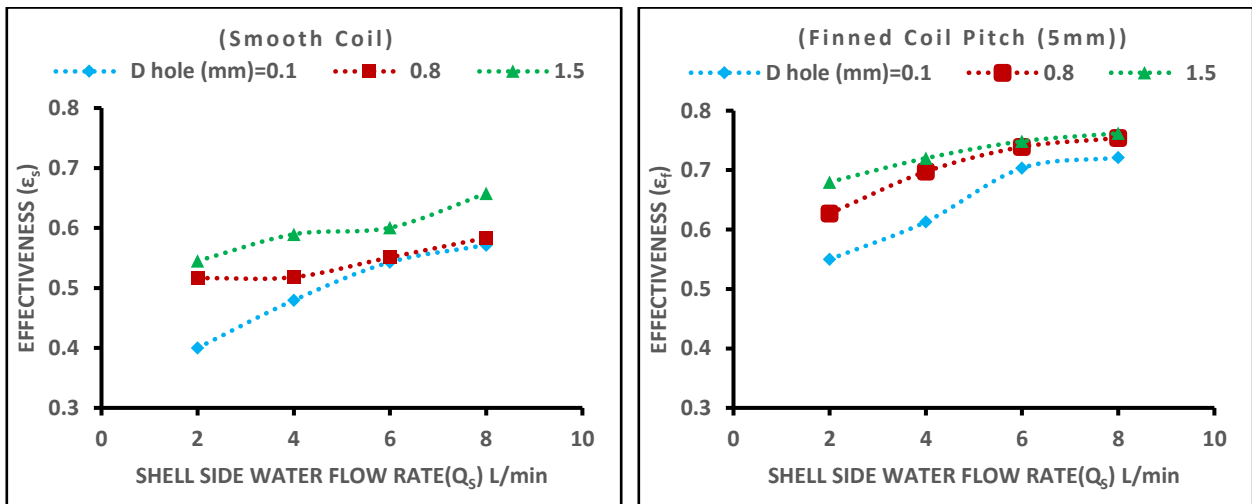
Figure 4. 18: Effect of bubble diameter on the effectiveness $(\varepsilon_s, \varepsilon_f)$ at $Q_a = 0.5$ L/min, $Q_h = 1$ L/min,and $P_a= 3$bar.

4.3.3 Effect of Bubble Diameter (Db) On(Δp) In Smooth and Finned Helical Coil Tube Heat Exchanger

The effect of bubble diameter on the pressure drop inside the shell of (smooth and finned tube) is given in Fig. 4.19. For the same operational condition used in figs 4.17 and 4.18. Obviously, the increased bubble diameter led to a development in pressure drop along the heat exchanger's shell side. As we mentioned before, this could be mainly due to the increase in the shell side Re with increasing the diameter of bubbles. Surprisingly, the bubble with a diameter of 1.5 mm and 0.8 mm has nearly the same effect on the pressure drop, contrary to the thermal improvement.
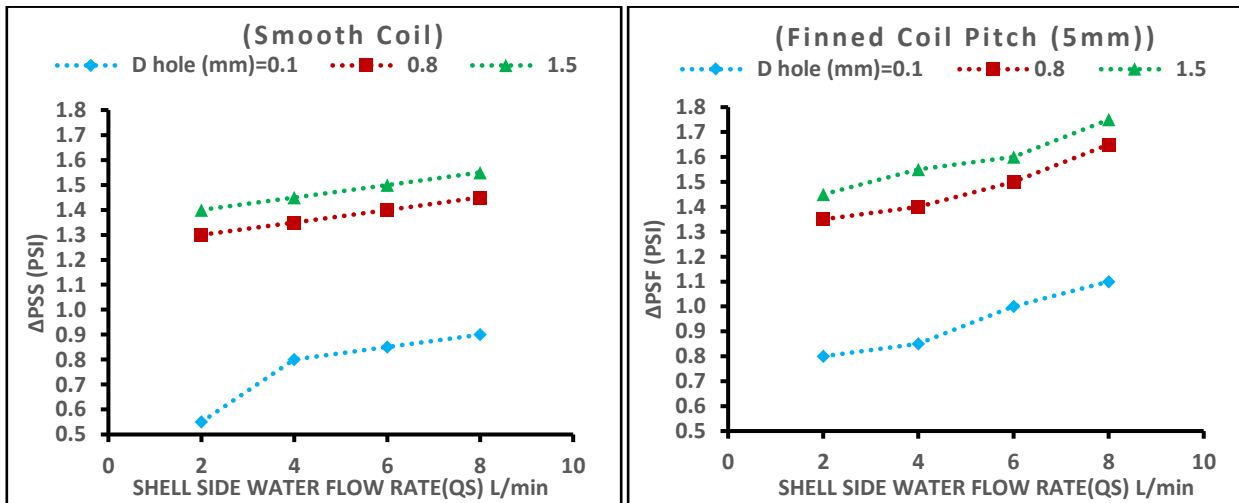
Figure 4. 19: Effect of bubble diameter on the pressure drop inside shell $(\Delta p_{ss}, \Delta p_{sf})$ at $Q_a = 0.5$ L/min, $Q_h = 1$ L/min,and $P_a= 3$bar.

Furthermore, we found that the pressure drop (Δp_{sc}) in the helical coil smooth tube is less than the pressure drop (Δp_{fc}) in the helical coil finned tube and vary according to the hot coil flow rate as shown in table (4.1).

Table 4.1: variation pressure drop $(\Delta p_{sc}, \Delta p_{fc})$ inside smooth and finned helical coil tube

Type of tube	Pitch fin	Hot water (L/min)	Δp (psi)
smooth helical coil	smooth	1	3.55
		1.5	3.7
		2	3.85
finned helical coil	5 mm	1	5.65
		1.5	5.75
	8 mm	1	5.5
		1.5	5.6
	10 mm	1	5
		1.5	5.5

4.4 Comparison of The Overall Heat Transfer Coefficient (U_s, U_f) In the Helical Coil (Smooth and Finned) Tube Heat Exchanger

Figure 4.20 states the effect of injection air bubbles on the overall heat transfer coefficient (U_s, U_f) .As mentioned previously, the injection of air into the water will generate bubbles inside the cold water. As a result of the difference in density between the water and the air, the bubbles will move vertically to the top. As a result of the movement of the bubbles, the turbulence will increase inside the shell. As a result, the thermal layers formed on the surface of the helical coil tube will be destroyed, which is one reason to increase the transfer of heat from hot water to cold water. The second main reason is the increase in cold water velocity due to injecting the bubbles into a shell, increasing the Reynolds number, subsequently increasing the heat transfer rate.

Similarly, when using spiral fins, the inner fins will cause an additional rotational movement (secondary flow) inside the hot water pipe. In contrast, the outer fins will act as barriers to break down the thermal layer formed on the surface of the

helical tube, which will increase the rate of heat transfer between the two liquids. Regarding pitch (p_f), the smaller pitch means the number of fins increases on the surface of the tube, which increases the surface area for heat transfer.

It can be concluded from Figs 4.20 and 4.21 that the highest improvement ratio of the overall heat transfer coefficient (U_f/U_s) for (p_f) (5,8, and 10mm) was (107%, 73%, 49%), respectively, and (U_{fa}/U_s) for (p_f) (5,8, and 10mm) was (281%, 261%, 248%) respectively.
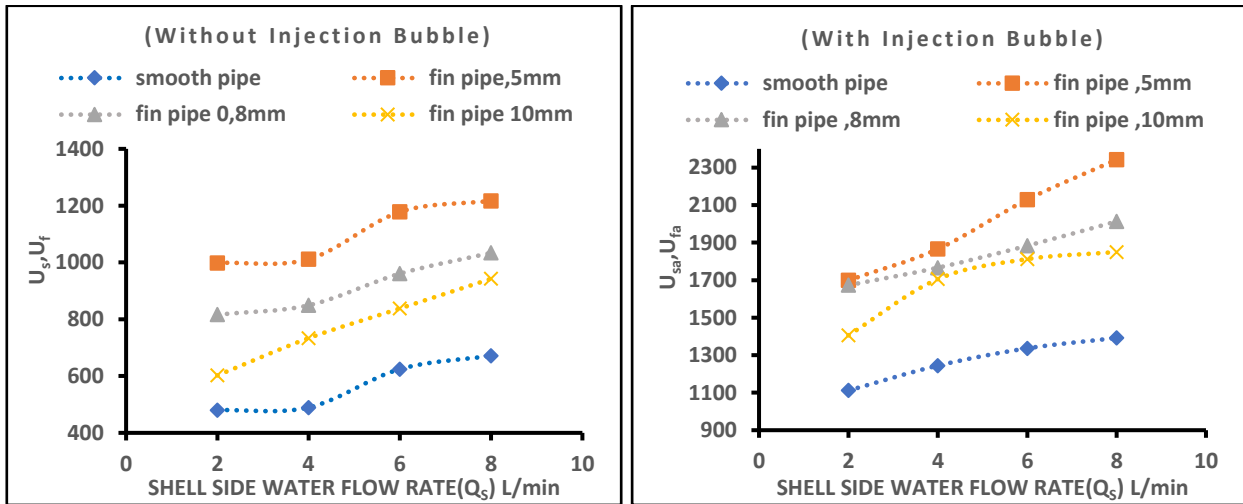
Figure 4.20: Comparison of overall heat transfer coefficient (U_s, U_f) $Q_h = 1.5$ L/min, $P_a = 3$bar, and $D_b = (1.5$mm).
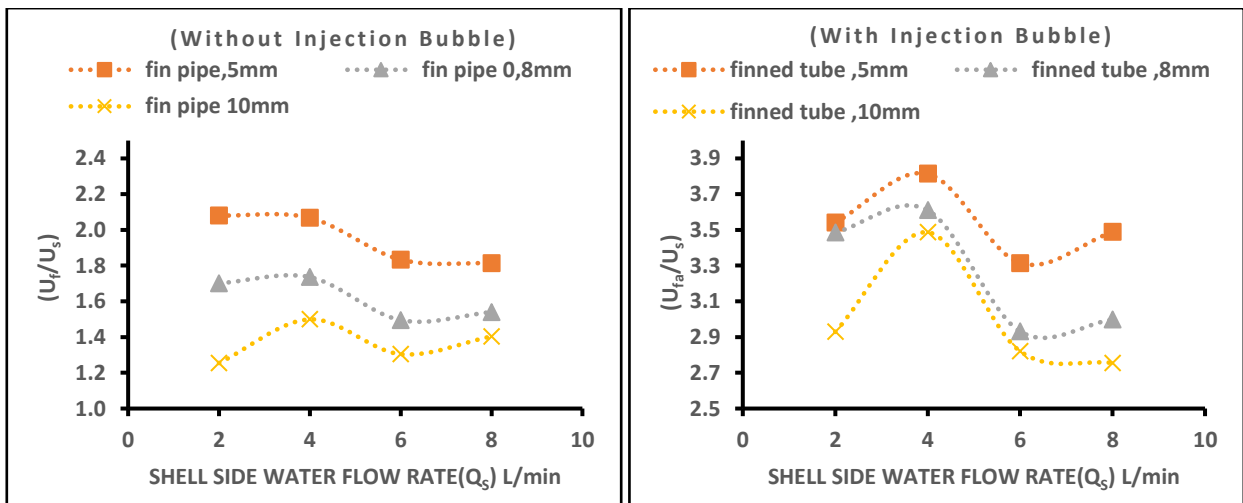
Figure 4.21: explained the highest improvement ratio of the (U_f/U_s), and (U_{fa}/U_s) at $Q_h = 1.5$ L/min, $P_a = 3$bar, and $D_b = (1.5$mm).

4.5 Temperature Distribution Along Vertical Shell and Helical Coil (Smooth, Finned) Tube Heat Exchanger

The present section tries to clarify the behavior of the temperature distribution along the heat exchanger to helical coil (smooth and finned) tube together, which has not been addressed in the literature. Four thermocouples were installed in equal space along the shell side of heat exchange; in addition to four thermocouples were used to measure the inlet and outlet temperatures of hot and cold water (see Figs 3.1, 3.2).

Figures 4.22 to 4.25 illustrate the transient temperature distribution along the shell side in addition to the coil side temperature for the smooth and finned helical coil tube heat exchanger.The obtained results showed that a mutual thermal mixing took place once the air as tiny bubbles was injected into the heat exchanger's shell side. Hence, a high heat transfer rate was obtained, which was indicated by the sudden rising temperature along the heat exchanger. Moreover, it was observed that the time is taken to reach temperature stability along the heat exchanger in both tube states (smooth and finned) before bubble injection ranged from (20 to 25 min).

In general, while the inlet temperature of the coil and shell remains constant during the whole process (35^0C and 15^0C), respectively, the injected air as bubbles in the shell side results in a sudden change in the temperature along the heat exchanger. Obviously, the temperature distribution increases directly once the air is injected ($Q_a = 0.5$ L/min) into the shell side. However, this rises in temperature is developed with the increased airflow rate until achieving the steady-state conditions at the end. Along with this, the outlet temperature of the coil (hot fluid) is consistently decreased with time until reaching its minimum value but the invariant value at the end of the individual run. Although the increase in the temperature along the heat exchanger is distinctive at a low airflow rate ($Q_a = 0.5$ L/min), the temperatures become almost closest to each other at all points along the height with increasing the airflow rate. This could indicate that the natural movement of air bubbles due to bouncy force, which results from the difference in density between air and water,

leads to intensive thermal mixing of the water inside the shell. Such behavior of the temperature leads to sustain the temperature difference at its maximum level. This, of course, leads to increased heat exchange between the hot and the cold fluid and increases the heat exchanger's thermal performance.

The figures 4.22 to 4.25 show that the transient time to reach a steady state of temperature in the case of the smooth tube is higher than the finned tube, as is the case for the difference in the distance between the spiral fins in the tube, it was found that the smaller distance between the fins, the less transient time due to effect of fins and number of it. Furthermore, the more miniature coil outlet temperature obtains at finned tube pitch (5mm).

(Transient time) smooth tube > (Transient time) finned tube

$$(\text{Transient time})(P_f = 10\text{mm}) > (\text{Transient time})(P_f = 8\text{mm}) > (\text{Transient time})(P_f = 5\text{mm})$$
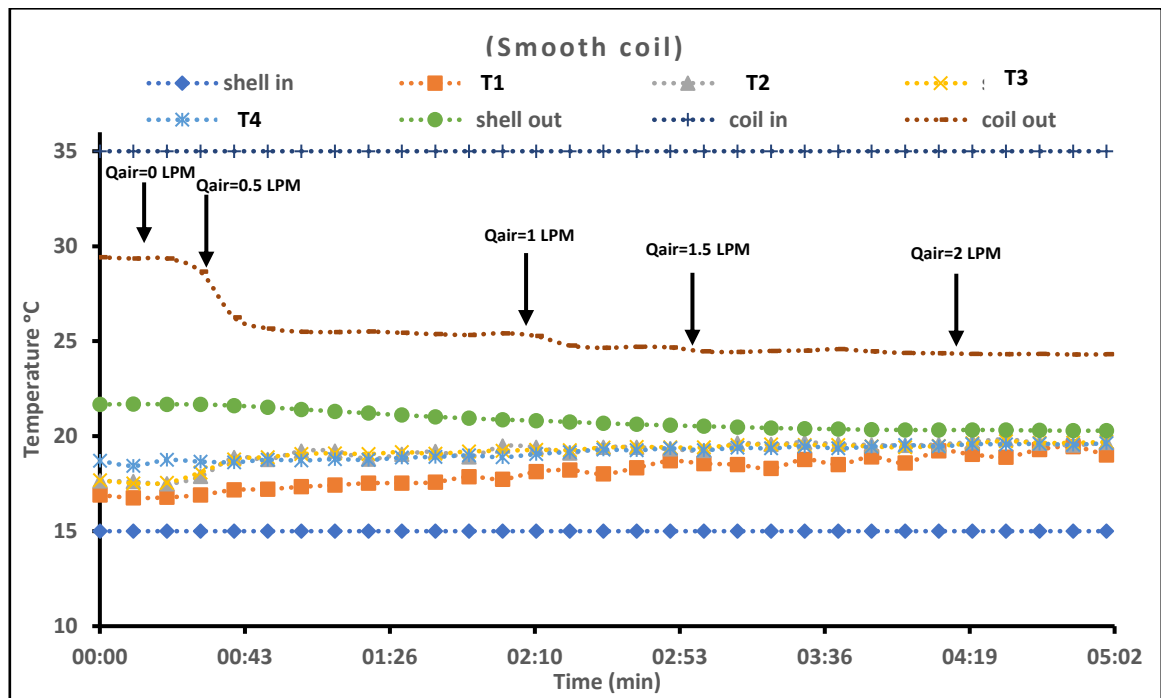
Figure 4.22: Temperature distribution with time along heat exchanger at, $D_b = 1.5\text{mm}$, $Q_h = 1.5\ \text{L/min}$, $Q_s = 6\ \text{L/min}$, and $P_a = 3\text{bar}$.
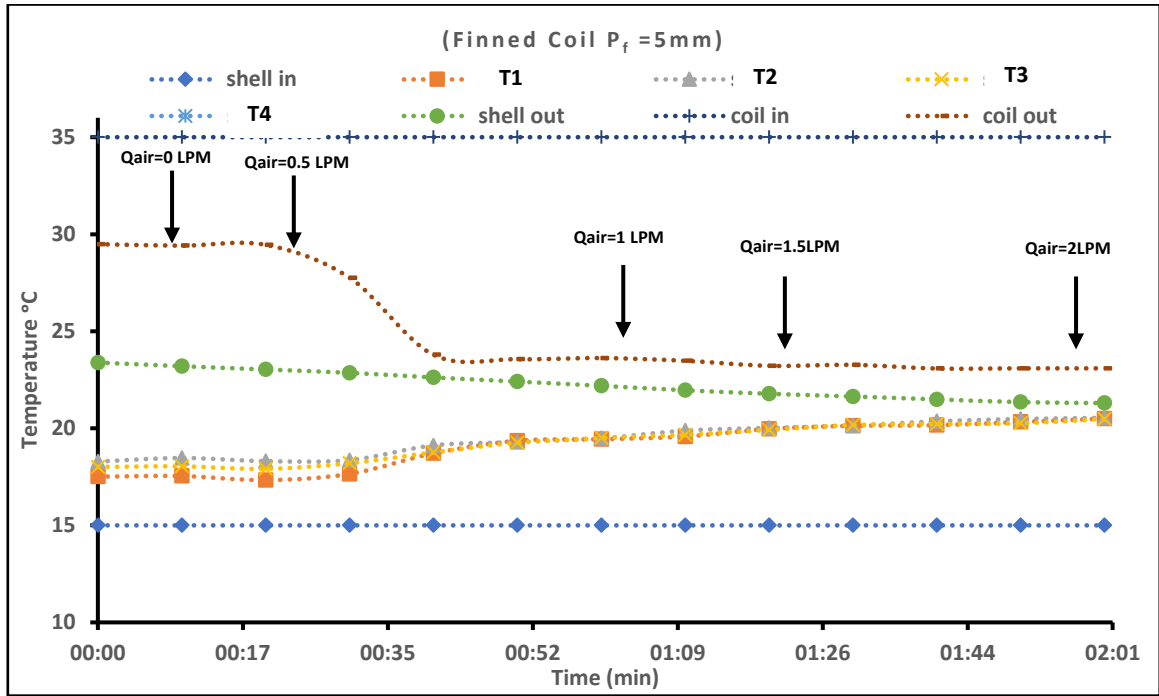
Figure 4.23: Temperature distribution with time along heat exchanger at, $D_b =$ 1.5mm, $Q_h = 1.5$ L/min, $Q_s = 6$ L/min, $P_a= 3$bar ,and $P_f = 5$mm .
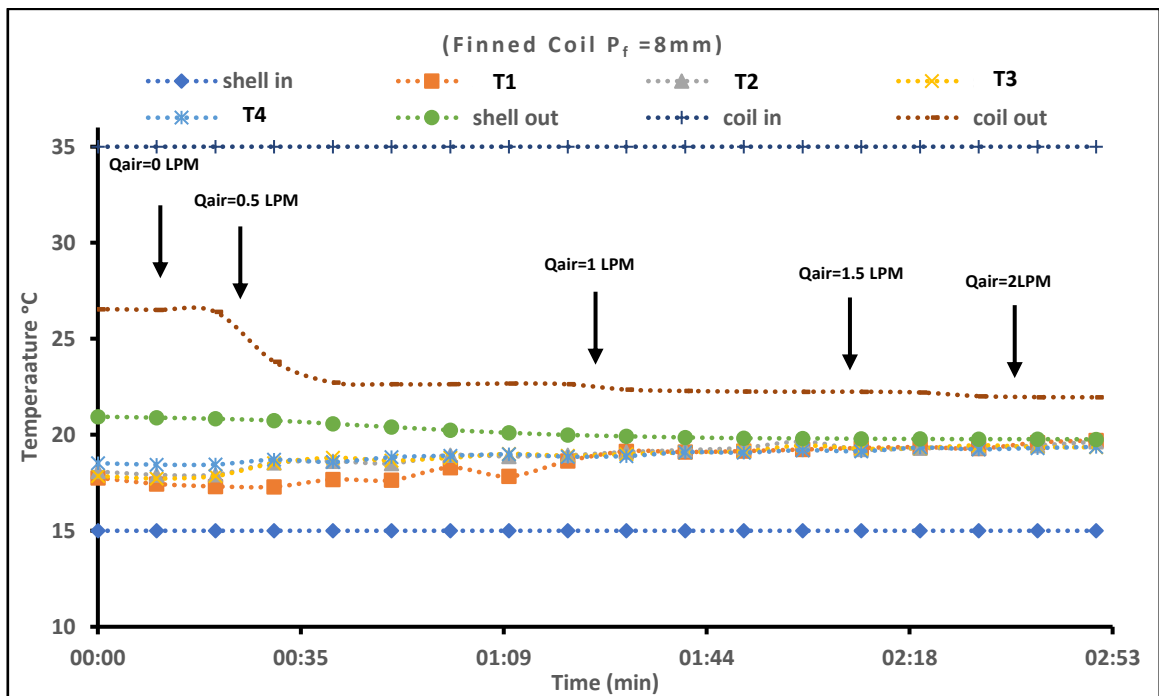
Figure 4.24: Temperature distribution with time along heat exchanger at, $D_b =$ 1.5mm, $Q_h = 1.5$ L/min, $Q_s = 6$ L/min, $P_a= 3$bar ,and $P_f = 8$mm .
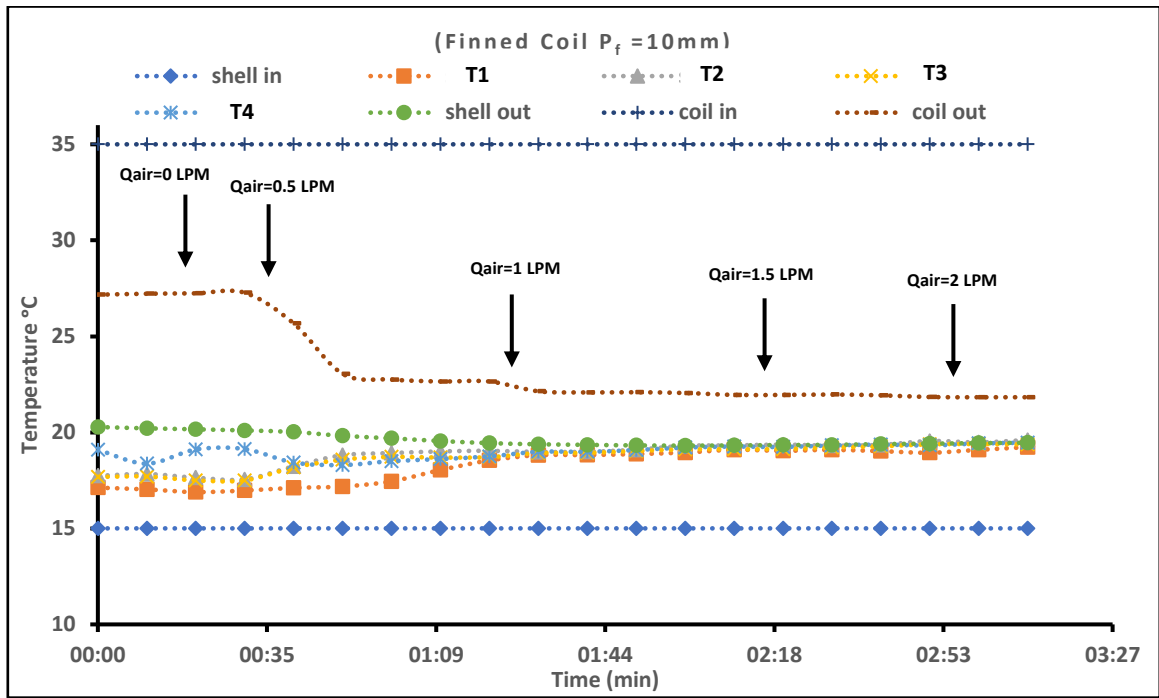
Figure 4.25:Temperature distribution with time along heat exchanger at, D_b = 1.5mm, Q_h = 1.5 L/min, Q_s = 6 L/min, P_a= 3bar ,and P_f = 10mm.

Chapter Five

Conclusions and Recommendations

CHAPTER FIVE

CONCLUSIONS AND RECOMMENDATIONS

INTRODUCTION

The current study aims to investigate the effect of tiny air bubble injection on the thermal performance of a counter-current flow for vertical shell and helically coil (smooth and finned) tube heat exchanger experimentally in laminar flow ($316 \leq$ Re ≤ 1523). The investigation involves heat transfer characteristics such as overall heat transfer coefficient (U), effectiveness (ε), air pressure (p_a) effect on the thermal performance of heat exchanger, pressure drop (Δp), and temperature distribution along the heat exchanger column.

5.1 conclusions

The experimental findings of the current work, presented in Chapter 4, demonstrated that the injection of air bubbles dramatically improves the thermal performance of a vertical shell and helically (smooth and finned) coiled tube heat exchanger. According to the obtained results, the following conclusions can be drawn.

1. Air bubbles injection into the shell side of the helically coiled tube heat exchanger results in a significant improvement in the overall heat transfer coefficient (U_s) and effectiveness (ε_s) for all cases under study. However, depending on the Qa and Qs, the maximum enhancement ratio of (U_{sa}/U_s) was up to 152 %, and ($\varepsilon_{sa}/\varepsilon_s$) was 111% compared with pure water (without bubble injection). The aforesaid maximum enhancement ratios were achieved when diameter bubble=1.5mm, $Q_s = 6$ L/min $Q_a = 2$ L/min, and $Q_h = 2$ L/min, While the minimum enhancement ratio of (U_{sa}/U_s) was 56%, and ($\varepsilon_{sa}/\varepsilon_s$) was 34%. Foresaid

2. minimum ratio occurred at diameter bubble=1.5mm, $Q_s = 8$ L/min, $Q_a = 0.5$ L/min, and $Q_h = 1$ L/min.

3. The amount of (U_{sa}/U_s) It decreases as the volume fraction increases. Moreover, the highest improvement ratio (U_{sa}/U_s) occurred at $Vd = 0.25, Q_a = 2$ L/min, $Q_s = 6$ L/min, and $Q_h = 2$ L/min, while, the lowest improvement ratio (U_{sa}/U_s) occurred at $Vd = 0.05, Q_a = 0.5$ L/min, $Q_s = 8$ L/min, and $Q_s = 1$ L/min.

4. The shell side pressure drop $(\Delta p_{ss}, \Delta p_{sf})$ It was found to be increased with increasing the airflow rate and bubble diameter. The maximum increment in pressure drop (Δp_{ss}) value due to the air injection was 1.7 psi at $Q_a = 2$ L/min, $D_b = 1.5$ mm, and $Q_s = 8,$ L/min .while the minimum increment in pressure drop value was 0.5 psi at $Q_a = 0.5$ L/min, $D_b = 0.1$ mm, and $Q_s = 2$ L/min.furthermore, The maximum increment in pressure drop (Δp_{sf}) value due to the air injection was 1.85 psi at $Q_a = 2$ L/min, $D_b = 1.5$ mm, and $Q_a = 8$ L/min.while the minimum increment in pressure drop value was 0.75 psi at $Q_a = 0.5$ L/min, $D_b = 0.1$ mm, and $Q_a = 2$ L/min.

5. The variation of air injection pressure (p_a) the value appears to have only a minor impact on improving heat transfer.

6. The maximum enhancement ratio of (U_{fa}/U_f) is clearly obtained at $Q_s = 4$ L/min, $Q_a = 2$ L/min, and $D_b = 1.5$mm is 92 %. and the minimum enhancement of (U_{fa}/U_f) is clearly obtained at $Q_s = 8$ L/min, $Q_a = 0.5$ L/min, and $D_b = 0.1$mm is 38 %. while the minimum enhancement obtained value of $(\varepsilon_{fa}/\varepsilon_f)$ was 23% at $Q_a = 0.5$ L/min, $Q_s = 8$ L/min, and bubble diameter (0.1mm) On the other hand, the maximum value of the$(\varepsilon_{fa}/\varepsilon_f)$ was 71% at $Q_a = 2$ L/min, $Q_s = 4$ L/min, and bubble diameter (1.5mm).furthermore,$(Q_s = 6$ L/min) and $(Q_a = 2$ L/min) are the optimum flow rates under the current experimental conditions to get on highest improvement ratio of (U_{fa}/U_f) and $(\varepsilon_{fa}/\varepsilon_f)$.

7. The transient time to reach a steady state of temperature in the case of the smooth tube is higher than the finned tube, as is the case for the difference in the distance between the spiral fins, it was found that the smaller distance between the fins, the less the transient time. Furthermore, the more miniature coil outlet temperature obtains at ($p_f = 5mm$).

8. The bubble diameter (D_b) has contributed to improving the heat exchanger thermal performance. The larger bubble diameter, the higher the thermal efficiency was.

5.2 Recommendations

The present work deals with the experimental study of enhancing the thermal performance of a vertical shell and coiled (smooth and finned) tube heat exchanger by using the air bubbles injection technique. However, the following recommendations for future work should be useful:

1. Study the influence of the number of air bubbles on the heat transfer characteristics of the vertical shell and coiled (smooth and finned) tube heat exchanger.
2. It is advised to do a special numerical analysis using CFD.
3. Measure the timing and velocity of air bubble generation, which affects the hydrodynamics and heat transfer in the heat exchanger. A clear Perspex tube and a high-speed camera may be used to accomplish this.
4. Study the economic feasibility of our study using the method of merged the passive and active methods, represented by using the air bubble injection technique and helical coil finned (internally - externally) tube.
5. Study the effect of merged (passive and active method) technices through using injection air bubbles inside shell and helical coil finned (internally - externally) tube heat exchanger.
6. Study the effect of merged (passive and active method) techniques on nusselt number, through using injection air bubbles inside the shell and helical coil finned (internally - externally) tube heat exchang

REFERENCE:

[1] H.Mahood,A.Campbell, R.Thorpe, and A.Sharif, "Heat transfer efficiency and capital cost evaluation of a three-phase direct contact heat exchanger for the utilization of low-grade energy sources," Energy Convers. Manag , vol. 106, pp. 101–109, 2015.

[2] Ali Sh. Baqir, A. S. "Theoretical and Experimental Study of Direct-Contact Evaporation of a Volatile Drops (N-Pentane) in an Immiscible Liquid (Distilled water)." PhD diss., Ph. D. Thesis, University of Basrah, Iraq, 2010.

[3]Ali Sh. Baqir, Hameed B. Mahood, Mudher S. Hameed, and Alasdair N. Campbell. "Heat transfer measurement in a three-phase spray column direct contact heat exchanger for utilisation in energy recovery from low-grade sources." Energy Conversion and Management 126 (2016): 342-351.

[4] Ali Sh. Baqir,H.Mahood,A.Campbell,and A.Griffiths,"Measuring the average volumetric heat transfer coefficient of a liquid–liquid–vapour direct contact heat exchanger," Applied Thermal Engineering, vol. 103, pp.47-55, 2016.

[5]H.Mahood,A.Campbell, Ali Sh. Baqir ,A.Sharif,and R.Thorpe,"Convective heat transfer measurements in a vapour-liquidliquid three-phase direct contact heat exchanger, "Heat and Mass Transfer, vol. 54, no. 6, pp. 1697-1705, 2018.

[6]Ali Sh.Baqir,H.Mahood,andA.Sayer,"TemperatureDistribution Measurements and Modelling of a Liquid-Liquid-Vapour Spray Column Direct Contact Heat Exchanger," Applied Thermal Engineering, vol. 139, pp. 542-551, 2018.

[7]H.Mahood,Ali Sh.Baqir,A.Yousif,A.Khadom,and A.Campbell,"Direct contact evaporation of a single two-phase bubble in a flowing immiscible liquid medium. Part I: twophase bubble size, "Heat and Mass Transfer, vol. 55, no. 9, pp. 2593-2603, 2019.

[8]N.Baqer,and Ali Sh. Baqir,"Numerical Investigation for Enhancement of Heat Transfer in Internally Finned Tubes Using ANSYS CFX Program," Basrah journal for engineering sciences, vol. 15, pp. 32-42, 2015.

[9]Ali Sh.Baqir,A.Qasim,and A.Adnan,"Experimental study for staggered perforated array of pins like fins in a rectangular air cross flow," The Iraqi Journal For Mechanical And Material Engineering, Vol.14, pp. 261-275, 2014.

[10] Ali Sh. Baqir, A.J., Majid, H.M. and Bassam, A.S. Circular fins with slanted blades attached on the copper pipe: Uniform heat flux and isothermal processes. International Journal of Mechanical Engineering and Technology (IJMET), 5(5), 2014.

[11]E.Somerscales and,A.Bergles,"Enhancement of Heat Transfer and Fouling Mitigation," Adv. Heat Transf, vol. 30, pp. 197–253, 1997.

[12]H.Mulaweh, "Experimental comparison of heat transfer enhancement methods in heat exchangers," International Journal of Mechanical Engineering Education,vol. 31, pp. 160–167, 2003.

[13]A.Dewan,P.Mahanta,K.Raju,and P.Kumar,"Review of passive heat transfer augmentation techniques," Proceedings of the Institution of Mechanical Engineers, Part A: Journal of Power and Energy, vol. 218, pp. 509–527, 2004.

[14]A. Science, "Experimental Measurement and Modelling of Heat Transfer in Spiral and Curved Channels," no. May, 2014.

[15]R.Kong,T.Deethayat,A.Asanakham,andT. Kiatsiriroat, "Heat transfer phenomena on waste heat recovery of combustion stack gas with deionized water in helical coiled heat exchanger," Case studies in thermal engineering , vol. 12, pp. 213–222, 2018.

[16]D.Austen and H.Soliman, "Laminar flow and heat transfer in helically coiled tubes with substantial pitch," Experimental Thermal and Fluid Science, vol. 1, pp. 183–194, 1988.

[17]A.Alimoradi, " Investigation of exergy efficiency in shell and helically coiled tube heat exchangers," Case Studies in Thermal Engineering,vol. 10,pp. 1-8, 2017.

[18]B.Barua, " On secondary flow in stationary curved pipes," The Quarterly Journal of Mechanics and Applied Mathematics,vol. 16,pp, 61-71,1963.

[19]C.Yildiz,Y.Biçer,and D.Pehlivan, " Heat transfers and pressure drops in rotating helical pipes," Applied energy,vol. 50,pp. 85-94,1995.

[20]G.Bonafoni,and R.Capata,"Proposed Design Procedure of a Helical Coil Heat Exchanger   for an Orc Energy Recovery System for Vehicular Application," Mechanics, Materials Science & Engineering Journal,2015.

[21]M. Lazova, H. Huisseune, A. Kaya, S. Lecompte, and G. Kosmadakis, "Performance   Evaluation of a Helical Coil Heat Exchanger Working under Supercritical Conditions in a solar organic Rankine cycle installation," Energies, vol.9, pp. 432-452, 2016.

[22]A. Kitagawa, K. Kosuge, K. Uchida, and Y. Hagiwara, "Heat transfer enhancement for laminar natural convection along a vertical plate due to sub-millimeter-bubble injection," Experiments in fluids, vol. 45, pp. 473–484, 2008.

[23]H. Sadighi Dizaji, S. Jafarmadar, M. Abbasalizadeh, and S. Khorasani, "Experiments on air bubbles injection into a vertical shell and coiled tube heat exchanger; exergy and NTU analysis," Energy Conversion and Management, vol. 103, pp. 973–980, 2015.

[24]A. Moosavi, M. Abbasalizadeh, and H. Sadighi Dizaji, "Optimization of heat transfer and pressure drop characteristics via air bubble injection inside a shell and coiled tube heat exchanger," Experimental Thermal and Fluid Science, vol. 78, pp. 1–9, 2016.

[25]M.Ahmadzadehtalatapeh, H.Yau," Energy Conservation Potential Of Heat Pipe Heat Exchanger: Experimental Study And Predictions," International Journal of Engineering, vol.25, pp.193-200, 2012.

[26]M.Kahrom, P.Haghparast, M.Javadi," Optimization of Heat Transfer Enhancement of Flat Plate Based on Pereto Genetic Algorithm," International Journal of Engineering, vol.23, pp.177-90, 2010.

[27]S.Lee," Thermal design: heat sinks, thermoelectric, heat pipes, compact heat exchangers, and solar cells," vol.23, 2020.

[28]Webb R, Kim Y, Principles of Enhanced Heat Transfer, 2nd ed., Taylor & Francis, New York, 2005.

[29]M. Kahani, S. Z. Heris, and S. M. Mousavi, "Effects of Curvature Ratio and Coil Pitch Spacing on Heat Transfer Performance of Al2O3/Water Nanofluid Laminar Flow through Helical Coils," J. Dispers. Sci. Technol., vol. 34, no. 12, pp. 1704–1712, 2013

[30]D. S. Austen and H. M. Soliman, "Laminar flow and heat transfer in helically coiled tubes with substantial pitch," Exp. Therm. Fluid Sci., vol. 1, no. 2, pp. 183–194, 1988.

[31]C. Yildiz, Y. Biçer, and D. Pehlivan, "Heat transfer and pressure drop in a heat exchanger with a helical pipe containing inside springs," Energy Convers. Manag., vol. 38, no. 6, pp. 619–624, 1997.

[32]H. Shokouhmand and M. R. Salimpour, "Experimental investigation of shell and coiled tube heat exchangers using wilson plots ☆," vol. 35, pp. 84–92, 2008.

[33]N. Jamshidi, M. Farhadi, D. D. Ganji, and K. Sedighi, "Experimental analysis of heat transfer enhancement in shell and helical tube heat exchangers," Appl. Therm. Eng., vol. 51, no. 1–2, pp. 644–652, 2013.

[34]GANAPATHY, V., "Design and Evaluate Finned Tube Bundles," Hydrocarbon Processing, Vol 75, No 9, pp. 103-111, Sep 1996.

[35]X. Li, H .Wu, H. Wang, P .Kou,and H.Tian, " Fluid flow and heat transfer characteristics in helical tubes cooperating with spiral corrugation, " Energy Procedia, vol.17,pp.791-800,2012.

[36]S.Sivalakshmi, M.Raja,and G.Gowtham, "Effect of helical fins on the performance of a double pipe heat exchanger, " Materials Today: Proceedings,vol.43,pp.11281131,2021

[37]A.E. Bergles, Techniques to enhance heat transfer, in: Handbook of Heat Transfer, McGraw-Hill, New York, 1998.

[38]T. Kuppan, Heat Exchanger Design Handbook, Marcel Dekker Inc., New York, 2000.

[39]P. Naphon, and S. Wongwises, "A review of flow and heat transfer characteristics in curved tubes, " Renewable and sustainable energy reviews, vol.10, pp.463–490,2006.

[40]S. Rozzi, R. Massini, G. Paciello, G. Pagliarini, S. Rainieri, and A. Trifirò, "Heat treatment of fluid foods in a shell and tube heat exchanger: comparison between smooth and helically corrugated wall tubes, " Journal of food engineering, vol. 79, pp.249–254,2007.

[41]A.García, P.Solano, G.Vicente,and A.Viedma, "The influence of artificial roughness shape on heat transfer enhancement: Corrugated tubes, dimpled tubes and wire coils, " Applied Thermal Engineering,vol.35,pp.196-201,2012.

[42]J.Solano, A.García, P.Vicente,and A.Viedma, "Flow field and heat transfer investigation in tubes of heat exchangers with motionless scrapers, " Applied Thermal Engineering ,vol.31,pp.2013-2024,2011.

[43]K.Wongcharee,and S.Eiamsa, " Heat transfer enhancement by using CuO/water nanofluid in corrugated tube equipped with twisted tape, "International Communications in Heat and Mass Transfer,vol.39,pp.251-257,2012.

[44]M.Miansari, A.Jafarzadeh, H.Arasteh,and D.Toghraie, "Thermal performance of a helical shell and tube heat exchanger without fin, with circular fins, and with V-shaped circular fins applying on the coil, " Journal of Thermal Analysis and Calorimetry,vol.143,pp.4273-4285,2021.

[45]M.Hashemian, S.Jafarmadar,and H.Dizaji," A comprehensive numerical study on multi-criteria design analyses in a novel form (conical) of double pipe heat exchanger," Applied Thermal Engineering, vol.102,pp.1228-1237, 2016.

[46]R.Samaroo, N.Kaur, K .Itoh, T.Lee, S.Banerjee,and M.Kawaji,"Turbulent flow characteristics in an annulus under air bubble injection and subcooled flow boiling conditions," Nuclear Engineering and Design,vol.268,pp.203-214, 2014.

[47]H.Dizaji, S.Khalilarya, S.Jafarmadar, M.Hashemian,and M.Khezri,"A comprehensive second law analysis for tube-in-tube helically coiled heat exchangers," Experimental Thermal and Fluid Science,vol.76,pp.118-125, 2016.

[48]S.Khorasani,and A.Dadvand," Effect of air bubble injection on the performance of a horizontal helical shell and coiled tube heat exchanger: an experimental study," Applied Thermal Engineering,vol.111,pp.676-683, 2017.

[49]G.Singh,and A.Nandan," Experimental study of heat transfer rate in a shell and tube heat exchanger with air bubble injection," International Journal of Engineering,vol.29,pp.1160-1166, 2016.

[50]E.El-Said,and M.Abou Alsood," Experimental investigation of air injection effect on the performance of a horizontal shell and multi-tube heat exchanger with baffles," Applied Thermal Engineering,vol.134,pp.238-247, 2018.

[51]Ali Sh.Baqir,H.Mahood,and A.Kareem,"Optimization and evaluation of NTU and effectiveness of a helical coil tube heat exchanger with air injection," Thermal Science and Engineering Progress,vol.14,pp.100420, 2019.

[52]A.Kreem,Ali Sh.Baqir,H.Mahood," Temperature Distribution Measurements along Helical Coiled Tube Heat Exchanger with Effect of Air Injection," International Engineering Conference (IEC), pp.85-89, 2019.

[53]T.Subesh, N.Dilip, K.Logesh, V.Ramesh, M.Venkatasudhahar,and D.Surrya," Study on performance of horizontal single pass shell and multi-tube heat exchanger with baffles by air bubble injection," International Journal of Ambient Energy,vol.41,pp.641-651, 2020.

[54]S.Ghashim,and A.Flayh," Experimental investigation of heat transfer enhancement in heat exchanger due to air bubbles injection, "Journal of King Saud University-Engineering Sciences, 2020.

[55]G.Sokhal, G.Dhindsa, K.Sokhal, M.Ghazvini, M.Sharifpur,and M.Sadeghzadeh," Experimental investigation of heat transfer and exergy loss in heat exchanger with air bubble injection technique," Journal of Thermal Analysis and Calorimetry,vol.28,pp.1-11, 2020.

[56]D. Panahi, "Evaluation of Nusselt number and effectiveness for a vertical shell-coiled tube heat exchanger with air bubble injection into shell side," Experimental Heat Transfer, vol. 30, pp. 179–191, 2017.

[57]H.Zavaragh, A.Kaleli, F.Afshari, and A.Amini, "Optimization of heat transfer and efficiency of engine via air bubble injection inside engine cooling system," Applied Thermal Engineering, vol. 123, pp. 390–402, 2017.

[58]S.Pourhedayat, H.Dizaji, and S.Jafarmadar, "Thermal-exergetic behavior of a vertical double-tube heat exchanger with bubble injection," Experimental Heat Transfer,vol.32, pp. 455-468, 2018.

[59]O.Shukla,and B.Yadav," CFD Analysis on Shell and Coiled Tube Heat Exchanger for Heat Transfer Augmentation Due to Air Bubbles Injection," International journal of innovative research in technology,vol.7,pp.256-261,2019.

[60]T.Suneetha,and P.Raghuram," Bubble size measurement and error analysis in a gas liquid injecter," Niscair-Csir,vol.19,pp. 442-446,2012.

[61]M.Murugan,R.Vijayan,A.Saravanan,andS.Jaisankar,"Performanceenhancement of centrally finned twist inserted solar collector using corrugated booster reflectors,"Energy,vol.168,pp. 858-869,2019.

APPENDIXES

Appendix (A): calibration curves

Calibreation method: Thermometer and thermocouples were put in ice cup as a first point for calibration.the calibration carried out under five variat temperature value.temperature values of thermocpouples were records from data loger and temperature of thermometer recorded directly. The temperature value of ice water warm up gradually by used water heater. Approximiatlly the temperature different between of thermometer and thermocouples was 0.5 °C at the most point as seen in the curves below.
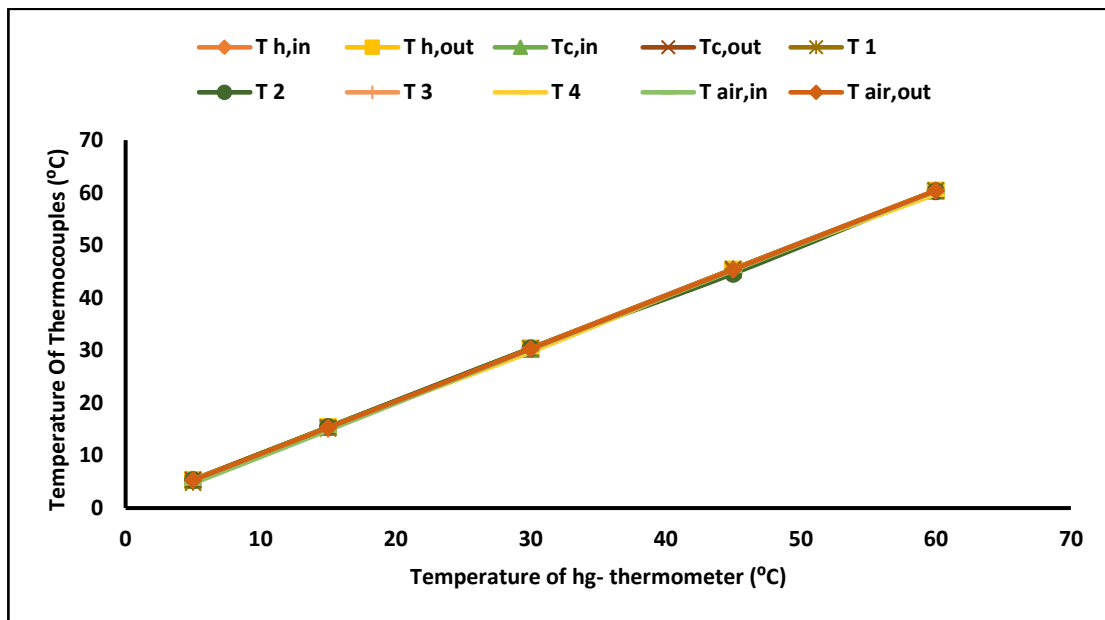
Figure A.1: Calibration curve of thermocouples

The rotometer was calibrated by using a graduated cylinder with L/min units, a water pump and a valve to control the amount of water flowing from the tank via the rotometer and a timer. After that, we set the amount of cold water flow to (2, 4, 6, 8 and 10) respectively through the control valve and measure the time taken for each flow separately. It was found that there is a reading error rate of (0.1-0.2 L/min) with the rotometer reading as shown in Figure (fig. A.2).
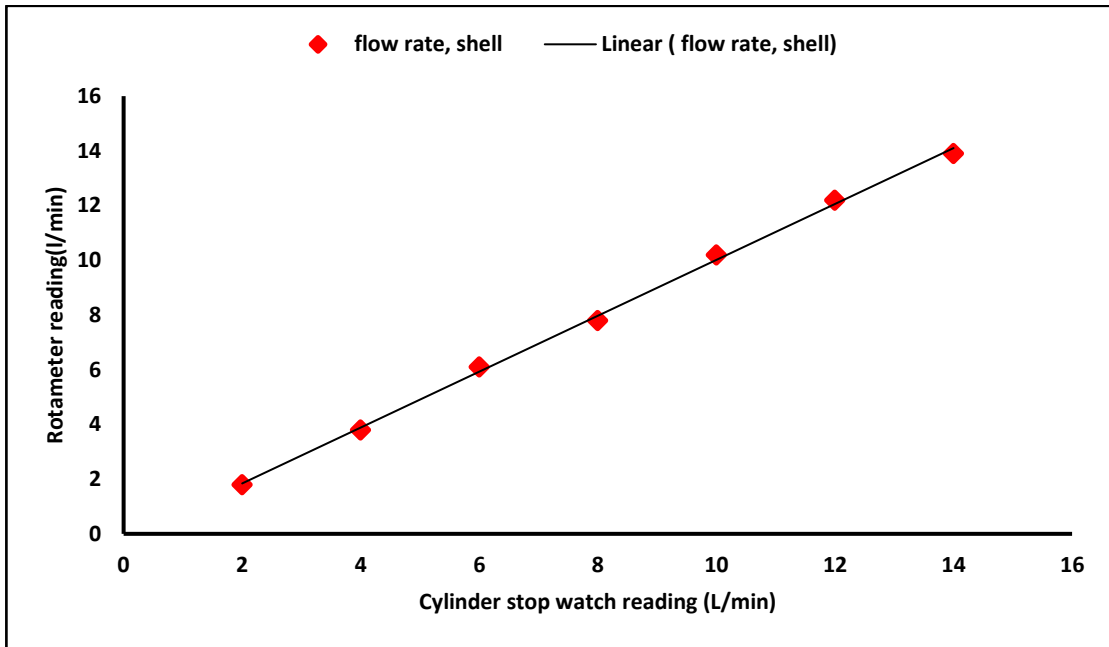
Figure A.2: Shell side rotameter calibration curve.

In the same way, the hot water rotometer was calibrated, but at different flowrate values (1,1.5,2, and 2.5 LPM), and we found an error rate of (0.2) by reading the hot water rotometer as shown in the figure (fig A.3).
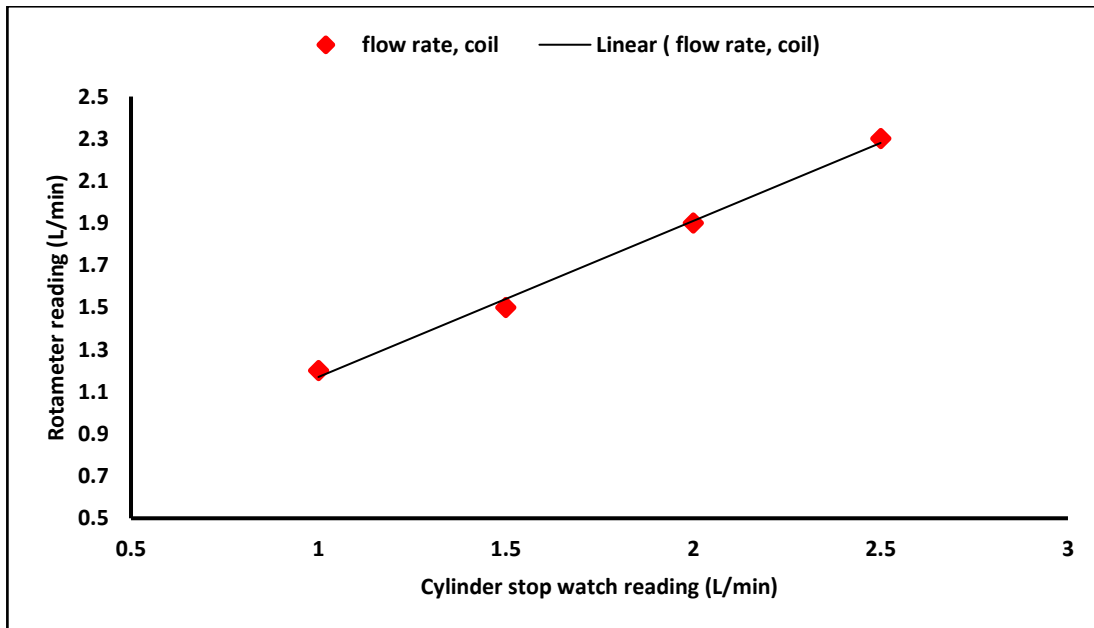
Figure A.3: coil side rotameter calibration curve.

Appendix (B): Laboratory Examination

To measure the dimensions, the sent sample was analyzed and the following was obtained:

Outer diameter =6 mm.

Inner diameter =4.4 mm.

Length sample =8.05 mm.

Fin depth = 0.4 mm.

Wall thickness = 0.8 mm.

spiral angle = 49

upper width fin =0.52 mm.

bottom width fin = 0.3 mm.

fin inner height = 0.2mm.

shape of inner tips fins is convex.

The name of the test device (Fesem Tescan mira3) and model France.

مركز كاك للفحوصات الكيميائية

00964783090350 & 009647718584090

بغداد ـ شارع فلسطين ـ ساحة الموال ـ مصرف الجنوب الاسلامي ـ الطابق الثاني

Figure B.1: Laboratory Examination paper.

Figure B.2: Front view of finned tube.

Figure B.3: Side view of finned tube.

Appendix (C): Uncertainty

The following equation can be used to calculate the uncertainty of experimental data **[61]**:

$$W_R = \sqrt{\sum_0^i \left(\frac{\partial R}{\partial X_i} \cdot W_{Xi}\right)^2} \tag{C.1}$$

Moreover, the result is given as:

$$R = f(X_1, X_2, \ldots, X_n) \tag{C.2}$$

Where:

W_R: Uncertainty in the result

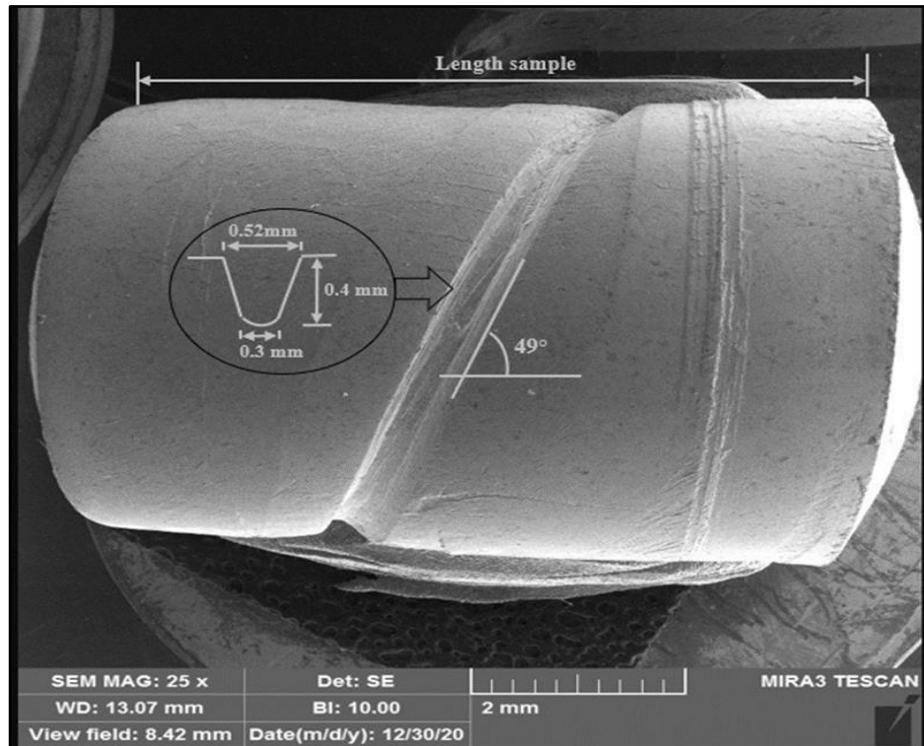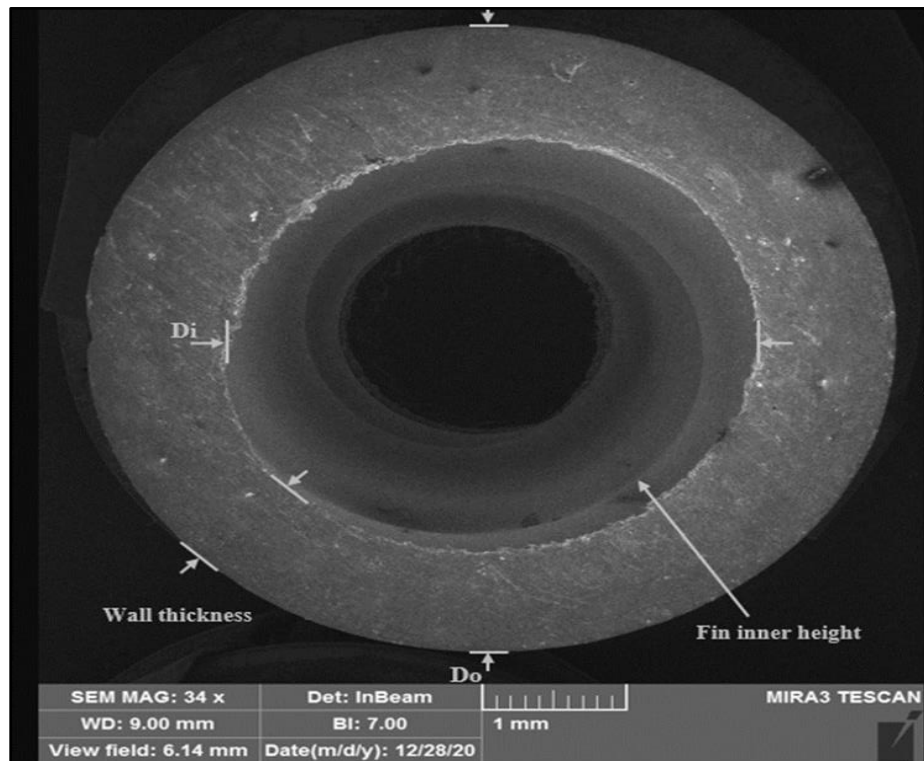$X_1, X_2, \ldots, X_n$: Independent variables, and

$W_1, W_2, \ldots, W_n$: Uncertainty in the corresponding variables.

The uncertainty of the performance parameters that have been experimentally obtained in the present study will calculate sequentially in the following sections using the general formula (C.1).

Overall Heat Transfer Coefficient (U)

The overall heat transfer coefficient (**U**) was calculated by Eq. (4.1) and rewritten below:

$$U = \frac{q}{A_s \cdot \Delta T_{LMTD}} \tag{C.3}$$

According to Eq. (C.1), the uncertainty of **U** is due to the errors of q, A_s And the temperatures ($T_{h,i}$, $T_{h,o}$, $T_{c,i}$ and $T_{c,o}$). However, the following general expression can be made:

$$W_U = \sqrt{\left(\frac{\partial U}{\partial q} W_q\right)^2 + \left(\frac{\partial U}{\partial \Delta T_{LMTD}} W_{\Delta T_{LMTD}}\right)^2 + \left(\frac{\partial U}{\partial A_S} W_{A_S}\right)^2} \tag{C.4}$$

This leads to:

$$W_U = \sqrt{\left(\frac{W_q}{A_s \cdot \Delta T_{LMTD}}\right)^2 + \left(-\frac{q \cdot W_{\Delta T_{LMTD}}}{A_s \cdot (\Delta T_{LMTD})^2}\right)^2 + \left(-\frac{q \cdot W_{A_S}}{A_S^2 \cdot \Delta T_{LMTD}}\right)^2} \tag{C.5}$$

Where ΔT_{LMTD} is the log-mean temperature difference, and it can be found by:

$$\Delta T_{LMTD} = \frac{(T_{h,i} - T_{c,o}) - (T_{h,o} - T_{c,i})}{\ln\left(\frac{T_{h,i} - T_{c,o}}{T_{h,o} - T_{c,i}}\right)} \tag{C.6}$$

Hence, the general uncertainty of ΔT_{LMTD} is **[50]**

$$W_{\Delta T_{LMTD}} = \frac{\sqrt{\begin{array}{l}\left(\left\{\left(\frac{[(T_{h,i} - T_{c,o}) - (T_{h,o} - T_{c,i})]}{(T_{h,i} - T_{c,o})}\right) - \ln\left(\frac{(T_{h,i} - T_{c,o})}{(T_{h,o} - T_{c,i})}\right)\right\}^2 \left[W_{T_{h,i}}^2 - W_{T_{c,o}}^2\right]\right) + \\ \left(\left\{\left(\frac{[(T_{h,i} - T_{c,o}) - (T_{h,o} - T_{c,i})]}{(T_{h,o} - T_{c,i})}\right) - \ln\left(\frac{(T_{h,i} - T_{c,o})}{(T_{h,o} - T_{c,i})}\right)\right\}^2 \left[W_{T_{h,o}}^2 - W_{T_{c,i}}^2\right]\right)\end{array}}}{\left(\ln\left[\frac{(T_{h,i} - T_{c,o})}{(T_{h,o} - T_{c,i})}\right]\right)^2} \tag{C.7}$$

Now, the second factor that affects the uncertainty of U is the heat transfer rate q which can be found by:

$$q = \dot{m}_h \, Cp_h \left(T_{h,i} - T_{h,o}\right) \tag{C.8}$$

Similarly, the uncertainty of q can be calculated as:

$$W_q = \sqrt{\left(\frac{\partial q}{\partial m_h} W_{m_h}\right)^2 + \left(\frac{\partial q}{\partial Cp_h} W_{Cp_h}\right)^2 + \left(\frac{\partial q}{\partial T_{h,i}} W_{T_{h,i}}\right)^2 + \left(\frac{\partial q}{\partial T_{h,o}} W_{T_{h,o}}\right)^2} \tag{C.9}$$

Using Eq. (C.8) results in:

$$W_q = \sqrt{\begin{array}{l}\left(Cp_h \cdot [T_{h,i} - T_{h,o}] \cdot W_{m_h}\right)^2 + \left(m_h \cdot [T_{h,i} - T_{h,o}] \cdot W_{Cp_h}\right)^2 + \left(m_h \cdot Cp_h \cdot W_{T_{h,i}}\right)^2 \\ + \left(- m_h \cdot Cp_h W_{T_{h,o}}\right)^2\end{array}} \tag{C.10}$$

Multiply equation (C.10) by $\left[\frac{m_h}{m_h}\right]\left[\frac{Cp_h}{Cp_h}\right]\left[\frac{T_{h,i} - T_{h,o}}{T_{h,i} - T_{h,o}}\right]$, results in:

$$W_q = \sqrt{\begin{array}{l}\left(\frac{m_h \cdot Cp_h \cdot [T_{h,i} - T_{h,o}] \cdot W_{m_h}}{m_h}\right)^2 + \left(\frac{m_h \cdot [T_{h,i} - T_{h,o}] \cdot W_{Cp_h}}{Cp_h}\right)^2 + \left(\frac{m_h \cdot Cp_h \cdot (T_{h,i} - T_{h,o}) \cdot W_{T_{h,i}}}{T_{h,i} - T_{c,i}}\right)^2 \\ + \left(\frac{- m_h \cdot Cp_h \cdot (T_{h,i} - T_{h,o}) \cdot W_{T_{c,i}}}{T_{h,i} - T_{c,i}}\right)^2\end{array}} \tag{C.11}$$

where: $q = \dot{m}_h \, Cp_h \left(T_{h,i} - T_{h,o}\right)$

Eq. (C.11) becomes:

$$\therefore W_q = q \sqrt{\left[\frac{W_{m_h}}{m_h}\right]^2 + \left[\frac{W_{Cp_h}}{Cp_h}\right]^2 + \left[\frac{W_{T_{h,i}}}{T_{h,i}-T_{h,o}}\right]^2 + \left[-\frac{W_{T_{h,o}}}{T_{h,i}-T_{h,o}}\right]^2}$$ (C.12)

The uncertainty of A_s Moreover, Cp_h can be ignored due to its minor effect [44].

Now the uncertainty of U can be obtained by Substitute Eq. C.7 and C.12 into Eq. C.5.

Effectiveness (ε)

The general equation that can be used to calculate the heat exchanger effectiveness is:

$$\varepsilon = \frac{q}{Q_{.max.}}$$ (C.13)

Using Eq. C. 1 above, the general uncertainty formula of ε is:

$$W_\varepsilon = \sqrt{\left(\frac{\partial\varepsilon}{\partial q}W_q\right)^2 + \left(\frac{\partial\varepsilon}{\partial Q_{.max.}}W_{Q.max}\right)^2}$$ (C.14)

Using Eq. C.13, yields:

$$W_\varepsilon = \sqrt{\left(\frac{W_q}{Q_{.max.}}\right)^2 + \left(-\frac{q.W_{Q.max}}{(Q_{.max.})^2}\right)^2}$$
(C.15)

Uncertainty of $W_{Q.max.}$ can be similarly obtained:

$$W_{Q.max.} = \sqrt{\left(\frac{\partial Q_{.max}}{\partial m_h}W_{m_h}\right)^2 + \left(\frac{\partial Q_{.max}}{\partial Cp_h}W_{Cp_h}\right)^2 + \left(\frac{\partial Q_{.max}}{\partial T_{h,i}}W_{T_{h,i}}\right)^2 + \left(\frac{\partial Q_{.max}}{\partial T_{c,i}}W_{T_{c,i}}\right)^2}$$ (C.16)

where

$$Q_{,max.} = C_{min.}\left(T_{h,i} - T_{c,i}\right)$$ (C. 17)

and $C_{min} = m_h * Cp_h$

Using Eq. C. 16 above, yield:

$$W_{Q.max.} = \sqrt{\left(Cp_h.\left[T_{h,i} - T_{c,i}\right].W_{m_h}\right)^2 + \left(m_h.\left[T_{h,i} - T_{c,i}\right].W_{Cp_h}\right)^2 + \left(m_h.Cp_h.W_{T_{h,i}}\right)^2 + \left(-m_h.Cp_hW_{T_{c,i}}\right)^2} \tag{C.18}$$

Multiply Eq. C.18 by $\left[\frac{m_h}{m_h}\right]\left[\frac{Cp_h}{Cp_h}\right]\left[\frac{T_{h,i} - T_{c,i}}{T_{h,i} - T_{c,i}}\right]$, results:

$$W_{Q.max.} = \sqrt{\left(\frac{m_h.Cp_h.\left[T_{h,i} - T_{c,i}\right].W_{m_h}}{m_h}\right)^2 + \left(\frac{m_h.\left[T_{h,i} - T_{c,i}\right].W_{Cp_h}}{Cp_h}\right)^2 + \left(\frac{m_h.Cp_h.\left(T_{h,i} - T_{c,i}\right).W_{T_{h,i}}}{T_{h,i} - T_{c,i}}\right)^2 + \left(\frac{-m_h.Cp_h.\left(T_{h,i} - T_{c,i}\right).W_{T_{c,i}}}{T_{h,i} - T_{c,i}}\right)^2} \tag{C.19}$$

But:

$$Q_{max.} = m_h.Cp_h.\left(T_{h,i} - T_{c,i}\right)$$

Hence, Eq. (C.19), becomes:

$$\therefore W_{Q.max.} = Q.max\sqrt{\left[\frac{W_{m_h}}{m_h}\right]^2 + \left[\frac{W_{Cp_h}}{Cp_h}\right]^2 + \left[\frac{W_{T_{h,i}}}{T_{h,i} - T_{c,i}}\right]^2 + \left[-\frac{W_{T_{c,i}}}{T_{h,i} - T_{c,i}}\right]^2} \tag{C.20}$$

Finally, the uncertainty of ε can be obtained by substituting Eq. C.12 and Eq. C.20 into Eq. C.15.

Appendix (D): List of Publications

1. Improvement of Thermal Performance of Coiled Tube Heat Exchanger Utilizing Air Bubble Injection Technique.

Improvement of Thermal Performance of Coiled Tube Heat Exchanger Utilizing Air Bubble Injection Technique

Saif Salah Hasan[1*], Ali Shakir Baqir[1], Hameed B Mahood[2]

[1]Engineering Technical College, Al-Furat Al-Awsat Technical University, Al-Najaf 31001, Iraq
[2]Department of Chemical and Process Engineering, Faculty of Engineering and Physical Sciences, University of Surrey, Guildford GU2 7XH, UK

E-mail: saif.salah@student.atu.edu.iq

Abstract. The heat transfer enhancement in terms of temperature of a vertical helically coiled tube heat exchanger is carried out experimentally. The experiments were achieved in a heat exchanger with a 50 cm height and 15 cm internal diameter under four different cold and three hot water mass flow rates and four different airflow rates. At the same time, the temperature difference was taken invariant ($\Delta T=20°C$). To avoid some uncertainties, the hot side temperature of the heat exchanger was measured via k-type thermocouples. The results showed that the increase of air injection flow rate improved heat transfer from the hot stream flowing in the coil to the shell's cold stream. An intimate thermal mixing when air injected is clearly observed, which could be responsible for the heat exchanger's thermal enhancement. Finally, the injected air pressure was noticed to be having only a minor effect on thermal performance improvement.

Keywords: heat exchanger, coil tube, air injection bubbles, and sparger.

1. Introduction

Heat exchangers are equipment utilized to transfer thermal energy between two different thermal energy content streams. Hence, they are widely implemented in various industrial applications, such as in the power plants, chemical industries, refinery, food industry, and pharmaceuticals. Accordingly, a huge effort has been directed to improve the heat exchanger performance efficiency utilizing various techniques[1]. However, all enhancement techniques inevitably involve a significant increase in the pressure drop, cost, energy, materials, and heat exchangers weight. Minimizing the pressure drop while improving heat exchanger thermal efficiency increases the target of many investigators.

Among various enhancement techniques, such as using a twisted tape, corrugated tubing, wavy stripes, barbed wires, and internal and external fins, air injection as bubbles seems the most promising approach. This improvement technique's merit is in its capability to significantly improve the thermal efficiency of heat exchangers with a relatively low increase in the pressure drop. However, Dizaji et al. [2] has experimentally studied the thermal enhancement of a helically coiled tube heat exchanger

1

2. Air bubble injection technique for enhancing heat transfer in a coiled tube heat exchanger: an experimental study.

University of AlKafeel

Publication Acceptance Letter

Manuscript ID: ENG-279

Authors: Saif S. Hasan1, Hameed B. Mahoodb2, Ali S. Baqir3

Email of Correspoinding Author: saif.salah@student.atu.edu.iq

Affiliation: Al-Furat Al-Awsat Technical University1,3, University of Surrey2

Dear (author) we are plased to inform you that, after peer-review process, your manuscript entitled

Air Bubble Injection Technique for Enhancing Heat Transfer in a Coiled Tube Heat Exchanger: An Experimental Study

has been accepted for presentation in the

3rd INTERNATIONAL SCIENTIFIC CONFERENCE OF ALKAFEEL UNIVERSITY(ISCKU 2021)

which was held at the University of Alkafeel on the 22nd - 23rd of March 2021

Your paper will be published by **American Institute of Physics** (ISSN: 1551-7616) after pass all the journal requirements.

With Best Regards

AIP | Publishing   Scopus

Prof. Dr. N. Al-Dahan
Rector of Alkafeel University

3. The Effect of Injected Air Bubble Size on the Thermal Performance of a Vertical Shell and Helical Coiled Tube Heat Exchanger.

ARTICLE

The Effect of Injected Air Bubble Size on the Thermal Performance of a Vertical Shell and Helical Coiled Tube Heat Exchanger

Saif S. Hasan[1], Ali Sh. Baqir[1] and Hameed B. Mahood[2,*]

[1]Engineering Technical College, Al-Furat Al-Awsat Technical University, Al-Najaf, 31001, Iraq

[2]Department of Chemical and Process Engineering, Faculty of Engineering and Physical Sciences, University of Surrey, Guildford, GU2 7XH, UK

[*]Corresponding Author: Hameed B. Mahood. Email: hbmahood@yahoo.com

ABSTRACT

In the present study, the effect of injecting air bubble size on the thermal performance of a vertical counter-current shell and coiled tube heat exchanger is experimentally investigated. The experiments were accomplished in a cylindrical shape heat exchanger with a 50 cm height and 15 cm outer diameter. Copper coil with 3.939 m equivalent length and 0.6 cm outer diameter was used to carry the hot fluid (water). Four different cold fluid (shell side) flow rates ($Q_s = 2$, 4, 6 and 8 LPM) under laminar flow conditions ($316 \leq Re \leq 1223$), constant hot (coil side) flow rate fluid rates ($Q_h = 1$ LPM), four different injected air flow rates ($Q_a = 0.5$, 1, 1.5 and 2 LPM), invariant temperature difference ($\Delta T = 20°C$), and constant bubble's number (1400) were tested. To demonstrate the effect of bubble size, a sparger with orifice diameters of 0.1, 0.8, and 1.5 mm was manufactured and used in the study. The overall heat transfer coefficient (U), NTU, effectiveness, and pressure loss were invested. The experimental results clearly showed that the heat exchanger's thermal efficiency significantly improved with increasing the shell side flow rate and the injected air flow rate. The maximum improvement in U, NTU, and effectiveness was 153%, 153%, and 68%, respectively. The thermal performance of the heat exchanger was shown to be improved with increasing the bubble size. Although the latter finding agrees with recent CFD published results, more studies need to be confirmed.

KEYWORDS

Sparger; smooth helical coil; vertical shell; heat exchanger; injection bubbles

Nomenclature

A_s	Heat transfer area (m^2)
c_p	Specific heat (J/kg. k)
di	Inner coiled tube diameter, mm
D_c	Curvature diameter (mm)
H	Height column (mm)
K	Thermal conductivity (W/m °C)
L	Tube length (mm)
LMTD	Logarithmic mean temperature difference (°C)
$\dot{m}$	Mass flow rate (kg/s)

4. Enhancement of Thermal Performance of Helically Coiled Tube Finned (Internally, and Externally) Of Heat Exchanger Utilizing Air Bubble Injection Technique.

[FJIMSE] Editor Decision External

Inbox

Dr. Essam Al-Zaini Yesterday
to me, Prof.Dr.Ali, Dr.Hameed

saif salah Al Karaawi, Prof.Dr.Ali shakir , Dr.Hameed B Mahood:

We have reached a decision regarding your submission to Al-Furat Journal of Innovation in Mechanical and Sustainable Energy Engineering, "Enhancement of Thermal Performance of Helically Coiled Tube Finned (Internally, and Externally) Of Heat Exchanger Utilizing Air Bubble Injection Technique".

Our decision is to: Resubmit for Review

_____
_____
Al-Furat Journal of Innovation in Mechanical and Sustainable Energy Engineering

MT: Enhancement of Thermal Performance of Helically Coiled Tube Finned (Internally, and Externally) Of Heat Exchanger Utilizing Air Bubble Injection Technique

The paper presents an experimental study of a heat exchanger type shall with an internally helical coil with injecting air bubbles into a shell inlet. Different flow rates for hot, cold, and the injected air was considered.

The general presentation of the paper is very good, however, some points to improve the next version would be recommended

W B-Review report1.docx

Appendix (E):summary of the obtained improvement values,and comparison of the present study results with Kareem [51,52].

Table E.1: summary of the obtained improvement values.

No	Type	Parameters	Value	Qs (L/M)	Qh (L/M)	Qa (L/M)	Db (mm)	Ps (mm)	Number of bubbles per meter
1	Smooth tube	(Usa/Us) max	152%	6	2	2	1.5	/	1400
		(Usa/Us) min	56%	8	1	0.5	1.5	/	1400
2		(εsa/εs) max	111%	6	2	2	1.5	/	1400
		(εsa/εs) min	34%	8	1	0.5	1.5	/	1400
3	Finned tube	(Ufa/Us) max	92%	4	1.5	2	1.5	5	1400
		(Ufa/Us) min	38%	8	1.5	0.5	0.1	5	1400
4		(εfa/εf) max	71%	4	1.5	2	1.5	5	1400
		(εfa/εf) min	23%	8	1.5	0.5	0.1	5	1400
9		Uf/Us max	107%	4	1.5	2	1.5	5	1400
10		Ufa/Us max	281%	4	1.5	2	1.5	5	1400

Table E.2: comparison of the present study results with Kareem et al. [51,52].

Authors	Kareem AR [51-52] , (smooth tube)	present study (finned tube)	
		smooth tube	(finned tube) pitch 5mm
Q_h (L/M)	1.5	1.5	1.5
Q_s (L/M)	6	6	6
Q_a (L/M)	2	2	2
$\Delta T(°C)$	20	20	20
D_b (mm)	/	1.5	1.5
$U(w/m^2.k)$	1426	1336	2130
U_{sa}/U_s	63%	150%	/
U_{fa}/U_f	/	/	81%
ε	0.6	0.57	0.74
$\varepsilon_{sa}/\varepsilon_s$	31%	110%	/
$\varepsilon_{fa}/\varepsilon_f$	/	/	50%

الخلاصة

يتطلب نقل الطاقة الحرارية بشكل فعال استخدام مبادل حراري قادر على نقل الطاقة الحرارية الكاملة لمصدر الطاقة بأقل تكلفة ممكنة. المبادلات الحرارية التقليدية ذات النمط السطحي لها عيوب كبيرة ، مثل مقاومة انتقال الحرارة العالية للسطح وطبقة الترسبات ، اضافة الى التكلفة العالية. نتيجة لذلك ، فإن أي محاولة لتحسين خصائص نقل الحرارة لمبادل حراري من النوع السطحي من شأنه أن يعزز الأداء الحراري. تقنية الحقن بالفقاعات الهوائية والأنبوب الحلزوني ذو الزعانف هما من أكثر الطرق الواعدة للتحسين التي تم اقتراحها مؤخرًا بصورة منفصلة. لذلك ,في هذه الدراسة ، تم دراسة التأثير المزدوج للحقن بالهواء والأنبوب الحلزوني المزعنف داخليا وخارجيا على الأداء الحراري لمبادل حراري عمودي ذو تيار معاكس ,تم فحصه تجريبيًا باستخدام معايير تشغيل مختلفة تمامًا مقارنة بالدراسات الادبية السابقة. حيث تم حقن الهواء في الجانب الصدفي للمبادل الحراري على شكل فقاعات هواء بقطر متغير (0.1،0.8 ، 1.5 مم) عن طريق سبارجر (أنبوب بلاستيكي حلزوني الشكل) يمتلك (1400) ثقب وهي طريقة حقن جديدة.

أجريت الدراسة لتحسين المعايير التشغيلية من حيث تحديد افضل void fraction (معدلات التدفق الحجمي للهواء والماء) والذي كان 0.25 وتحت تدفق صفحي يتراوح بين (1223 $\geq$ Re $\geq$ 316) . وتم النظر في تأثير المعايير الرئيسية المتغيرة على معامل انتقال الحرارة الكلي ، والفعالية ، وتوزيع درجة الحرارة على طول جانب الغلاف ، وجانب القشرة ، وانخفاض الضغط وتأثير ضغط الهواء المحقون مع وبدون حقن فقاعات الهواء والمقارنة بينهما. إلى جانب ذلك ،تمت دراسة تأثير قطر الفقاعة على الأداء الحراري للمبادل الحراري.

أظهرت النتائج التجريبية تحسنًا ملحوظًا في معامل انتقال الحرارة الكلي وفعالية المبادل الحراري نتيجة حقن فقاعات الهواء. وبالفعل، بالنسبة للأنابيب الملساء ، كان الحد الأقصى من التحسين (U_{sa}/U_s), $(\varepsilon_{sa}/\varepsilon_s)$ 152% و 111% ، على التوالي تم الحصول عليها عندما (Qs = 6LPM ، Qa = 2 LPM، و Qh = 2LPM. اما بالنسبة للأنابيب المزعنفة ، كان الحد الأقصى لتعزيز معامل نقل الحرارة الكلي ، والفعالية هو 92% , 71 % على التوالي عند(Qs = 4LPM ، Qa =2 LPM ,Qh =2LPM، وقطر فقاعة = 0.1mm .

كذلك بينت النتائج ان أعلى نسبة تحسين لمعامل انتقال الحرارة الكلي (U_f/U_s) لزعانف (5،8 ، و 10 ملم) كانت (107% ، 73% ، 49%) ، على التوالي ، و(U_{fa}/U_s) لزعانف (5،8 ، و 10 ملم) كانت (281% ، 261% ، 248%) على التوالي.

دراسة تجريبية لتحسين نقل الحرارة باستخدام حقن فقاعات الهواء داخل مبادل حراري من نوع الصدفة وانبوب مزعنف داخليا وخارجيا

رسالة مقدمة الى

قسم هندسة تقنيات ميكانيك القوى

كجزء من متطلبات نيل درجة الماجستير في

هندسة تقنيات ميكانيك القوى/ الحراريات

تقدم بها

سيف صلاح حسن رحيمه

ماجستير في هندسة تقنيات ميكانيك القوى

اشراف

الاستاذ الدكتور

علي شاكر باقر

1442

جمهورية العراق

وزارة التعليم العالي والبحث العلمي

جامعة الفرات الاوسط التقنية

الكلية التقنية الهندسية/النجف

دراسة تجريبية لتحسين نقل الحرارة باستخدام حقن فقاعات الهواء داخل مبادل حراري من نوع الصدفة وانبوب مزعنف داخليا وخارجيا

سيف صلاح حسن رحيمه

ماجستير في هندسة تقنيات ميكانيك القوى

1442